Etude du rôle de FW2.2 dans le développement du fruit de tomate

Lamia Azzi

THÈSE

Présentée à

L'UNIVERSITÉ BORDEAUX 1

ÉCOLE DOCTORALE SCIENCES DE LA VIE ET DE LA SANTÉ

Par

Lamia AZZI

Le 16 décembre 2013

POUR OBTENIR LE GRADE DE DOCTEUR

SPÉCIALITÉ : BIOLOGIE VÉGÉTALE

Etude du rôle de FW2.2 dans le développement du fruit de tomate

Directeur de thèse : Christian CHEVALIER

Membres du Jury

Mme. BERTIN Nadia. .....Rapporteur
M. SCHNITTGER Arp .....Examinateur
M. GRANELL RICHART Antonio .....Rapporteur
M. ROLIN Dominique .....Président

THÈSE

Présentée à

L'UNIVERSITÉ BORDEAUX 1

ÉCOLE DOCTORALE SCIENCES DE LA VIE ET DE LA SANTÉ

Par

Lamia AZZI

Le 16 décembre 2013

POUR OBTENIR LE GRADE DE DOCTEUR

SPÉCIALITÉ : BIOLOGIE VÉGÉTALE

Etude du rôle de FW2.2 dans le développement du fruit de tomate

Directeur de thèse : Christian CHEVALIER

Membres du Jury

Mme. BERTIN Nadia. .....Rapporteur
M. SCHNITTGER Arp .....Examinateur
M. GRANELL RICHART Antonio .....Rapporteur
M. ROLIN Dominique .....Président

Remerciements

Je remercie les membres du jury de m'avoir fait l'honneur d'évaluer mon travail de thèse. Merci pour tout l'intérêt que vous y avez porté et pour la discussion que j'ai pu avoir avec vous à ce sujet, elle a été très enrichissante pour moi. Un remerciement tout particulier à mon président de jury, Dominique Rolin, qui me voit comme un « géant vert » (pour une fille d'1m60, c'est un comble). Vous avez été mon professeur en licence et en master, votre gentillesse et votre pédagogie ont éveillé mon intérêt pour la biologie végétale et font en partie ce à quoi j'en suis arrivée aujourd'hui.

Mes remerciements vont évidemment à mon directeur de thèse, Christian Chevalier. Il y a trois ans et demi, vous m'avez accueillie dans votre bureau (toute paniquée que j'étais…) pour un entretien et vous avez bien voulu de moi en tant que thésarde. Je vous remercie pour la confiance que vous m'avez accordée et le soutien que vous m'avez apporté. Vos conseils avisés, votre rigueur scientifique, votre patience et votre présence bienveillante m'ont aidé à évoluer et auront été précieux pendant ces trois ans.

Je n'en serais également pas là sans Frédéric Gévaudant. Je t'adresse mes plus sincères remerciements (le tutoiement a mis du temps à venir, mais là je crois y arriver !). D'abord mon professeur en licence et master, puis mon responsable de stage en M1, tu as été un encadrant hors pair, tant d'un point de vue scientifique que d'un point de vue humain, très présent, doué d'une patience hors norme (là, je m'incline) face aux nombreuses boulettes que j'ai pu faire, d'un stoïcisme inébranlable dans des moments où j'aurais moi-même montré de l'agacement et d'un sens de l'humour nécessaire dans des moments où il y en avait le plus besoin : eh oui, qui eut cru pouvoir transformer des BY2 en champignons ? Nous, on a réussi ! Couler 300 grandes boîtes de LB en une après-midi ? Finger in the nose ! Merci pour toute l'implication dont tu as fait preuve pendant ces trois ans, ce travail est autant le mien que le tien. Je garderai toujours en mémoire l'image d'un encadrant souriant qui assume avec fierté se déguiser en Lady Gaga et je te souhaite bon courage pour la suite (j'espère être conviée à ton HDR ?) et beaucoup de succès ! Encore merci pour tout !

Je remercie Michel Hernould pour son aide et ses connaissances intarissables sur bien des sujets. Ce n'est pas pour rien que je vous considère comme l'encyclopédie vivante du laboratoire ! Merci pour votre gentillesse, votre patience, un certain pot de 750g d'une célèbre pâte à tartiner apporté au Japon pour nous remonter le moral, votre humour, parfois décalé, parfois caustique, et vos charades à tiroir qui ont toujours leur effet escompté ! Les discussions (scientifiques ou pas) que nous aurons pu avoir dans le bureau des thésard/coin café autour d'un café et d'un morceau de chocolat m'ont beaucoup apporté, j'en garderai un excellent souvenir.

Merci à Aurélie Honoré pour toute l'aide que tu m'auras apporté pendant ma thèse, tu m'as soulagé de beaucoup de choses et j'ai adoré parler origami avec toi. Je suis sûre que

ces problèmes de tomates qui ne pollinisent pas ou qui font de la pourriture apicale finiront par se résoudre !! Je te souhaite une très bonne continuation.

Merci à ma Landaise de voisine de bureau et partenaire dans le crime, Céline, la G2 squatteuse de bureau G1, toujours présente quand une bêtise est à faire, avec qui la traversée de ces 3 ans aura été plus simple. Je garderai un excellent souvenir de nos Game of Thrones, Walking Dead, Vente Privée, 9gag et toute autre distraction associée à la pause du midi. Merci d'avoir été là quand ça allait et (surtout) quand ça n'allait pas, tu as été d'un grand soutien, à grands coups de tout ce qui peut être à base de chocolat, quelque soit l'heure de la journée, et de photos de chatons, de chiots, de lapins et de tout ce qui ressemble à un animal mignon sur le net. Je te souhaite bon courage pour la fin, plus que 8 mois, tu commences à voir la lueur au bout du tunnel, que tu le veuilles ou non !

Je pense à tous les petits docteurs en devenir. Nono, tu vas voir, tout va bien se passer, mais pense à essayer de ne pas te saborder en te plantant une pipette pasteur dans le pouce tous les mois ! Tracey, arrête de râler, on sait que ça ne va pas, vraiment… Cynthia, non, tes tomates ne te veulent pas que du mal ! Rémi, les grosses vaches attendent toujours les gâteaux que tu leur dois ! Je vous souhaite tout le courage qu'il faut pour mener à bien votre travail et beaucoup de bonheur pour la suite !

Je pense aussi à ceux qui sont passé par là : Mathieu, Thomas et Guillaume pour votre humour grinçant, mais aussi Antoine, Julien Lisa et Julie pour votre aide quand j'en ai eu besoin. Merci aux étudiants qui ont mis leur patte plus ou moins chanceuse dans mon travail et à ceux qui ont partagé notre bureau et sont devenus des amis.

Et à ceux qui ont soutenu en même temps que moi : Johann, Justine, Eric, Julien, Maud, Claireline, Shaam, Lila et Isa, on y est arrivé !!

Je remercie toute les personnes de l'UMR1332 que j'ai pu côtoyer pendant ces trois ans, leur gentillesse étant ce qui les caractérise : Frédéric Delmas, pour tout les conseils que tu as pu m'apporter, les décontaminations de graines à la bertholite et tous les gâteaux/bonbons que ton beau-frère a pu nous fournir et que tu as toujours généreusement partagé avec nous ; Nathalie Frangne, pour ton sourire et l'aide que tu m'as apportée pendant ces trois ans et surtout pendant l'année de monitorat (fais attention, j'arriverai à te piquer tes bottines un jour !) ; JP pour toutes les pauses partagées, les discussions chien et les machines PCR que tu m'as très gentiment prêtées, toujours avec un immense sourire, bien sûr ; Cécile, pour les râleries partagées et les discussions bouquins et fringues (dis-donc, il est mignon ce petit pull !) ; Amèlia et Mathieu, bon courage pour la suite, si ça vous tente toujours, on peut ouvrir une boutique de fleuriste ! ; aux gens du haut, Aurélie, Batoune, Marc, Martine, Joana, Pierre, Laurent, Christophe, Benoît, j'en oublie forcément et je m'en excuse, merci pour votre soutien quand j'en ai eu besoin.

Isabelle, merci pour tous les soins que tu as apportés à mes plantes et tout l'amour et la patience que tu leur as fournis au moment où je rêvai de les arroser à la javel… Je reste sûre que ton sourire et ton optimisme apportent bien plus que l'eau et les solutions nutritives aux plantes !

Merci aux filles du BIC pour leur aide à la microscopie, toujours avec le sourire (« Lysiane ! Ya un problème, je vois rien ! – T'as ouvert le shutter ? – … C'est bon, je vois quelque chose ! »).

Merci à Jean-Baptiste Thibaut, Benoit Lacombe et Claire Corratgé-Faillie pour l'accueil chaleureux qu'ils m'ont réservé et l'aide qu'ils ont pu m'apporter dans la réalisation du voltage-clamp.

A Florence, la secrétaire la plus énergique au monde, merci pour ta patience quand je rechignai à faire la moindre petite démarche qui ressemblait vaguement à de l'administratif. Tu as été une vraie mère poule, que ce soit pour moi ou pour tous les autres étudiants qui sont passé dans le labo !

Je ne peux oublier mes amis, toujours présents quand j'en ai eu besoin : Marie-Ange (merci pour les virées shopping et les soirées sushi !) et Julien, Eric et Benoit, Maud et Cyril, Elsa et Julien, Fabien et Lucie, Amélie et Christina, Shaam, Marie, Lila, Isa. Vous retrouver autour d'un verre ou d'un repas, se raconter les derniers potins et refaire le monde pendant des heures ont toujours été un plaisir et d'un grand réconfort.

Je remercie accessoirement Joe Hisaishi, les Blonde Redhead, Mono, Explosions in the Sky et Mogwai pour leur soutien musical. L'inspiration est parfois venue grâce à eux !

Je remercie mes parents pour leur amour inconditionnel, leur soutien et leurs encouragements, à 1600 comme à 12000km d'ici, et d'avoir toujours pensé à m'apporter du réconfort fourré d'amandes et de miel dans leurs valises pendant leurs visites. C'est grâce à vous que j'en suis là aujourd'hui et je vous en serais toujours reconnaissante. Merci à ma petite sœur, pour tout ce que tu as pu m'apporter et pour tout ce dont tu as pu me soulager à une période cruciale, autant techniquement que téléphoniquement, tu as été parfaite chouchounette ! Merci à mes grands-parents pour leur sourires, leurs encouragements et d'avoir toujours cru en moi. Et merci à ma belle famille pour tous les encouragements et tout le soutien qu'elle m'aura apporté.

Et enfin, merci à toi Benoit, merci d'être ce que tu es. Tu t'es certainement senti un peu dépassé par les états dans lesquels j'ai pu me mettre parfois, mais ce travail est en partie le fruit de ton soutien inconditionnel. T'entendre dire que tu étais fier de moi le soir de ma soutenance a été une fierté pour moi aussi. Je suis heureuse de partager ta vie et, c'est bon, on va pouvoir partir en vacances tranquillement !

Contents

Abbreviation list

Genes

ADE2	Phosphoribosylamino-imidazole-carboxylase
APC/C	Anaphase Promoting Complex/Cyclosome
BIN	Brassinosteroid Insensitive GSK3-like kinase
BRI	Brassinosteroid Insensitive receptor kinase
CCS52	Cell Cycle Switch 52
CDK	Cyclin-Dependent Kinase
CFP	Cyan Fluorescent Protein
CKIIβ	Casein Kinase II beta subunit
CNR	Cell Number Regulator
CorA	Magnesium channel
CYC	Cyclin
CYP450	Cytochrome P450
DEFL	Defensin Like
E2F	Elongation Factor
EGFP	Enhanced Green Fluorescent Protein
EYFP	Enhanced Yellow Fluorescent Protein
FAS	Fasciated locus
FCR	Fungal Cadmium Resistance
FS8.1	"Square" shape locus
FUR4	Uracil permease
FW2.2	Fruit Weight chromosome 2 arm2
FWL	FW2.2 like
GFP	Green Fluorescent Protein
HIS3	Imidazoleglycerol-phosphate dehydratase
IMA	Inhibitor of Meristem Activity
IQ domain	Calmodulin binding domain
KLUH	Cytochrome P450 / Fruit size locus
KRP	Kip-Related Protein
LC	Locule number locus
MCA	Mid-1 Complementing Activity
MIF	Mitosis Inducing Factor
PCR	Plant Cadmium Resistance
PLAC8	Placenta-specific 8
RBR	Retinoblastoma-Related
SF	FW2.2 small fruit allele
SMR	Siamese-Related
SUC	Invertase
UPS	Ubiquitin Proteasome System
WUS	Wuschel
YCF	Yeast Cadmium Factor
YFP	Yellow Fluorescent Protein

Nucleic acids

35S	Cauliflower mosaic virus 35S promoter
ATP	Adenosine 5' triphosphate
BAC	Bacterial artificial chromosome
cDNA	Complementary desoxyribonucleic acid
DNA	Desoxyribonucleic acid
dNTP	Desoxyribonucleotide 5' triphosphate
mRNA	messenger RNA
PCR	Polymerase chain reaction
RNA	Ribonucleic acid
RNA-seq	RNA sequencing
RT-PCR	Real time-polymerase chain reaction
SNP	Single nucleotide polymorphism
UTR	Untranslated regions
WGS	Whole genome sequencing

Units

°C	Celsius degree
µA	Microampere
bp	Base pair
cM	CentiMorgan
g	Acceleration
kb	Kilobase
kbp	Kilobase pair
kDa	KiloDalton
mm	Millimeter
mV	Millivolt
s, min, h	second, minute, hour

Others

3-AT	3-amino-1,2,4-triazole
BC	Before Christ
BiFC	Bimolecular Fluorescence complementation
BLAST	Basic Local Alignment Searching Tool
BY2	Bright Yellow 2 cells
Cd	Cadmium
cv	Cultivar
DAA	Days after anthesis
et al.	*et alii*
i.e.	*id est*
ICP-MS	Inductively Coupled Plasma-Mass Spectrometry

ICP-OES	Inductively Coupled Plasma Optical Emission Spectrometry
LB	Lysogeny Broth culture medium
MS	Murashige and Skoog culture medium
MSMO	Modified Murashige and Skoog culture medium
NIL	Nearly isogenic lines
QTL	Quantitative trait locus
w/w, w/v, v/v	weight/weight, weight/volume, volume/volume
Zn	Zinc

Figures list

I. Introduction

Figure 19: Comparison of FW2.2 protein sequence with characterized homologous proteins of plants and PLAC8 proteins from mammals. All the aligned protein sequences share the same PLAC8 domain. Zm: *Zea mays*; Os: *Oryza sativa*; Sl: *Solanum lycopersicum*; At: *Arabidopsis thaliana*; Gm: *Glycin max*; Mm: *Mus musculus*; Rn: *Rattus norvegicus*; Hs: *Homo sapiens*; Bt: *Bos torus.*

Figure 20: Alignment of the 17 FWLs and the FW2.2 protein sequences. The PLAC8 domain is shaded in green.

Figure 21: Gene expression patterns of *SlFW2.2* and its homologues in different plant organs and at different stages of fruit development in the *Solanum pimpinellifolium* cv LA1589. The y axis represent the normalized expression (in RPKM) and the x axis the organs and their stage of development. The FWLs genes have been separated in 4 groups according to their higher plant tissue expression. DAA: days post anthesis; 0 DAA: anthesis stage; 10 DAA1 and 10 DAA2: 10 DAA fruit n°1 and n°2; 33 DAA: ripening fruit; Cotyl: cotyledons; Hypo: hypocotyl; Meri: vegetative meristem; ML: mature leaves; Root: whole root; YFB: young flower buds; YL: young leaves.

Figure 22: Expression of *SlFW2.2* in *Solanum lycopersicum* cv M82, line TA1143 (large fruit allele), in different organs and in different parts of the flower at two different stages of the flower development. It is noticeable that the higher levels of *FW2.2* expression are detected in the vegetative plant parts. YL: young leaves; ML: mature leaves; Root: whole root; 6: 6 millimeters long flower; 9: 9 millimeters long flower; C: carpel; St: stamen; P: petal; Se: sepal.

Figure 23: Exon composition of the *SlFW2.2* homologue genes obtained using FLAGdb++. The genes have been seperated in 4 groups, according to their exon length composition. The Gene IDs indicated are the same than described Table 1.

Figure 24: Evolutionary relationship between the tomato FW2.2 and FWLs protein as a part of a large plant protein family. The proteins do not segregate according to their putative function. Red: proteins from *Solanum lycopersicum*; Blue: proteins from *Arabidopsis thaliana*; Green stars: proteins implied in plant and fruit developmental processes; Yellow stars: proteins implied in transport and/or resistance to heavy metal resistance . At: *Arabidopsis thaliana*; Bd: *Brachypodium distachyon*; Gm: *Glycin max*; Lj: *Lotus japonicus*; Mt: *Medicago truncatula*; Os: *Oryza sativa*; Pta: *Pinus taeda*; Ptr: *Populus trichocarpa*; Rc: *Ricinus communis*; Sl: *Solanum lycopersicum*; Vv: *Vitis vinifera*; Zm: *Zea mays*.

Figure 32: BY2 cells content in total irons (A), manganese (B), phosphorus (C) and zinc (D) in the three BY2 cells lines (indicated with a color code). The cells overexpressing FW2.2 whether fused with the EYFP or the HA tag accumulate higher levels of the 4 elements than the cells overexpressing the GFP protein.The *x* axis indicates the developmental stage (in DAA) and the *y* axis indicates the mineral content in milligrams per 100 grams of dry weight (mg/100g of DW).

Figure 33: Growth test of *Arabidopsis thaliana* overexpressing the *SlFW2.2* gene or the fusion of the *EYFP* gene with the *SlFW2.2* gene. Plants overexpressing the *GFP* gene were used as a negative control. There is no clear difference of growth between the different plants.

Figure 34: Global oocytes depolarization according to an imposed voltage. For the imposed voltages and the global depolarization measurement, the uninjected or injected oocytes were placed in ND96 medium supplemented or not with 1 mM cadmium (Cd) or zinc (Zn). No visible depolarization has been observed on any of the oocytes.The *x* axis indicates the imposed voltage value (in mV) and the *y* axis indicates the global depolarization value (in µA).

Figure 35: (A), *Arabidopsis thaliana* plants presenting a visible size reduction.(B), plant height and (C), silique length of the transformants overexpressing *FW2.2* under the control of the 35S promoter (35S::FW2.2) compared to wild type plants (Col-0). The measurements were performed on 10 wild type plants and 84 transgenic plants coming from 11 independent transformation events. The p-values obtained from the T-test were both <0.0005.

Figure 36: Leaf epidermis cell outline of *Arabidopsis thaliana* plants overexpressing the (A) *GFP* gene (considered as a negative transformation control) or the (B) *FW2.2* gene under the control of the *35S* promoter, observed with a magnification factor of 20. The leaf epidermis cell outlines of the *FW2.2* overexpressor have been obtained from 2 independent plant transformation lines.The transformants leaves display a dramatic cell phenotype with a reduced cell size and an increased stoma density.

Figure 37: Measurement of the cell number (A) and stoma number (B) per mm² in the *Arabidopsis* transformants leaves. The cell number and stoma number per mm² are both clearly increased in the *FW2.2* overexpressors.

Figure 38: Scanning electron micrographs of the adaxial leaf epidermis of wild-type (WT) and *CyclinD3.1* overexpressor (CycD3 OE) in *Arabidopsis* plants (from Dewitte *et al.* 2003).

Figure 39: BY2 cell shape in the control cells (GFP) and the cells overexpressing the *FW2.2* gene. A) Scatterplot showing the width to length relationship in both control (*GFP)* and *FW2.2* overexpressing BY2 cells. B) The typical morphologies of cells after 7-8 days of culture are illustrated.

Figure 40: Scatterplot showing the length and width of both control and auxin deprived cells (from Winicur *et al.* 1998). The *FW2.2* overexpressing cells show higher length values and lower width values compared to the control *GFP* overexpressing cells, which reveals an elongated shape.

Figure 41: Expression of cell cycle control genes in the TA1143 line (large fruit allele – blue bars) and the TA1144 line (small fruit allele – red bars) during the tomato fruit development. The TA1143 anthesis stage and TA1144 20DAA stage have not been treated. The genes expressions have been measured using RT-PCR and show some differences between the two lines. The *x* axis indicates the developmental stage (in DAA) and the *y* axis indicates the relative mRNA abundance.

Figure 42: Comparison of the *SlFW2.2* and *SlKRP4* gene expression in the two NILs during the tomato fruit development.The expression of the *SlKRP4* gene is opposite in the two lines. The *x* axis indicates the developmental stage (in DAA) and the *y* axis indicates the relative mRNA abundance.

Figure 43: Endoreduplication index in the fruit pericarp of the two lines TA1143 (large fruit allele) and TA1144 (small fruited line). The endoreplication index is a little bit higher in the large fruit at the beginning of the fruit development but then becomes higher in the small fruits after 5 DAA.

Figure 44: Interaction test between the FW2.2 protein and the FWL protein using the Split-Ubiquitin technique. The yeast cells have been plated on a SD-LTHA medium supplemented with 50mM 3-aminotriazole to test the interaction strength and grown during 3 days. The pfur4 protein is an ER resident membrane protein that serves as a negative control (when fused to the modified N-terminal part of the ubiquitin (NubG) it cannot interact with the C-terminal part of the ubiquitin (Cub)) and as a positive control when fused to the wild-type N-terminal part of the ubiquitin (NubI). Three colonies of each transformation tests have been picked up on the double transformants selection medium (SD-LT) and dropped on the interaction selection medium (SD-LTHA) after having their OD_{590nm} harmonized and being diluted 100 (10^{-2}), 1000 (10^{-3}) and 10000 (10^{-4}) times to be then grown during 3 days. All the FWLs proteins tested seem to interact with FW2.2.

IV. Discussion and perspectives

Tables list

Introduction

I. Introduction

The fruit is a specialized organ specific to the Angiosperms, the flowering plants, which are the most advanced form of the plant kingdom. In Angiosperms, the ovules (female gametes) are enclosed in an ovary, unlike the Gymnosperms (with naked ovules). Following pollination and fertilization, the ovary develops into the fruit, which has evolved as a suitable environment for seed maturation and seed dispersal mechanisms.

Fleshy fruits include important crops such as grape, apple, citrus, peach, strawberry, melon and tomato that represent a major source of vitamins, fibers, carbohydrates, and phytonutrient compounds essential for human nutrition. Fleshy fruits are subjected to permanent selection and breeding programmes mainly focused towards the improvement of fruit production: enhancing yield, optimizing cultural practices, coping with pests and pathogens through the selection of resistant cultivars. Besides fruit production, efforts are made at increasing the fruit storage period to answer the distributors' demand for longer shelf-life thus making compatible market places and distant production areas. In recent years, breeders have worked at satisfying consumers' demands for new varieties with enhanced organoleptic qualities.

Two processes are highly specific to fleshy fruits: (i) the large accumulation of water and solutes (sugars, organic acids, secondary metabolites), which gives the fleshy characteristics to the fruit and contributes to organoleptic quality traits, and (ii) the ripening phase during which traits underlying the sensory quality of the fruit are acquired (colour, texture, flavour, aroma). Until recently, studies on fleshy fruit species were mostly focused on developmental studies mostly devoted to ovary formation, fruit set and fruit maturation. However, despite their nutritional and economic importance, essential fruit quality traits such as morphological traits (size, weight and shape) (Tanksley 2004), conservation (the relation between cell number, cell size and wall composition) (Coombe 1976) and the organoleptic and nutritional traits of ripe fruit are determined well before ripening, during the early development of fleshy fruit species. This results from a complex interplay between developmental processes such as cell division, cell expansion, cell differentiation (Gillaspy et al. 1993) and the establishment of the composition in primary and secondary metabolites (Carrari et al. 2006).

In the context of improvement of quality traits of plant products, tomato fruit is an excellent model for a fundamental and applied perspective, to investigate the developmental mechanisms controlling fruit size and fruit quality. It is thus critical to identify the cellular and molecular determinants involved in the complex interplay between the establishment of cell size and final fruit size through the cell expansion process, and the high metabolic activity occurring inside expanding cells within the fruit.

A. Tomato as a model for fruit development

The Solanaceae are an economically important family of flowering plants. This family comprises a large variety of important agricultural crops, medicinal plants, spices, weeds, and ornamentals, such as the tuber-bearing potato, a number of fruit-bearing vegetables (*e.g*. eggplant and pepper) and ornamental flowers (petunias, *Nicotiana*). Tomato (*Solanum lycopersicum* Mill.) belongs to the *Solanaceae* family and is the second most cultivated plant in the world, which allows the production of more than 100 million tons of tomato fruits per year. This represents the first ranking in world fruit production and represents the main income for major vegetable seed companies. In addition, the organization of genomes within the *Solanaceae* presents an exceptionally high degree of conservation, thus rendering this a unique subject to explore the basis of phenotypic diversity and adaptation to natural and agricultural environments.

Tomato displays a highly favourable biology with short life cycle, high multiplication rate, easy crosses and self-pollination. The wide range of genetic resources covered by the large morphological diversity encountered in cultivated tomato varieties has been exploited, together with the development of genomic tools over the last 15 years, to unveil the genetic basis of fruit size and shape determination.

B. Tomato fruit growth

The early fruit development in tomato can be divided into three distinct phases (Gillaspy et al. 1993). During the first phase, the ovary develops and "takes" the decision to set fruit upon pollination and fertilization. Then the ovary walls enlarge through an intense activity of cell divisions in the second phase. Thereafter fruit growth corresponding to the third phase is mainly sustained by cell expansion leading to a fruit which exhibits its almost final size and is able to ripen. At the end of the cell expansion phase, individual cells in the fleshy part (mesocarp tissue) of the fruit can reach spectacular levels in volume: more than a 30,000-fold increase from initial cell volume, sometimes corresponding to >0.5 mm in diameter (Cheniclet et al. 2005). Of importance, this spectacular cell hypertrophy is closely correlated with an increase in nuclear DNA ploidy levels due to endoreduplication. Indeed high levels of endopolyploidy occur in the course of fruit development within the mesocarp and the jelly-like tissue embedding the seeds (Bergervoet et al. 1996; Joubès et al. 1999; Cheniclet et al. 2005; Bertin et al. 2007). The typical ploidy levels encountered in tomato fruit can reach up to 512C (where C is the haploid DNA content), unmatched values by other species such as Arabidopsis, maize or Medicago, classical model plants in which endoreduplication was studied (Melaragno et al. 1993; Vilhar et al. 2002; Kondorosi et al. 2005). The large variation in fruit weight correlates with the mean ploidy level achieved in pericarp cells which itself correlates with the mean cell size, thus highlighting the contribution of cell size to final fruit weight and the putative role of endoreduplication in driving fruit growth (Chevalier et al. 2011). Endoreduplication is such an important process during tomato fruit development that modifying the expression of genes involved in the regulation of the cell cycle and commitment into endoreduplication affects fruit growth and thus alters fruit size (Chevalier et al. 2011).

C. The cell cycle control

Plant yield and organ size depend upon plant growth and development which involve fundamental cellular processes such as cell division and cell expansion in close interaction with genotype and environmental cues (Beemster *et al.*, 2003). The cell division activity provides the building blocks, setting the number of cells that will compose an organism whereas the cell expansion activity then determines its final size. Therefore the control of the onset and exit of the cell cycle which leads to cell divisions is a crucial matter to understand plant and organ development.

Cell division or mitosis is the ultimate step in the cell cycle that leads to the transmission of the genetic information from one mother cell to two daughter cells. The mitotic cycle in eukaryotic cells is composed of four distinct phases: an undifferentiated DNA pre-synthetic phase with a 2C nuclear DNA content, termed the G1 phase; the S phase during which DNA is synthesised, with a nuclear DNA content intermediate between 2C and 4C; a second undifferentiated phase (DNA post-synthetic phase) with a 4C nuclear DNA content, termed the G2 phase; and the ultimate M phase or mitosis. The classical cell cycle thus involves the accurate duplication of the chromosomal DNA stock during the S-phase and its subsequent equal segregation in the nascent daughter cells following cytokinesis at the end of the M phase.

The progression within the cell cycle is regulated by a class of conserved heterodimeric protein complexes consisting in a catalytic subunit referred to as Cyclin-Dependent Kinase (CDK) and a regulatory cyclin (CYC) subunit whose association determines the activity of the complex, its stability, its localization and substrate specificity (Inzé and De Veylder 2006). The CDK/CYC complexes operates at the boundaries between the G1 and S phases, and between the G2 and M phases, to phosphorylate target proteins whose inhibitory or activatory posttranslational modifications are essential for passing these cell cycle checkpoints (Figure 1). The progression along the various cell cycle phases and at the phase transitions are regulated by specific CDK/CYC complexes. The commitment to the S phase is dependent upon CDKA/CYCD complex activities which phosphorylate the RETINOBLASTOMA-RELATED 1 (RBR1) protein (Guttierrez et al. 2002). The hyperphosphorylation of RBR1 leads to the release of sequestered E2F transcription factors

required to drive the expression of S phase genes. Then CDK/CYCA complexes control the progression through the S-phase and the commitment to mitosis whose proper completion depends on CDKA/CYCB complex activities. The kinase activity of the complexes is not only dependent on the presence of a regulatory CYC subunit, but is also finely tuned by the phosphorylation/dephosphorylation status of the catalytic (kinase) subunit itself.

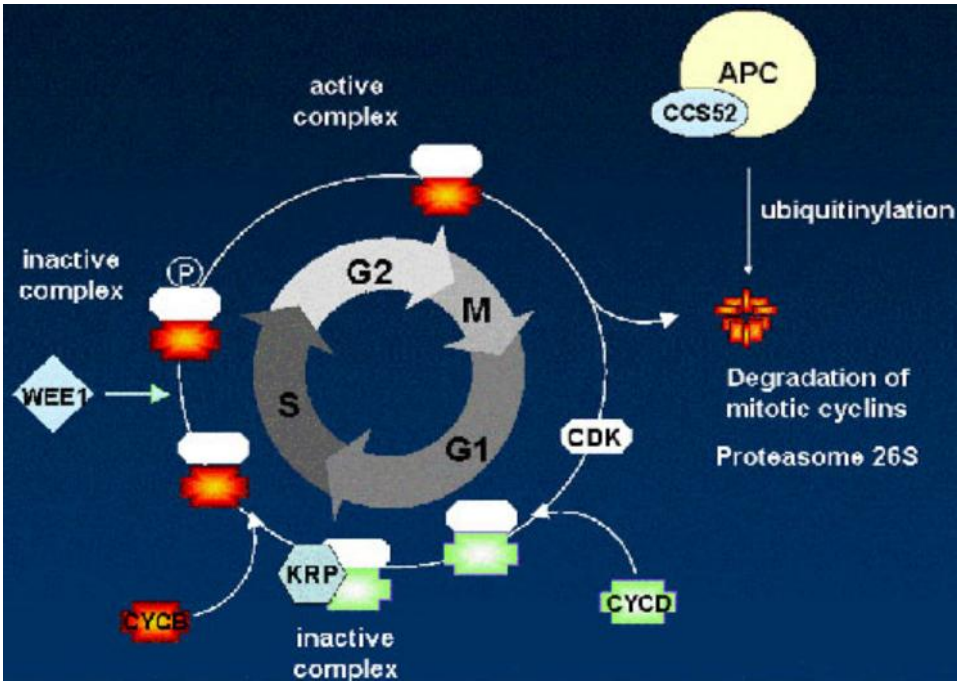

Figure 1: Cell cycle control and regulation of CDK-cyclin complex activities

The loss of CDK/CYC complex activity is then required to exit from mitosis. This occurs upon the proteolytic destruction of the cyclin moiety via the ubiquitin proteasome system (UPS), involving a specific E3-type ubiquitin ligase named the Anaphase-Promoting Complex/Cyclosome (APC/C) which is activated through its association with the CCS52 protein (Heyman and De Veylder, 2012). Additionally the CDK/CYC complexes are inactivated by the specific binding of CDK inhibitors of the Kip-Related Protein- (KRP) (Torres Acosta et al., 2011) and SIAMESE-Related- (SMR) type (Churchmann et al., 2006). The CDK inhibitors are also subject to specific degradation mechanisms involving UPS (Marrocco et al., 2010).

As part of developmental programs or in response to environmental constraints, cells are able to modify the typical cell cycle into the endoreduplication cycle or endocycle where mitosis is lacking (Joubès and Chevalier, 2000; Edgar and Orr-Weaver, 2001; De Veylder *et*

al., 2011). As already mentioned, endoreduplication is largely associated to cell differenciation / cell expansion during tomato fruit growth. During endoreduplication, successive rounds of DNA duplication occur in iterative S phases separated by an undifferentiated G phase, leading to the production of polytenic chromosomes with multivalent (2, 4, 8, 16...) chromatids without any change in chromosome number (Bourdon et al. 2012). As a consequence high nuclear DNA contents/ploidy levels can be reached, thus impacting the morphology of both nucleus and cell (Bourdon et al. 2012).

As recently reviewed by De Veylder et al. (2011), the proper unfolding of the cell cycle and the commitment to endoreduplication are a matter of CDK/CYC activity levels. The progression through the G2-M transition requires the activity of a Mitosis Inducing Factor (MIF) above a certain threshold. The absence or reduced activity of this MIF is sufficient to drive cells into the endoreduplication cycle (Inzé and De Veylder, 2006). *In planta* functional analyses identified the M-specific CDKB1;1 as the likely candidate kinase to be part of MIF when bound to the A-type cyclin CYCA2;3, able to inhibit endoreduplication when fully active (Boudolf et al. 2009). The stability of the regulatory CYCA2;3 is the key process in the regulation of CDKB1;1 activity, since the selective degradation of CYCA2;3 achieved by the CCS52A-mediated activation of APC provokes the commitment to endoreduplication by reducing or suppressing the MIF activity.

D. Domestication of tomato

Wild progenitors of tomatoes are herbaceous green plants with small round-shape green fruits growing in the Andes. By 500 BC, the first domesticated variety of tomato, a little yellow fruit, similar in size to a cherry tomato, was already grown by the Aztecs in southern Mexico and probably other areas. This domesticated variety was already bearing larger fruits than the wild ancestors.

The origin of its spreading throughout the world is unclear, but Spanish Hernán Cortés and Genoese Christopher Columbus may have been the first to transfer the small yellow tomato to Europe in the 16th century. After the Spanish colonization of South America, they

distributed the tomato throughout their colonies in the Caribbean and the Philippines, from where it spread to the entire Asian continent.

Human domestication and selection has clearly provoked changes in the morphology, the physiology and the environmental adaptation (Figure 2). For example, the presumed wild ancestor of the modern tomato, the *Solanum lycopersicum* cv Cerasiforme, produces two-loculed fruits weighing only few grams, whereas some varieties of the modern cultivated tomato plants are able to produce fruits that contain many locules and can reach about 1000 grams.

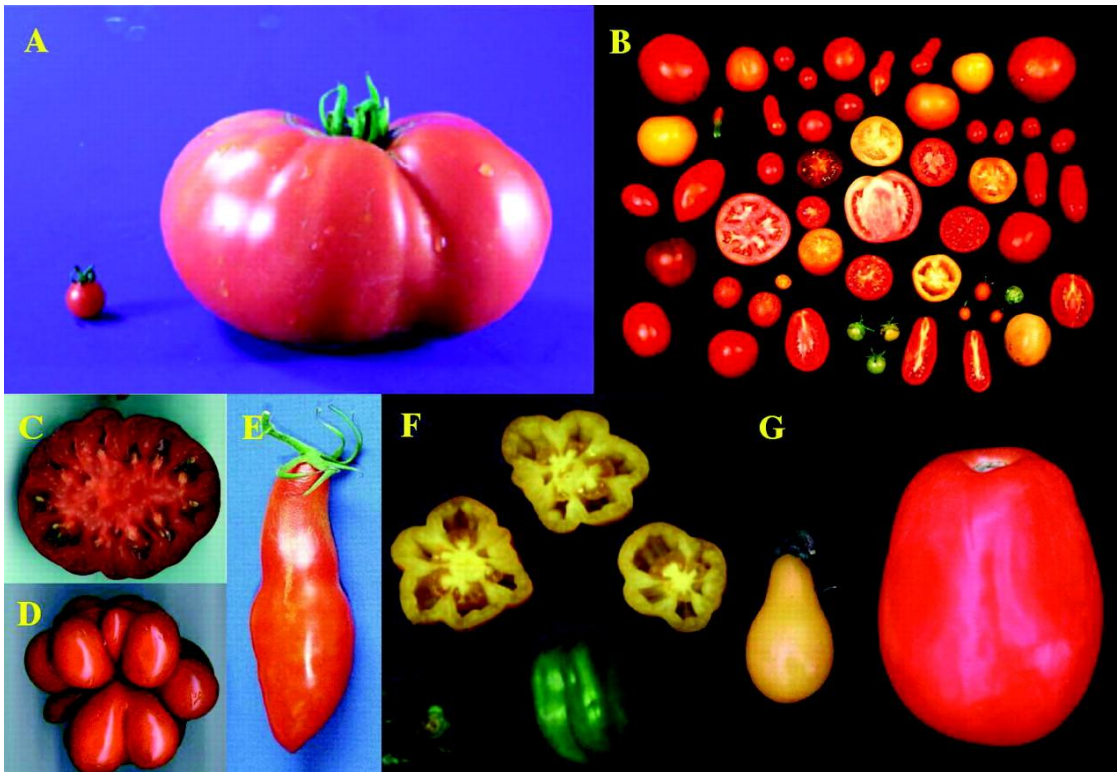

Figure 2: Modern tomatoes highly vary from their wild relatives by their size and shape (from Tanksley, 2004).

E. QTLs influencing fruit mass

Traits that differentiate modern crops from their related wild species are due to quantitative trait loci (QTLs). For instance in tomato, a quantitative trait mapping study, in which a cross between domesticated tomato *Solanum lycopersicum* and its wild relative

Solanum cheesmanii have been performed, highlighted that fruit size is influenced by a relatively small number of genes (a total of 11 QTLs) (Paterson *et al.* 1991). Another cross between *Solanum pimpinellifolium* and *Solanum lycopersicum* revealed that 67% of the phenotypic variation in fruit size can be linked to only six loci (Lippman and Tanksley, 2001). What is also noticeable in these studies is that all the wild species alleles are related to a reduction in size.

These QTLs influence fruit weight by directly controlling the size, or changing the shape and/or the structural organization of the fruit.

These fruit weight QTLs explain 4.7 to 42% of the phenotypic variance observed and a major QTL common to both green and red fruited species located on the arm 2 of the chromosome 2 can explain 30% of the fruit size variation (Alpert *et al.* 1996).

1- QTLs influencing fruit shape

Three major loci are known to modulate fruit shape.

The first to be isolated is the *OVATE*locus that is responsible of a pear-shaped, elongated tomato fruit shape (Ku *et al.* 1999). This *OVATE* locus corresponds to a gene that encodes a putative nuclear protein whose function is unknown, expressed from the floral stage until the second week after anthesis. The elongated shape is associated with domestication and is due to a loss of function mutation in the *OVATE*coding sequence: the domesticated allele presents a mutation in its second exon which results in the appearance of a premature stop codon (Liu *et al.* 2002).

The second locus that influences fruit shape is the *SUN* locus. It has been discovered during studies focusing on the *OVATE*locus where fruits displaying an elongated shape did not harbour the mutation on *OVATE*(Van der Knapp and Tanksley 2001). This locus differs from the *OVATE*locus by the way it controls shape: *SUN*induces a uniform elongation of the tomato fruit (Van der Knapp *et al.* 2002). The *SUN*inducing effect has been shown to be due to the locus duplication in the elongated fruit genome. This duplication is due to transposon insertion that provokes an increase in the IQD12 gene expression (coding for a IQ67 domain containing protein – the IQ domain is known to be involved in calmodulin binding (Bürstenbinder *et al.* 2013)) in the flower after pollination and in the fruit while the expression of the *DEFL1* (a putative secreted defensin – usually expressed in *Solanum pimpinellifolium*, the wild ancestor), is not detectable (Xiao *et al.* 2008). It has been shown

that *SUN* influences the fruit size by repressing the cell division in the transversal direction and promoting the cell divisions in the longitudinal direction (Wu *et al.* 2011).

The *FS8.1* locus is responsible of the "square" shape of tomato fruit: longer round and slightly elongated. The effect of the *FS8.1* gene is noticeable at the flower stage: the carpel has already the elongated and blocky shape. The gene appears to act only during the floral and carpel development and has almost no activity during the fruit development (Ku *et al.* 2000).

2- QTLs controlling the structural organization of the fruit

Many wild species and cultivated varieties present flowers with two to four carpels that develop into locules after the pollination. However some domesticated species produce very large fruits with a very high number of locules, the most popular being the tomato "Coeur de boeuf" variety. This modification of the locule number is also associated with an increased fruit weight. Two loci are responsible for this locule multiplication: the *FASCIATED*and *LOCULE NUMBER*loci.

These two loci drive the same increasing effect on locule number through the increase in the carpel number, suggesting that their effect starts during flower initiation. The *fasciated* mutation has a more drastic effect on the locule number increase than the *locule number* locus.

*FASCIATED*influences the size of the floral meristem 12 days before the flower initiation, as well as the number of floral organs (Barrero *et al.* 2006). The *fasciated* mutation is recessive, suggesting that the difference between the wild and domesticated allele are likely due to a loss-of-function mutation. The function of the protein remains unknown.

The *LOCULE NUMBER*locus was not that much characterized. However it was shown that the difference of effect between the wild and domesticated allele was controlled by two single nucleotide polymorphisms located in a non-coding sequence located 1000 bp downstream of the *WUSCHEL* stop codon (Muños *et al.* 2011), suggesting that this locus may have a regulatory function.

These two QTLs act epistatically as the larger fruits are produced when the two mutations can be detected.

3- QTLs controlling fruit size

Five loci have been identified as QTLs that influence the fruit size: *fw1.1*, *fw2.2*, *fw3.1*, *fw3.2* and *fw4.1* (Grandillo *et al.* 1999). Unlikely to *FASCIATED*and *LOCULE NUMBER*loci, they impact the fruit mass without changing the shape and structural organization of the fruit.

The *fw3.2* QTL is the second major fruit size QTL has been studied and showed that it consists in a single nucleotide polymorphism (SNP) that influences the expression of the *KLUH/cytochrome P450* (*CYP450*) gene. An increased fruit size has been correlated with an increased expression of this gene in both reproductive and vegetative organs (Chakrabarti *et al.* 2013).

Historically fw2.2, the major fruit size QTL, was the first to be cloned and subject of a partial characterization.

F. Isolation of *FW2.2*

1- Localization of the *fw2.2* QTL

A first cross between the wild species *Solanum pimpinellifolium* (LA1589) and the domesticated species *Solanum lycopersicum* cv M82-1-7, used as the male parent, followed by a backcross with the *Solanum lycopersicum* cv E6203, as the female parent, (Alpert *et al.* 1995) have been performed to evaluate the fruit weight trait in the descendants. This population has been named the *Pimpinellifolium* population. A second backcross between the *Solanum pennellii* introgression line containing the distal portion of the chromosome 2, generated by Eshed and Zamir (1995), and *Solanum lycopersicum* cv M82-1-8 was used similarly to evaluate this trait. This population has been named the *Pennellii* population.

Restriction fragment length polymorphism (RFLP) analyses were made on the genomic DNA of the two obtained populations in order to observe the marker segregation on the chromosome 2, which agreed with the high-density linkage map previously published (Tanksley *et al.* 1992). Fruit weight analysis of the *Pimpinellifolium* and the *Pennellii* populations showed a significant association with two markers, the TG167 and TG91 which allowed localize a major fruit size QTL on the distal portion of the chromosome 2, between these two markers (Alpert *et al.* 1995 and 1996) (Figure 3).

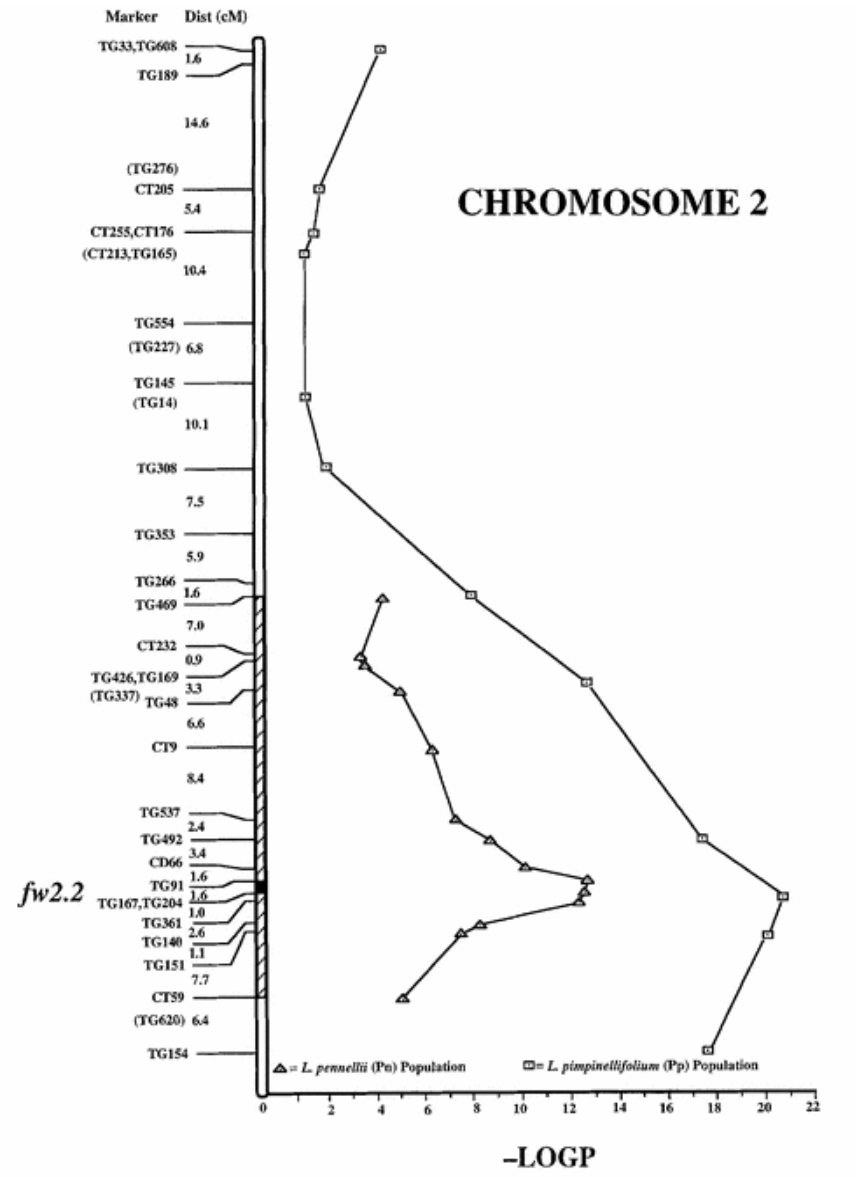

Figure 3: Position of *fw2.2* QTL on the chromosome 2, mapped using *Pennellii* and *Pimpinellifolium* populations (from Alpert *et al.* 1995).

A high resolution mapping then allowed the fine positioning of the *fw2.2* QTL within a 150 kbp interval region (Alpert *et al.* 1996).

2- *fw2.2* in the *Solanum* genus

The *Solanum* genus includes various wild species related to *Solanum lycopersicum*. The wild relatives are known to be small-fruited and considered as the ancestral relatives (Rick, 1976), whereas the domesticated species bear large fruits. This suggested that the wild and domesticated *Solanum* species differ by their *fw2.2* allele (Alpert *et al.* 1995). A comparison of sequences between the *Solanum lycopersicum* cv M82 and the *Solanum pennelliifw2.2* allelesrevealed that they do not differ in their coding sequence; however they present nucleotide polymorphisms in their 5' and 3' untranslated regions (UTR) (Frary *et al.* 2000). A comparative sequencing of the nine *Solanum* species revealed that all the wild small-fruited relatives bear the same allele, from which the *Solanum lycopersicum* "domesticated" large fruit allele of *fw2.2* seems to derive with the accumulation of macromutations in the non-coding sequences (Nesbitt *et al.* 2002) (Figure 4).

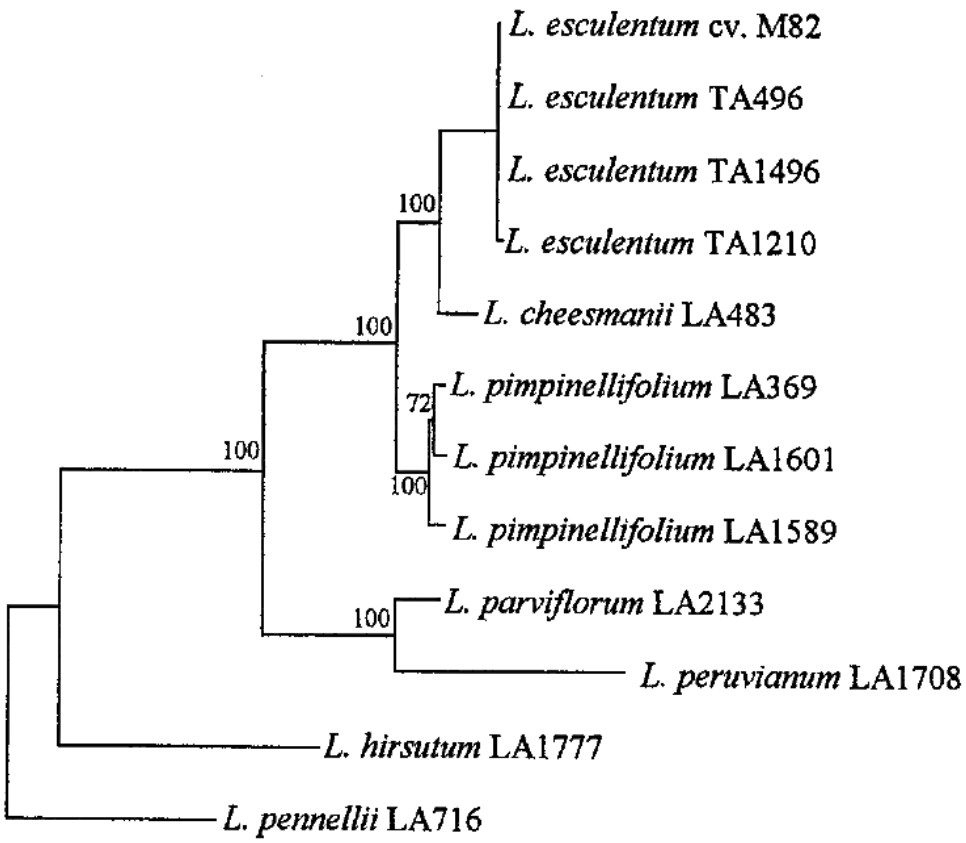

Figure 4: Phylogenic tree from combined sequences of *Solanum* species, comparing the *fw2.2* coding sequence 5'UTR sequence, among others (from Nesbitt *et al.* 2002).

These macromutations accumulation are likely to be the origin of changes in fruit size and domestication of tomato.

G. Allelic effect

1- Allelic expression

As the two alleles only differ with their 5'UTR sequences, the difference between large and small fruit cannot be attributed to any functional differences in the FW2.2 protein itself (Nesbitt *et al*. 2002). From this observation, a differential pattern of expression for the two alleles of *fw2.2* could be considered.

The expression of the two alleles have been measured (Cong *et al.* 2002) in the pericarp of the two NILs previously described, in order to determine if the *fw2.2* alleles are differing in their expression timing (Figure 5). It appears that the two alleles display expression patterns that differ during the fruit development in the two lines.

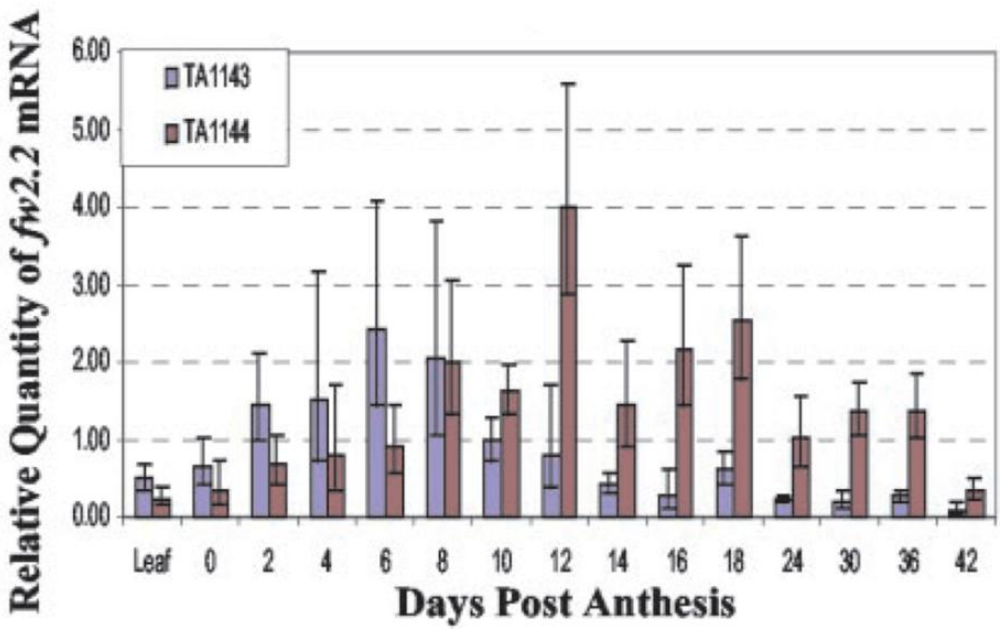

Figure 5: Accumulation of *fw2.2* transcripts during tomato fruit development in the TA1143 and TA1144 nearly isogenic lines (from Cong *et al.* 2002).

The alleles are characterized by time-shifted expressions: the large fruit allele (TA1143 line) presents an early fruit expression that peaks around 8th days after pollination (DAP) and then decreases slowly, whereas the expression level for the small fruit allele (TA1144 line) is increasing gradually from the beginning of the fruit development to reach its maximal expression around the 14 DAP.

What is also noticeable is the difference of expression of *fw2.2* at the anthesis (0) stage. The TA1143 line presents a higher expression than the TA1144 line, suggesting that the action of *fw2.2* starts earlier to control fruit growth.

The difference in the 5'UTR seems to be the cause of the shifted expression between the two alleles.

Such a dramatic phenotypic change in crop plants due to a change in the regulatory regions has also been described for maize. The *teosinte branched 1* gene controls the number of inflorescences, the sex determination and regulates the number and length of axillary branches by controlling the apical dominance (Doebley *et al.* 1997). This gene is directly involved in maize domestication and has been shown to present important nucleotide polymorphisms in the regulatory regions and no change in the coding sequence which results in an increased expression in the domesticated form of maize (Wang *et al.* 1999).

The expression of *fw2.2* seems to be mainly localized in the fruit, but can also be detected in roots, hypocotyl, young leaves and flower buds (Figure 6).

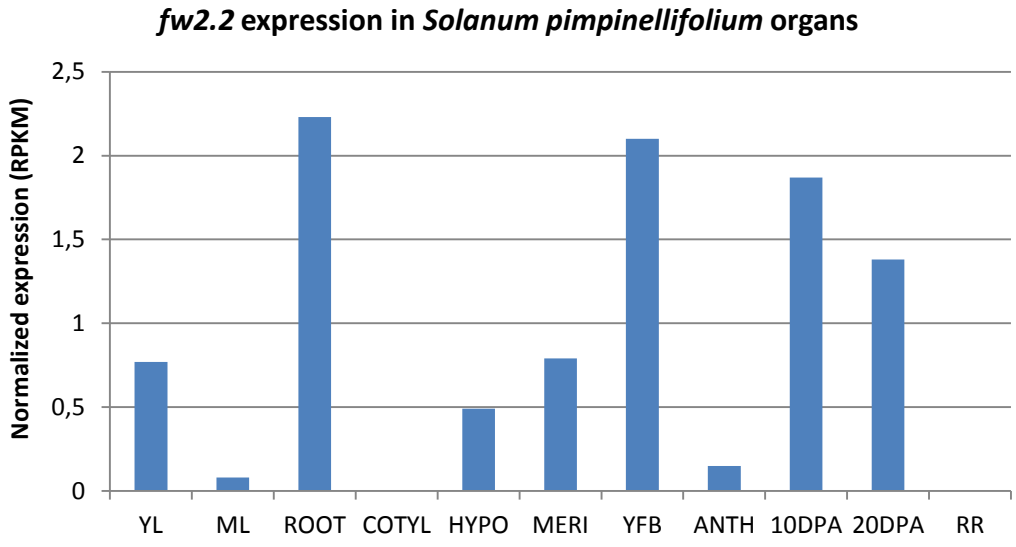

Figure 6: Expression of *fw2.2* in different organs of *Solanum pimpinellifolium* cv. LA1589. The expressions have been determined using Illumina RNA-seq (Huang *et al.* 2013; datas available on http://ted.bti.cornell.edu/cgi-bin/TFGD/digital/home.cgi and http://www.ncbi.nlm.nih.gov/sra/ with the SRA061767 accession number). YL: young leaves, ML: mature leaves, ROOT: whole roots; COTYL: cotyledons; HYPO: hypocotyls; MERI: vegetative meristems; YFP: young flower buds; ANTH: anthesis flowers; 10, 20DAA: fruits at 10 or 20 DAA; RR: red ripe fruits.

The detection of a relatively high expression of *fw2.2* in the young flower buds suggests that the protein is already acting during flower initiation, when floral organs develop, and may regulate their size at this early stage. These expression results confirm that the role of *fw2.2* may not be restricted to the fruit development but also may influence the whole plant development.

In situ hybridizations have been performed on cross sections of the pericarp and the placenta of the two TA1143 and TA1144 lines, at 6 DAA and 12 DAA (Cong *et al.* 2002). This experiment revealed that the transcripts were differentially localized during the fruit development. At 6 DAA, the transcripts were localized in the inner pericarp for the TA1143 line whereas they were localized around the vascular bundle regions of the TA1144 line. At 12 DAA, no signal is detectable in the pericarp of the TA1143 line but present in the TA1144 line. However, at these two stages of development, a strong signal is detectable in the placenta of the two lines, suggesting that the expression of *fw2.2* can be higher in these tissues. These observations suggest that *fw2.*2 can have, in addition to a time shifted expression, a spatial expression.

2- Allele influence on plant development

Nearly isogenic lines (NILs), generated with a cross between *Solanum pennellii* and *Solanum lycopersicum* cv M82-1-8 (Alpert *et al.* 1995; Eshed and Zamir 1994), only differing at the 0.8 cM *fw2.2* locus have been studied and revealed that *fw2.2* allele not only affect fruit size, but also the plant development (Figure 7).

The plants bearing the small fruit allele (TA1144 line) display an increased number of inflorescences and flowers compared to that bearing the large fruit allele (TA1143 line) (Nesbitt *et al.* 2001). The flowers from the big fruited line also show an increased ovary size. This difference is not due to increased sink strength, as a flower removal experiment does not allow the fruit size difference recovery between the two lines, but increased the gap.

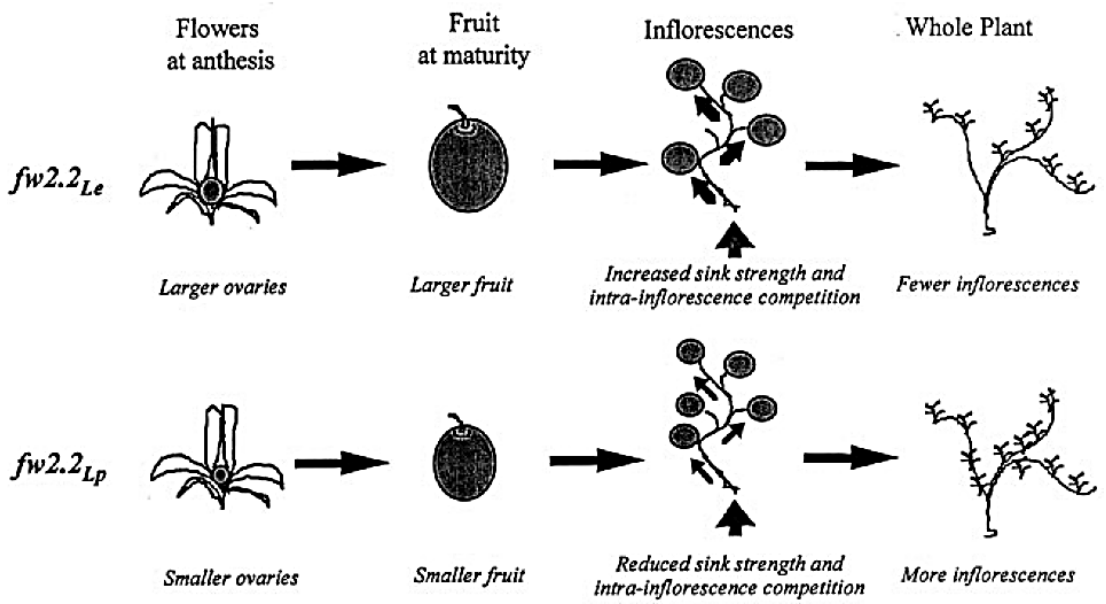

Figure 7: Effect of *fw2.2* allele on plant development. Plants carrying the large fruit allele ($fw2.2_{Le}$) are represented on the upper part of the figure and the plants carrying the small fruit allele ($fw2.2_{Lp}$) are represented on the bottom part (from Nesbitt *et al.* 2001). Plants carrying the large fruit allele display larger fruits, flowers with larger ovaries, less fruits per truss and less trusses than the plants carrying the small fruit allele.

Altogether this information suggests that the role of FW2.2 is not only limited to the fruit development but also acts in processes implied in whole plant physiology. The work of Baldet (2006) proposed that FW2.2 may be implied in the relation between sugar supply and cell proliferation in the ovary.

3- Allele influence on fruit size

The small fruit allele is partially dominant on the large fruit allele (Alpert *et al* 1995). It was actually shown that a transformation of tomato with a DNA fragment, isolated from a cosmid library of *Solanum pennellii* genomic DNA, harboring the sequences of the promoter and the gene of the small fruit allele of *fw2.2*, provoked a significant fruit size reduction in transgenics with the large fruit allele genetic background (Frary *et al.* 2000) (Table 1).

Table 1: Effect of *fw2.2* small fruit allele on the Mogeor cultivar fruits. The cosmid 50 holds the *fw2.2* small fruit allele, whereas the cosmids 62, 69 and 84 hold cDNAs isolated with a cDNA library screen. Only plants transformed with the cosmid 50 containing the small fruit allele of *fw2.2* have fruits with a reduced size (from Frary *et al.* 2000).

Cosmid	Cultivar	Average fruit weight (g)		*P* value
		+Transgene	−Transgene	
50*	TA496	41.6 (18)	56.4 (7)	<0.0001
50*	TA496	47.7 (23)	68.1 (12)	<0.0001
50	Mogeor	25.4 (21)	40.9 (7)	<0.0001
62	Mogeor	46.5 (18)	48.0 (9)	0.70
62	TA496	51.0 (21)	51.3 (3)	0.94
69	Mogeor	50.0 (14)	51.7 (10)	0.58
84	Mogeor	49.4 (18)	47.9 (5)	0.71

Another study showed that the relative *fw2.2* transcript level highly influences fruit size (Liu *et al.* 2003). Gene dosage series on a panel of plants displaying 1, 2, 3 or 4 copies of the small fruit allele showed that the fruit size and mass correlates highly and negatively with *fw2.2* transcripts level at 9 DAA (state with the higher accumulation of *fw2.2* transcripts) respectively (Figure 8). This correlation is also observed for the placenta size.

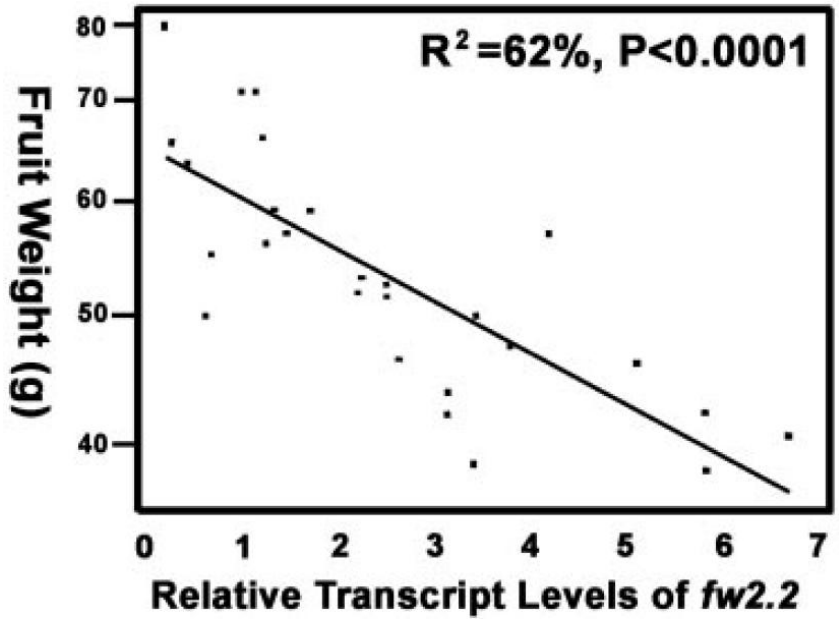

Figure 8: Relationship between *fw2.2* transcript level at 9DAA and final fruit weight (from Liu *et al.* 2003). The higher is the expression of *FW2.2* at 9DAA, the smaller the fruits is at its final developmental stage.

As a higher *fw2.2* expression level leads to a smaller fruit size, we can easily imagine that its role is implied in mitosis control, and more precisely in mitosis inhibition. This hypothesis has been first put forward by Cong et al. (2002).

4- Influence on fruit development

Interestingly, where a study showed that a change in the fruit size is correlated with a change in the cell number and the cell expansion (Gillaspy *et al.* 1993), several studies emphasized interesting points about the *fw2.2*-induced fruit size variation.

The first focused on the cell size in tomato flower carpels. Frary et al. (2000) showed that there is no difference in the cell size between the carpels of the two NILs despite a clear carpel size and weight difference, which means that the carpel of the large-fruited lines have a higher number of cells than the carpels of the small-fruited lines. In addition, a semi-quantitative RT-PCR experiment showed that the expression of *fw2.2* was significantly higher in the carpels of the TA1144 line at the 3-5mm flower bud stage, than in the carpels of the TA1143 line. This means that the control of the final fruit size begins at earlier stages, during the setting up of all floral organs.

The second focused on the cell size in fruit pericarps of the two NILs. Cong et al. (2002) showed that the two lines do not present any difference in cell size in their pericarp (Figure 9). The *fw2.2*-induced fruit size variation is clearly not due to a cell size difference.

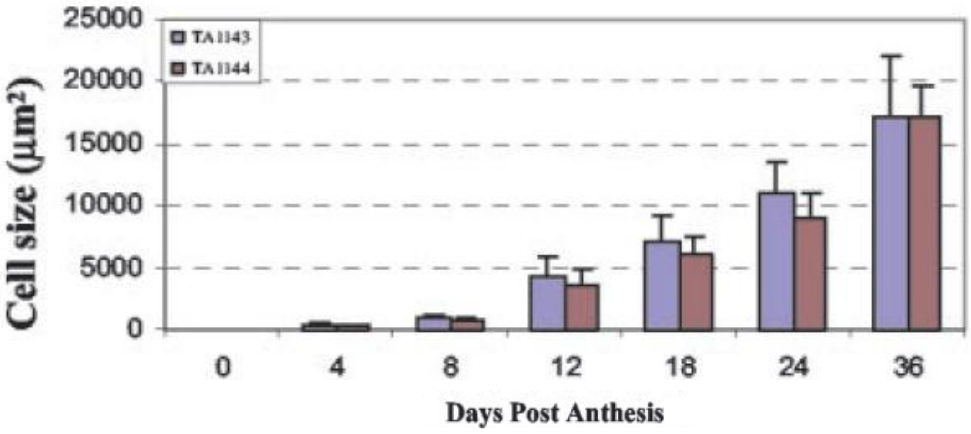

Figure 9: Evolution of the pericarp cell size in the two NILs during fruit development in the two NILs (from Cong *et al.* 2002). The pericarp cell size measurements do not highlight a significant size difference between the two lines.

The third observation came from the same work and showed that the number of cell layers in the pericarp and consequently the pericarp thickness were the same between the two NILs (Figure 10).

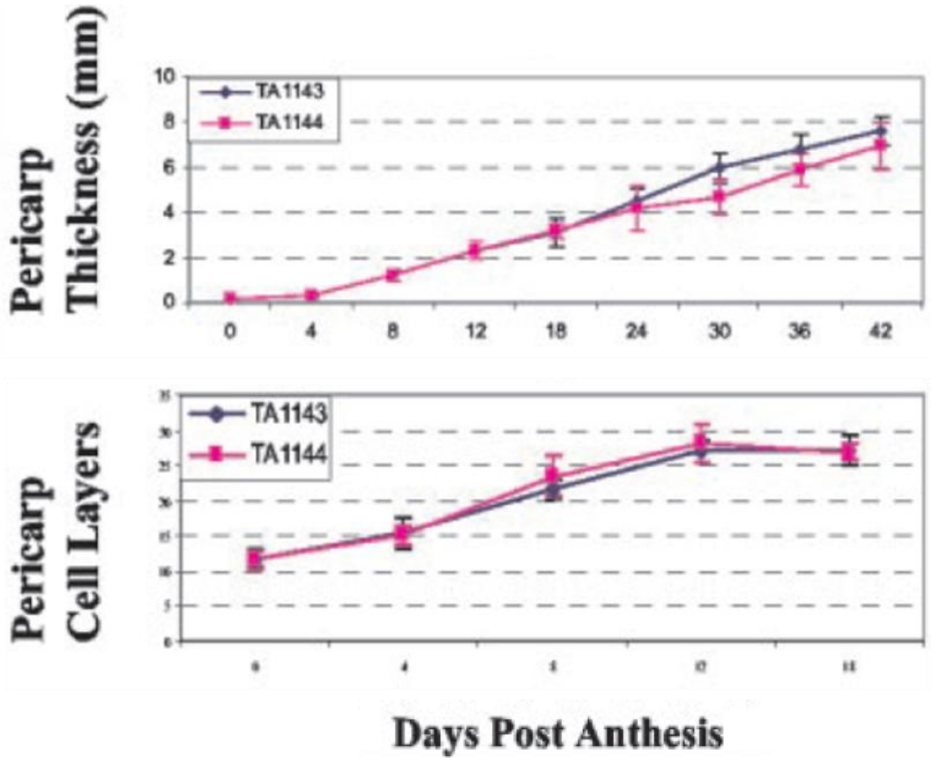

Figure 10: Evolution of the pericarp thickness and number of cell layers in the pericarp during tomato fruit development in the two NILs (from Cong *et al.* 2002). The pericarp thickness and number of cell layers measurements do not highlight a significant difference between the two lines.

As the placenta size is negatively correlated to the *fw2.2* expression level and the *fw2.*2-induced fruit size variation is not due to an increased cell size or a pericarp thickening due to an increased number of cell layers, this means that *fw2.2* may control the cell division activity occurring in the whole pericarp and placenta, in a two and three dimensional way, respectively.

The last observation highlighted the fact that the mitotic index, which measures the rate of dividing cells within a tissue, is varying between the two NILs during tomato fruit development (Figure 11). It is indeed higher in the small fruited line at the beginning of the fruit development and then decreases quickly from 4 DAP to be almost equal to zero around 18 DAP. Hence a near arrest in mitotic activity is observed in the pericarp and the placenta. Concerning the large fruited line, the mitotic index is slightly lower at the beginning of the

fruit development but the mitotic activity is clearly maintained during a longer time in both pericarp and placenta, which certainly leads to larger fruits.

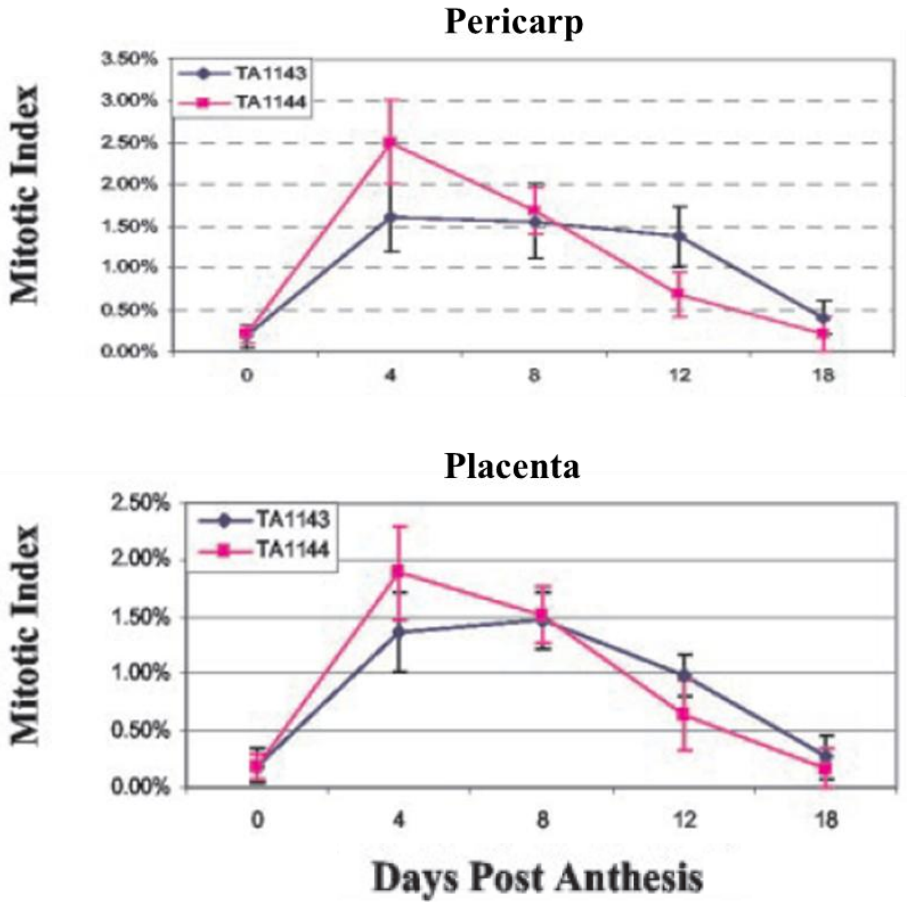

Figure 11: Evolution of the mitotic index in the pericarp and the placenta during tomato fruit development in the two NILs (from Cong *et al.* 2002). The mitotic index is higher at the first stages of fruit development in the small fruits than in the large fruits but then collapses, whereas a higher mitotic activity is maintained for a longer time in the large fruits.

According to Gillaspy (1993), the fruit development can be divided in two phases: the first phase is characterized by an intense activity of cell divisions which lasts until the 7 to 10 DAP and the second phase corresponds to a fruit growth mostly by cell expansion. The first phase seems to be very active in the TA1144 fruits compared to that of the TA1143 fruits but slows down earlier than in the large fruits.

Focusing on the first phase, the mitotic activity in the fruit can be easily correlated to the *fw2.2* expression level (see Figure 5): the higher the level, the lower the mitotic activity.

This last observation reinforces the hypothesis that *fw2.2* can be a negative regulator of the mitosis.

5- Protein subcellular localization

The role of FW2.2 as a negative regulator of mitosis may imply that its localization is cytosolic or nucleic. The study of Cong and Tanksley (2006) raised an interesting point as the study of the amino acid sequence of the FW2.2 protein using TopPred revealed that it possesses two transmembrane domains. In addition, a transient expression of FW2.2 fused to the reporter protein GFP in young tomato leaves showed that the protein localizes at or close to the membrane (Figure 12).

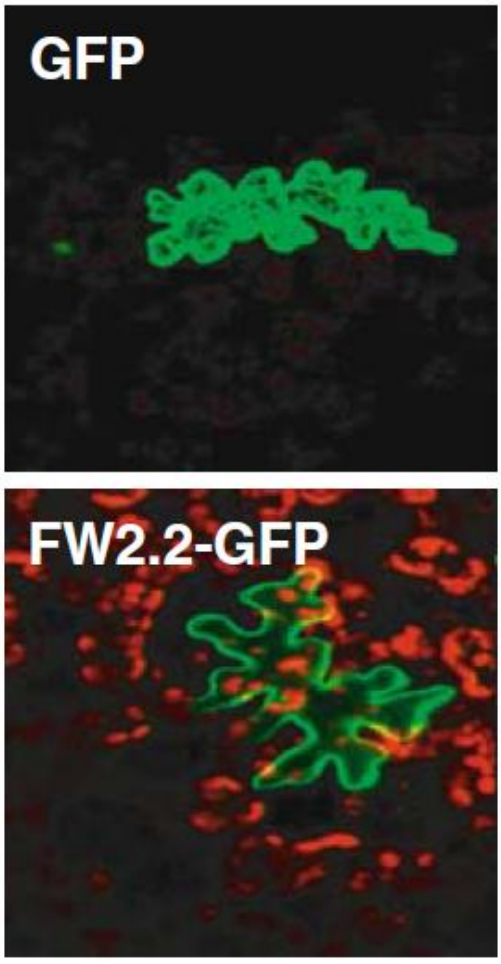

Figure 12: Subcellular localization of the FW2.2 protein tagged with the GFP in tomato young leaf cells (from Congand Tanksley,2006).

This unexpected subcellular localization raises the question of how FW2.2 can influence the cell division while being membranous.

6- Model proposed for the control of the cell cycle

If *fw2.2* is a mitosis inhibitor, this means that it has an influence on the cell cycle or is a protein directly involved in the cell cycle control.

Regarding its localization in the cell, this atypical assignment to the membrane dismisses the possibility that it can be a protein directly involved in the cell cycle control but rather a protein that can influence the cell cycle progression.

To verify this hypothesis, a tomato fruit cDNA library screen has been performed using the two hybrid system and the cytosolic part of the FW2.2 protein with the aim to explain how a membrane protein can influence the cell cycle (Cong and Tanksley,2006). One of the isolated positive clones corresponded to a homologue of the regulatory subunit of the Casein Kinase (CKIIβ).

A colocalization assay allowed the observation that the two proteins localized proximal to the membrane (Figure 13), also suggesting a physical interaction that can explain the influence of FW2.2 on the cell cycle, CKIIβ1 being a protein known to play an important role in cell proliferation in yeast and mammalian cells (Homma *et al.* 2005).

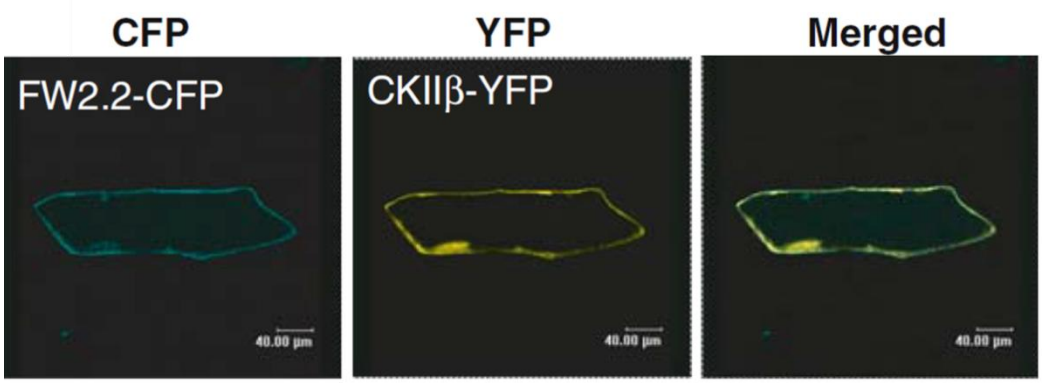

Figure 13: Colocalization assay of the FW2.2 and the CKIIβ1 proteins respectively fused with the CFP and the YFP in onion epidermal cells (from Cong and Tanksley, 2006). Both proteins seem to share the same subcellular localization.

H. *fw2.2* in the plant reign

Various homologues of *fw2.2 can be found* all over the plant reign and also in mammals. Several studies have been made on these homologues and it appears that some of them have an impact on fruit size, while others do not.

1- First homology identified

The study of Galaviz-Hernandez (2003) identified FW2.2 as a homologue of the PLAC8 protein, produced in human (*Homo sapiens*) trophoblast giant cells and in the derived spongiotrophoblast layer. They share a high content of conserved cysteines and amino acid sequence, which give its name to this conserved part of the protein: the PLAC8 domain (Figure 14).

Proteins from other plant organisms have been found to share high homologies with HsPLAC8 and it appears that these proteins come from placenta developing organisms only. No homologue proteins have been found in non-placental eukaryotes such as drosophila and nematode.

HsPLAC8 protein is produced almost exclusively in the placenta and has been shown to be implied in the brown fat differentiation and the control of the body weight, but also the white adipocytes differentiation and cell number control (Jimenez-Preitner *et al.* 2011 and 2012). Therefore, it seems likely that these proteins have a common role in tissue development.

2- Homologues with developmental influence

Other genes have been identified as homologues of *fw2.2*, also influencing the fruit or plant size and development, and have been the subjects of several more or less successful studies in elucidating their functional role.

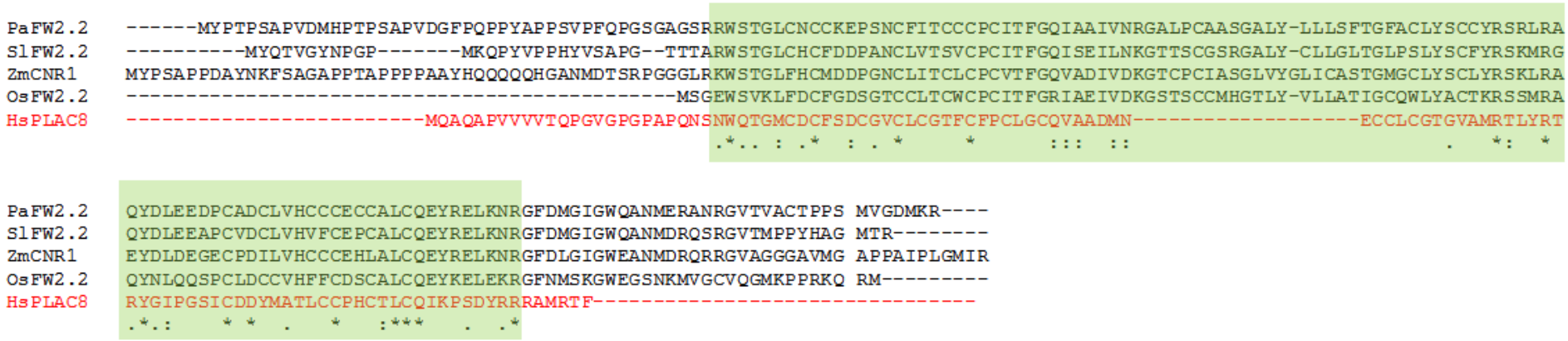

Figure 14: Alignment of several homologue sequences of FW2.2 in the plant and animal reign. The PLAC8 domain, common to all these proteins, is highlighted in green. Pa: *Persea americana*;Sl: *Solanum lycopersicum*;Zm: *Zea mays*; Os: *Oryza sativa*; Hs: *Homo sapiens*.

a- Soybean homologue

In soybean, a member of the *FW2.2-like* gene family, *GmFWL1*, has been identified as a key factor for the nodule organogenesis and the control of chromatin condensation (Libault *et al.* 2010). Its nodule-specific and rapid induction of expression after *Bradyrhizobium japonicum* infection, compared to that of other *GmFWLs*, imply its specific role in these organs. The production of this protein influences the numbers of developing nodules: a silencing of the *GmFWL1* gene provokes a decrease in the number of nodules forming on the hairy roots.

Cells from the nodules present smaller nuclei, due to higher level of chromatin condensation. As *GmFWL1* expression is strongly and quickly induced in the roots during nodule organogenesis, it has been considered to be involved in the early cellular remodeling processes implied in the plant response to rhizobium infection.

b- Avocado homologue

In avocado (*Persea Americana*), another member of the *FW2.2-like* genes has been identified and suggested to be a negative regulator of fruit cell division (Dahan *et al.* 2010). The “Hass” avocado cultivar has the specificity to produce both normal sized fruits and small fruits, with no specific pattern of distribution on the tree. These two kinds of fruits are only differentiated by their mesocarp cell number; the cell size remains unchanged (Cowan *et al.* 1997).

In his study, Dahan *et al.* (2010) showed a correlation between the cell division arrest and the increase of *PaFW2.2* transcripts, which led to the assertion that FW2.2 is a negative regulator of the cell division in avocado.

c- Maize homologue

In maize (*Zea mays*), Guo *et al.* (2010) revealed the existence of 12 homologues of FW2.2, sharing the same conserved PLAC8 domain. Two of these homologues, CNR1 and CNR2 present the higher identity and are specifically expressed in tissues with growth activity.

Knowing the potential role of *fw2.2* in the cell division regulation, these homologues represent the best candidate for a negative regulator of cell number in maize. An overexpression of these two genes in maize revealed that *CNR2* overexpressors do not show any obvious phenotype, whereas *CNR1* overexpressors are affected in their plant height and

organ size (tassel, ear and leaf) in correlation with *CNR1* transcript levels. To correlate the effect of *CNR1* with its expression level, a downregulation of this gene has been performed using RNA interference and the results were significant: a high correlation exists between *CNR1* levels and the plant and organ size. In addition, the cell size has been measured between transgenic and wild type maize plants and it appears that there is no significant size difference. This means that *CNR1* regulates the organ size by controlling the cell number and not the cell size. Obviously, *CNR1* and *FW2.2* share the same role.

d- *Prunus* homologues

Twenty three members of the *FW2.2/CNR* family have been identified in the *Prunus* genus and two of these members, *PavCNR12* and *PavCNR20* (*Pav: Prunus avium*), appeared to be associated to QTLs (De Franceschi *et al.* 2013). Further analysis showed that *PavCNR12* is a fruit size QTL, also present in the sour cherry (*Prunus cerasus*) and the peach (*Prunus persica*). Olmstead et al. (2007) reported that the size variation observed in different domesticated cherry cultivar is mainly due to an increase in cell number rather than a change in the cell size.

This QTL displays 3 alleles that do not differ by their protein-coding region, the 3 alleles contributing differentially to fruit size. Furthermore, a high sequence variation in the promoter region of this QTL suggests that the effect of *PavCNR12* depends on the expression regulation, the same way the alleles of *SlFW2.2* control tomato fruit size.

e- Rice homologue

In rice (*Oryza sativa*), 8 homologues have been identified (*OsFW2.2-like* 1 to 8, the *OsFWLs*) and two of them have been found to be implied in plant development regulation (Xu *et al.* 2013).

The first homologue, *OsFWL3*,is specifically expressed in the panicle, suggesting its implication in fruit development. A knock-out of this gene provokes an increased grain length and glume size. As the cell size between the knock-out and wild-type grains does not change, *OsFWL3* may influence the organ size through the control of the cell number.

The second homologue, *OsFWL5*, is expressed in seed, root, leaf, flag leaf and sheath during all the rice developmental cycle. Its expression does not give any information of its

role, but a knock-out mutant for this gene produces taller plants. Its expression seems to be negatively correlated to the leaf growth activity.

3- Homologues related to heavy metal resistance and ion transport

Some of the homologues of *FW2.2* found have been studied and do not seem to influence fruit size or plant development but are rather associated with a heavy metal resistance in the plants that are expressing them.

a- Maize homologue

Based on the *At*PCR1 and CorA proteins as predictive models, the structure of the maize CNR1 protein has been established, because PCR1 comes from the same family than CNR1 and CorA which display two transmembrane helical motifs (Guo *et al.* 2010). This structure prediction proposed the pentamerization of CNR1 proteins in order to form a channel in the membrane that could facilitate the passage of cations. This model has not been experimentally demonstrated.

b- *Arabidopsis thaliana*

i. PCR proteins

From a screen of an *Arabidopsis thaliana* cDNA library using the cadmium sensitive *ycf1* (Yeast Cadmium Factor protein 1) *Saccharomyces cerevisiae* mutant (strain DTY167), a cDNA has been isolated that confers a cadmium resistance to this yeast mutant (Song *et al.* 2004). This cDNA encodes for a 16 kDa protein called *At*PCR1 (*Arabidopsis thaliana* Plant Cadmium Resistance 1) and the expression of AtPCR1 in the *ycf1* yeastmutant confers the ability to grow on a medium supplemented with cadmium (Figure 15). Its expression is mainly localized in the aboveground parts of the plant, more specifically in the leaves.

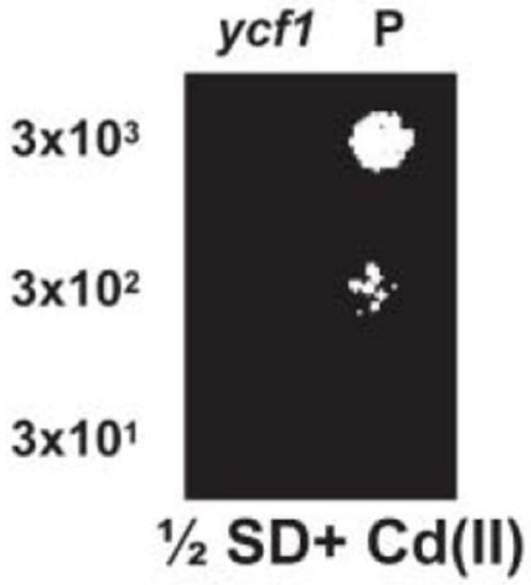

Figure 15: *ycf1* yeast mutant growth on a ½ SD medium supplemented with cadmium after a transformation with an empty vector (*ycf1*) or a vector containing the *AtPCR1* cDNA (P) (from Song *et al.* 2004).

A structural analysis of this protein coupled with a yeast and an *Arabidopsis thaliana* transformation with *PCR1* fused with the GFP coding sequence showed that it is localized in the plasmalemme.

*At*PCR1 shares high sequence homology with *Sl*FW2.2, presenting the same PLAC8 domain. Nine homologues of *At*PCR1 exist within the Arabidopsis genome and 4 of them (*AtPCR2*, *8*, *9* and *10*) have been tested to determine whether they can confer the same cadmium resistance effect to transformed yeasts. The 9 homologues also share sequence homologies with *Sl*FW2.2 and also present the PLAC8 domain.

A transformation of the *ycf1* yeast mutant with the 4 isolated clones showed that *At*PCR2, 9 and 10 confers a more or less strong cadmium resistance to the mutant. In the PLAC8 domain, two motifs are highly conserved: the CCXXXCPC motif localized in the N-terminal part of a transmembrane domain and the QXXRELK motif localized in the C-terminal part of the cytosolic domain. Further analyses using partially or totally deleted AtPCR1 protein for the CCXXXCPC motif showed that this motif and more precisely the cysteine residues are directly implied in the cadmium resistance.

To complete this study, an overexpression of *AtPCR1* in *Arabidopsis thaliana* confers to transformed plants a better growth ability on a medium supplemented with cadmium

(Figure 16), by reducing the cadmium uptake. But surprisingly the knock-out mutant *pcr1* did not show any difficulty to grow on a medium supplemented with cadmium.

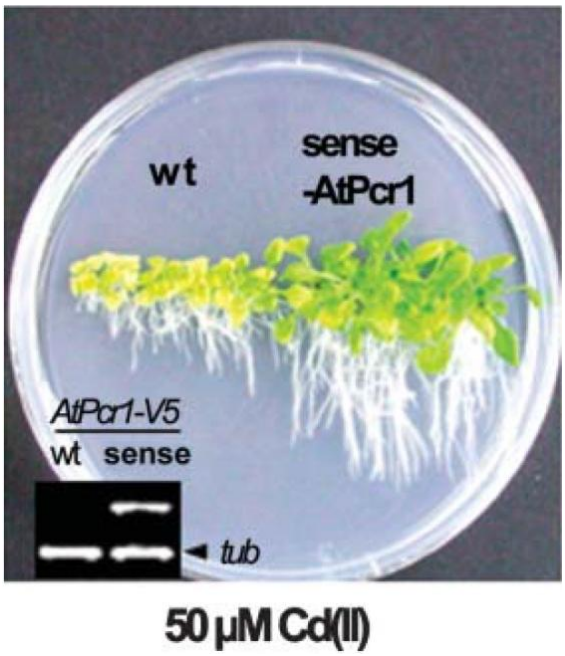

Figure 16: Wildtype and *AtPCR1* overexpressor plants of *Arabidopsis thaliana* growth on a medium supplemented with cadmium (from Song *et al.* 2004). Plants overexpressing the *AtPCR1* gene show better growth ability on a medium supplemented with cadmium.

*At*PCR2 has also been the subject of a complete study (Song *et al.* 2010) as it has the ability to confer a cadmium resistance to transformed yeasts. What differentiates it from AtPCR1 is the expression localization: while *AtPCR1* is expressed in the shoot parts of the plant, *AtPCR2* expression is almost ubiquitous. It is detected in roots, leaves (mainly restricted to the vascular tissues), stems, flowers and siliques. The protein also localizes at the plasmalemme.

The total content in metal ions of wild-type and a knock-out mutant *pcr2* has been measured and revealed that the zinc content in the knock-out mutant was modified. The *pcr2* mutant shows an altered development when grown on medium supplemented with zinc, iron, copper or cadmium, as well as it shows difficulties to grow on a medium lacking zinc (Figure 17). In the same way, an overexpression of *AtPCR2* allows a better plant development on medium supplemented with zinc or from which zinc has been removed.

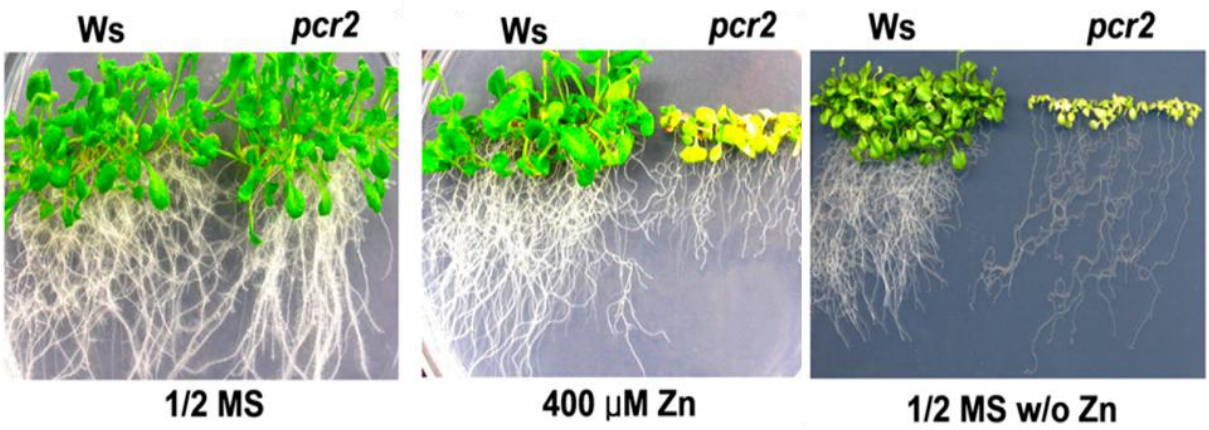

Figure 17: Wild type and *pcr2* knock-out mutant growth on medium supplemented with or without zinc (from Song *et al.* 2010). Knock out *pcr2* mutants show a higher sensitivity to zinc than the wild type plants.

These observations, coupled with the fact that an overexpression of *AtPCR2* in zinc sensitive yeast mutants at low and high concentrations provokes a growth impairment and a better growth compared to the control mutants respectively, confirm the idea that PCR2 is a zinc extruder.

ii. MCA proteins

Other proteins, such as the AtMCA (Mid1-Complementing Activity) proteins, are known to contain the PLAC8 domain and present a mechanosensing role in the root growth and also in stomatal dynamics and regulation of transpiration (Nakagawa *et al.* 2007; Conn *et al.* 2011). These proteins have been identified as Calcium-permeable channels whose abundance has been negatively correlated with calcium accumulation in the cells.

These proteins display another important domain, the ARPK domain, and localize at the membrane. Truncated versions of these proteins, conserving only the ARPK or the PLAC8 domain, allowed determine that the ARPK domain is responsible of the ion transport, whereas the PLAC8 domain did not show any specific activity (Nakano *et al.* 2011).

c- *Oidiodendron maius*

This mycorrhizal fungus has been isolated in Poland from heavy metal contaminated areas in which it was able to grow.

A screen of an *O. maius* cDNA library using the mutant yeast strain *yap1* inactivated for a cadmium resistance gene has been performed and allowed the isolation of a cDNA clone

that confers a cadmium resistance to the mutant yeast strain when inserted by transformation. The gene sequence isolated has been named *OmFCR* (*O. maius Fungal Cadmium Resistance*) (Abbà *et al.* 2011).

This cDNA encodes a 179 amino-acid long protein that share sequence similarities with the *At*PCR and *Zm*CRNs proteins, also displaying the PLAC8 motif. The protein sequence also contains a slightly modified CCXXXXCPC motif found to be directly implied in heavy metal transport, here found as CLXXXXCPC motif. An oligonucleotide directed site-specific mutagenesis have been performed in order to modify this motif and it appears that it is also implied in the cadmium resistance as its mutation induces a cadmium sensitivity in the mutant yeast strain transformed with the mutated cDNA.

A fusion of the protein with the EGFP allowed its localization determination in yeast: the protein seems to be assigned in the nucleus, whether the yeast is in contact with cadmium or not.

To determine how the protein exerts its heavy metal resistance, a two hybrid screen of a genomic library of *Saccharomyces cerevisiae* has been performed and allowed to reveal the interaction between *Om*FCR and one of the DNA mismatch repair system protein Mlh3p. Cadmium is known to target the major DNA repair systems (Giaginis *et al.* 2006) by inhibiting their ATP hydrolysis activity and the *Om*FCR protein can act as a signal transducer when associated with the Mlh3p protein in the signal cascade that controls the cell cycle progression.

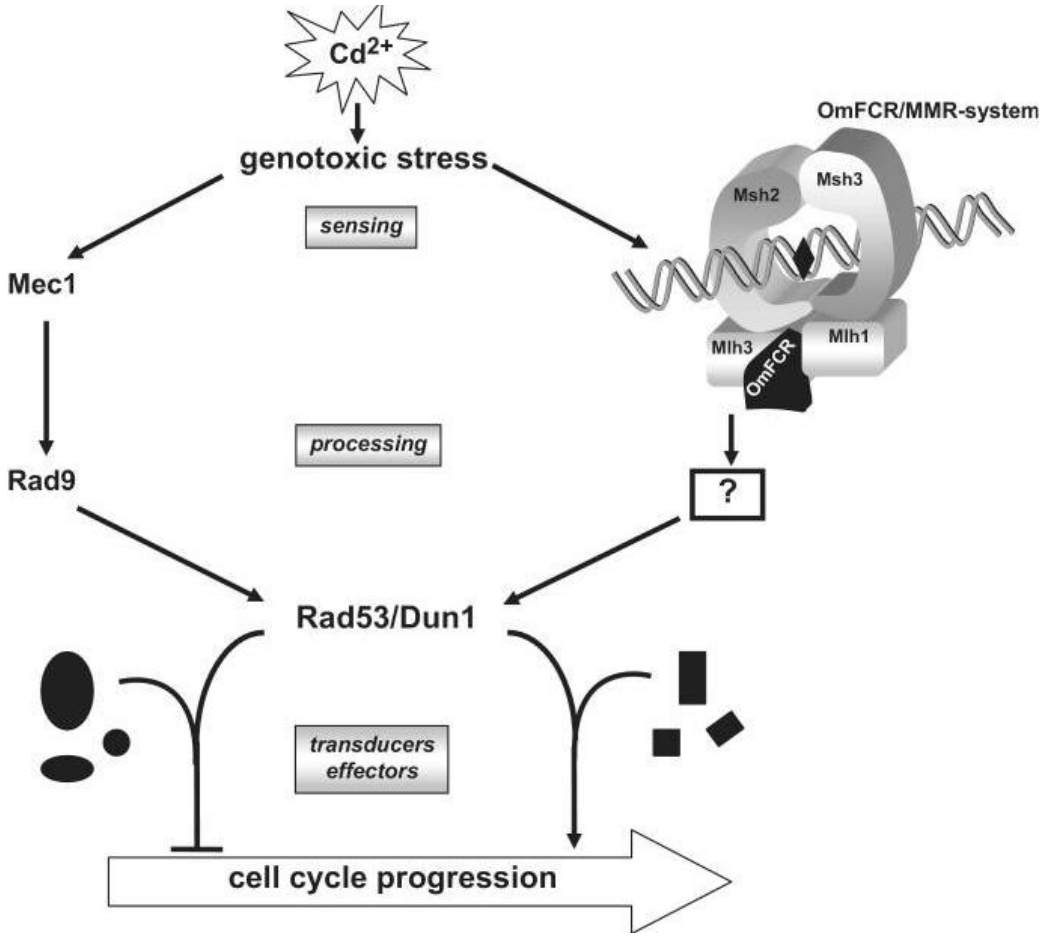

Figure 18: Model of the *Om*FCR function in the mismatch repair system, as a signal transducer in the phosphorylation cascade that controls the progression of the cell cycle (from Abbà *et al.* 2011).

This protein gives interesting informations about which role heavy metal resistance proteins can occupy within the cell. The *yap1* mutant yeast strain presents a slower growth than wild-type yeast that can be explained by a cell cycle progression arrest when the cells are exposed to cadmium due to the accumulation of mismatches on the genomic DNA that cannot be repaired (Figure 18).

II

Objectives
Hypotheses

II. Objectives of the Thesis : Hypothesis and scientific approach

There is no doubt that *fw2.2* is the major QTL controlling the fruit size. The study of its various homologues all over the plant reign gave hypothesis on its function but not how it possesses such a dramatic effect on the fruit size.

In the literature, the homologues of FW2.2 seem to belong to a large family in their inner organism. We can hypothesize that FW2.2 homologues also exist in tomato that could share the same function or have identical function to the proteins described in the former part of the introduction. The first part of this manuscript aims at determining if FW2.2 possesses actually homologues in tomato and figuring out if these homologous proteins may share the same role than FW2.2; the putative homologous gene and protein sequence structures have been studied; the gene expression in the tomato fruit and plant has been analyzed and a phylogenic study has been performed.

The study of AtPCR1, AtPCR2 and OmFCR showed that these three proteins are directly implied in the heavy metal resistance. These proteins are FW2.2 homologues and share a high sequence homology with this protein, sharing the same conserved PLAC8 domain. The fact that FW2.2 shares such a high sequence homology with these proteins led us to propose the first hypothesis that FW2.2 can also be implied in the heavy metal resistance being an ion transporter. In a second part of this work, we tried to determine if FW2.2 has a transporter function, and if it is the case, for which heavy metal it ensures a heavy metal resistance. A transporter function implies that the protein ensuring this role has a membrane localization, as this localization has not been clearly demonstrated, we managed to verify that FW2.2 localizes at the plasma membrane.

Previous works showed that *SlFW2.2* is mainly expressed in the fruits and has a mitosis negative regulation function. As its allelic effect is mainly observable on the fruits, leading to a fruit size difference, which is likely due to an inhibition of the mitosis in the carpel, the pericarp and the placenta, we asked ourselves what could be its developmental effect at the plant level and at the cell level. In the third part of this work, we tried to investigate what is the developmental role of FW2.2 and how it regulates the development, focusing on heterologous organisms.

Since FW2.2 can be a membrane protein, it is puzzling to know that it is influencing the cell cycle with such localization. It is legitimate to wonder through which pathway it applies a negative control on the mitosis. We can imagine that if the mitoses are inhibited by this gene, a difference in the regulation of the genes implied in the cell cycle control may be apparent. In the fourth part of this work, we investigated the expression of several cell cycle control gene in order to determine through which protein the effect of FW2.2 is acting.

As FW2.2 is a small protein, supposed to be addressed to the membrane, we hardly imagine that it can act alone as a transporter and hypothesized that it might make interactions with other proteins to form a functioning transporter. And even if the transporter function is not verified, its influence on the cell cycle is undeniable and let suppose that there might be a signal pathway between the membrane and the nucleus that makes possible the influence of FW2.2. This is why, in this fourth part of the work, we tried to determine if FW2.2 is able to make interactions with other proteins, using an interaction screening technique applicable to membrane proteins: the Split-Ubiquitin technique.

III

Results

III. Results

The study of Galaviz-Hernandez (2003) identified FW2.2 as a homologue of the PLAC8 protein in mammals. The alignment of the FW2.2 protein sequence with 4 mammalian PLAC8 protein and 6 FW2.2 plant homologue protein sequences shows that all of these proteins share the same PLAC8 domain (previously known as the DUF614 domain) (Figure 19). In this domain, several amino acids appear to be very conserved between all the proteins. Since some of them have been already characterized, this could indicate that these proteins may share the same function.

A. The *FW2.2-like* gene family in tomato

The FW2.2 protein shares homologies with numerous proteins in the plant and animal kingdom (Figure 19). The work of Guo *et al*. (2010) identified various homologues all over the plant reign but classified FW2.2 as a plant specific protein. In the phylogenic study of Guo *et al*. (2010), only the two alleles of FW2.2 were represented whereas the *FW2.2* gene family in different plant species is often enlarged. This observation led us to wonder whether *FW2.2* homologues could coexist in tomato displaying a putative identical function.

1- Identification of *FW2.2*-like genes in tomato

In order to identify the homologues of FW2.2 in *Solanum lycopersicum*, we used two online publicly available databases in order to align the protein sequence against tomato databases.

The first tool used was the Sol Genomics Network Blast tool, aligning the FW2.2 protein sequence against the “SGN tomato combined - WGS, BAC and unigene sequences” set with a maximum threshold of 1^{e-10}. This first blast alignment allowed the identification 7 coding sequences that align with FW2.2, with scores ranging from 31 to 53. These genes were named *FW2.2-like* (*FWLs*) 1 to 7 proteins.

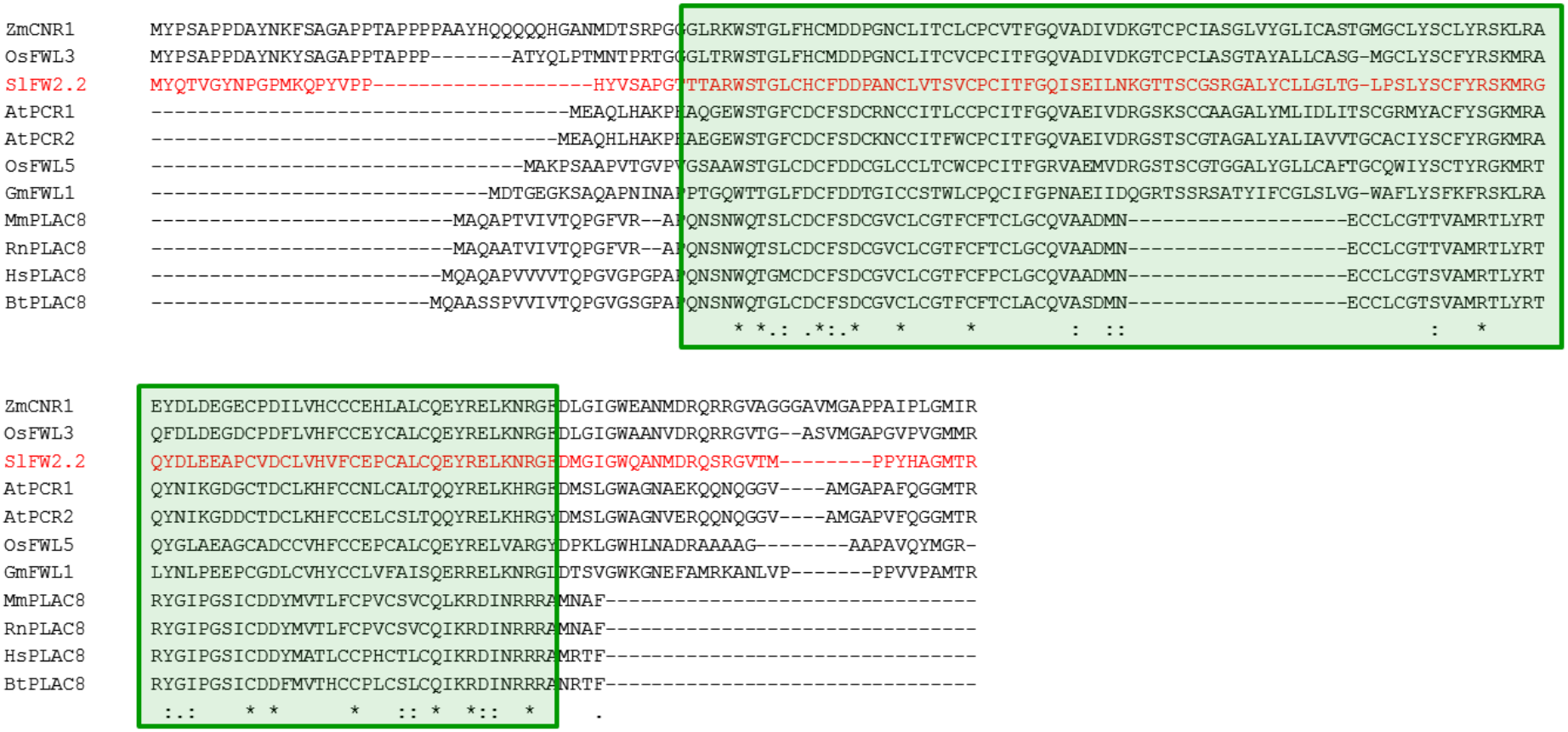

Figure 19: Comparison of FW2.2 protein sequence with characterized homologous proteins of plants and PLAC8 proteins from mammals. All the aligned protein sequences share the same PLAC8 domain. Zm: *Zea mays*; Os: *Oryza sativa*; Sl: *Solanum lycopersicum*; At: *Arabidopsis thaliana*; Gm: *Glycin max*; Mm: *Mus musculus*; Rn: *Rattus norvegicus*; Hs: *Homo sapiens*; Bt: *Bos torus.*

A newly available tool was used to investigate whether the homologues in tomato could be much more numerous than the ones isolated using the Sol Genomics Network. The FLAGdb++ (hosted at INRA Evry) tool presents the particularity to gather information from the Sol Genomics Network analyzed with prediction softwares.

The FLAGdb++ tool allowed indeed the identification of a larger panel of putative homologues, as it released a total of 20 sequences. In these 20 homologues, we could confirm the presence of the 7 homologues identified using the Sol Genomics Network and retrieve the majority of the sequence by blasting the isolated FLAGdb++ sequences against the Sol Genomics Network database (Table 2).

The alignment of the previously described protein sequences (Figure 19) revealed that they all share the PLAC8 domain common to all the homologues described in previous literature. A more accurate observation of the sequence homologies revealed that in the PLAC8 domain some amino acids appeared to be very conserved between all the homologues. These amino acids enter in the composition of two motifs that are common to all the proteins.

The first motif is the CCXXXXCPC motif, described in the *At*PCR protein and directly implied in the heavy metal resistance. The second motif is the QEYRELK motif, whose function is unknown.

These two motifs are highly conserved in their position and amino acid composition but undergo some modifications in their composition that could certainly provoke a protein function modification.

The alignment of all the FWLs proteins identified showed that they all share also the same PLAC8 domain with these two conserved motifs (Figure 20).

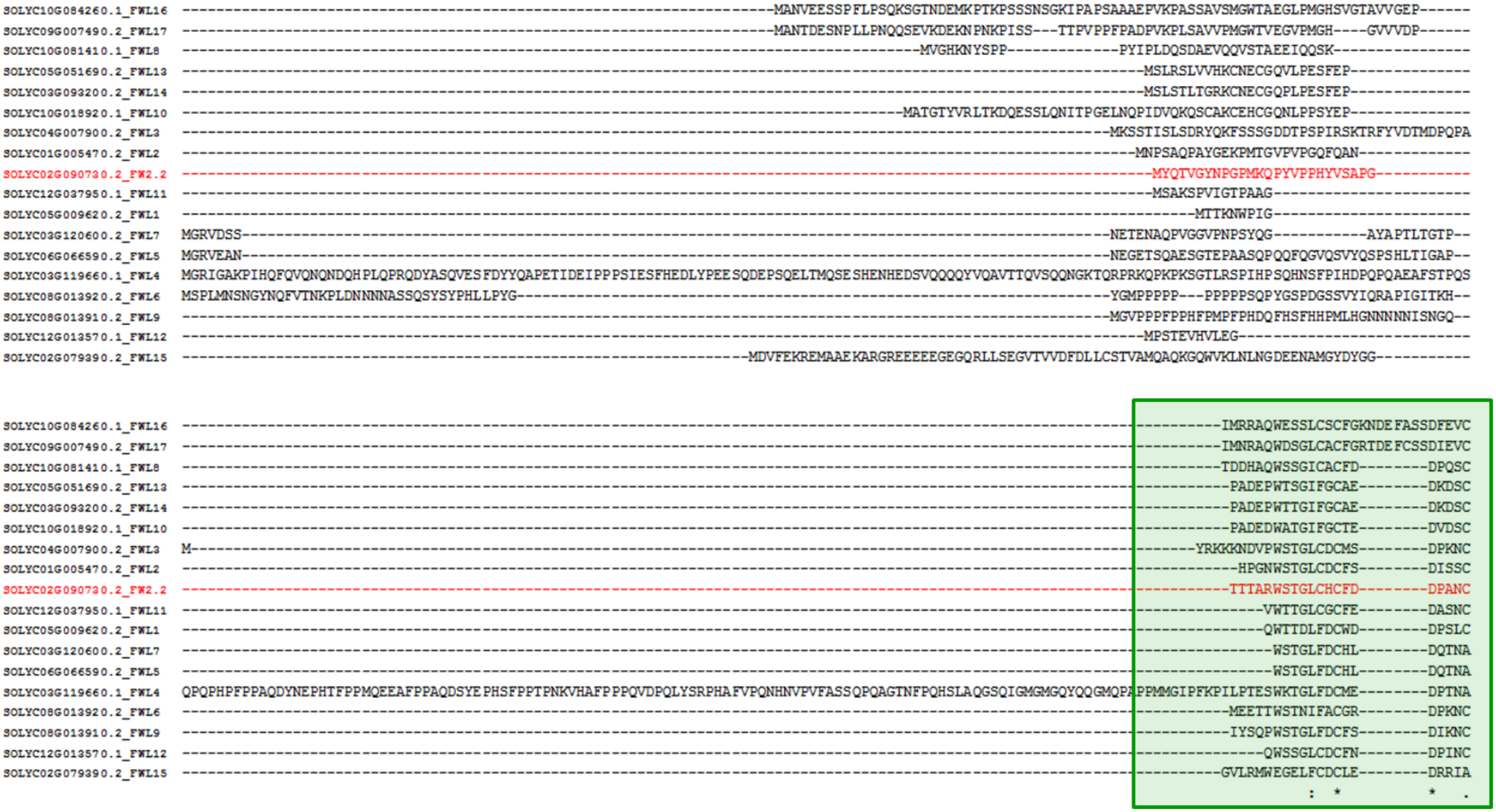
SOLYC10G084260.1_FWL16
SOLYC09G007490.2_FWL17
SOLYC10G081410.1_FWL8
SOLYC05G051690.2_FWL13
SOLYC03G093200.2_FWL14
SOLYC10G018920.1_FWL10
SOLYC04G007900.2_FWL3
SOLYC01G005470.2_FWL2
SOLYC02G090730.2_FW2.2
SOLYC12G037950.1_FWL11
SOLYC05G009620.2_FWL1
SOLYC03G120600.2_FWL7
SOLYC06G066590.2_FWL5
SOLYC03G119660.1_FWL4
SOLYC08G013920.2_FWL6
SOLYC08G013910.2_FWL9
SOLYC12G013570.1_FWL12
SOLYC02G079390.2_FWL15

Figure 20: Alignment of the 17 FWLs and the FW2.2 protein sequences. The PLAC8 domain is shaded in green.

Table 2: List of the homologous genes found using Sol Genomics Network and FLAGdb++.

Gene ID FLAGdb++	Corresponding SGN accessions	Gene name
SOLYC02G090730.2	Not provided	FW2.2
SOLYC05G009620.2	SGN-U567217	FWL1
SOLYC01G005470.2	SGN-U567416	FWL2
SOLYC04G007900.2	SGN-U574099	FWL3
SOLYC03G119660.1	SGN-U565461	FWL4
SOLYC06G066590.2	SGN-U578311	FWL5
SOLYC08G013920.2	SGN-U574857	FWL6
SOLYC03G120600.2	Not provided	FWL7
SOLYC10G081410.1	SGN-U278217	FWL8
SOLYC08G013910.2	SGN-U568551	FWL9
SOLYC10G018920.1	Not provided	FWL10
SOLYC12G037950.1	Not provided	FWL11
SOLYC12G013570.1	Not provided	FWL12
SOLYC05G051690.2	SGN-U585119	FWL13
SOLYC03G093200.2	SGN-U275082	FWL14
SOLYC02G079390.2	SGN-U563948	FWL15
SOLYC10G084260.1	SGN-U571867	FWL16
SOLYC09G007490.2	SGN-U562867	FWL17
SOLYC02G083540.2	SGN-U565830	SlMCA1
SOLYC03G095820.2	SGN-U565932	SlMCA2
SOLYC07G020970.1	Not provided	unnamed

From the analysis of the retrieved sequences, it appears that some of them can be excluded from the list of putative homologues due to the sequence shortness or homology with other proteins.

An alignment of all these proteins showed that four protein sequences display two sequence length abnormalities. FW2.2 is constituted of 163 amino acids and the other proteins were at least 400 amino acids long or as short as 30 amino acids.

The first length abnormalities concern the SOLYC03G119660.1 (FWL4), SOLYC03G095820.2 (*Sl*MCA2) and SOLYC02G083540.2 (*Sl*MCA1) proteins. These sequences are almost twice longer than the other protein sequences, with a N-terminal 150-200 amino-acid extension. The alignment of these proteins with the TAIR (Arabidopsis) database showed that SOLYC03G095820.2 and SOLYC02G083540.2 proteins were closer to *Arabidopsis* MCA (Mechanosensitive CAlcium channel) proteins than they were to PLAC8 proteins, which led us to name these proteins SlMCA2 and SlMCA1 respectively. The MCA

proteins also contain the PLAC8 domain, which can explain that using the FW2.2 sequence as a query in FLAGdb++ retrieved sequences belonging to the MCA family.

Although the FWL4 protein presents an important N-terminal extension, the sequence comparison against the TAIR database clearly revealed that it belongs to the PLAC8 family.

The second length abnormality concerns the SOLYC07G020970.1 protein. This protein is only 30 amino acids long; it aligns perfectly with the C-terminal end of the FW2.2 protein and gives no hit using neither the Sol Genomics Network nor the TAIR database. As a consequence, it corresponds surely to a prediction error.

These observations led the exclusion of the SlMCA1, SlMCA2 and SOLYC07G020970.1proteins from the FW2.2 homologue list and to the conservation of the FWL4 protein in our future analyses.

2- Expression pattern of the FWLs in different tissues of *Solanum pimpinellifolium* cv LA1589

SlFW2.2 is known to be expressed mainly in the young fruit, the roots and the flower buds. We then investigated whether the homologues of FW2.2 were also expressed in the same territories or displayed a different pattern of expression.

To monitor the expression of all these homologues, we used the Tomato Functional Genomic database, hosted by the Sol Genomic Network. This database provides RNAseq data for different cultivar and different organs and various stages of fruit development.

Using the gene IDs' accessions, we were able to retrieve a set of expression data in the *Solanum pimpinellifolium* cv LA1589 for all the homologues relative to different plant organs, as well as for 3 stages of fruit development. The analysis of the expression patterns for these genes allowed separate the homologues in 4 distinct groups, according to their territory of expression (Figure 21).

Group 1

Group 2

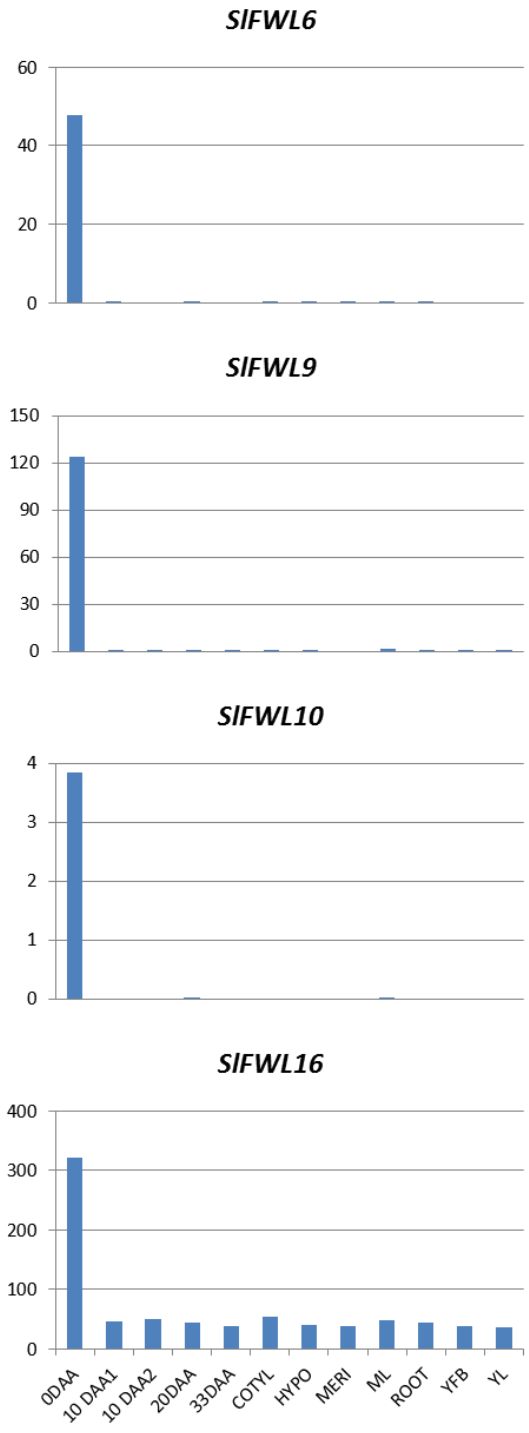

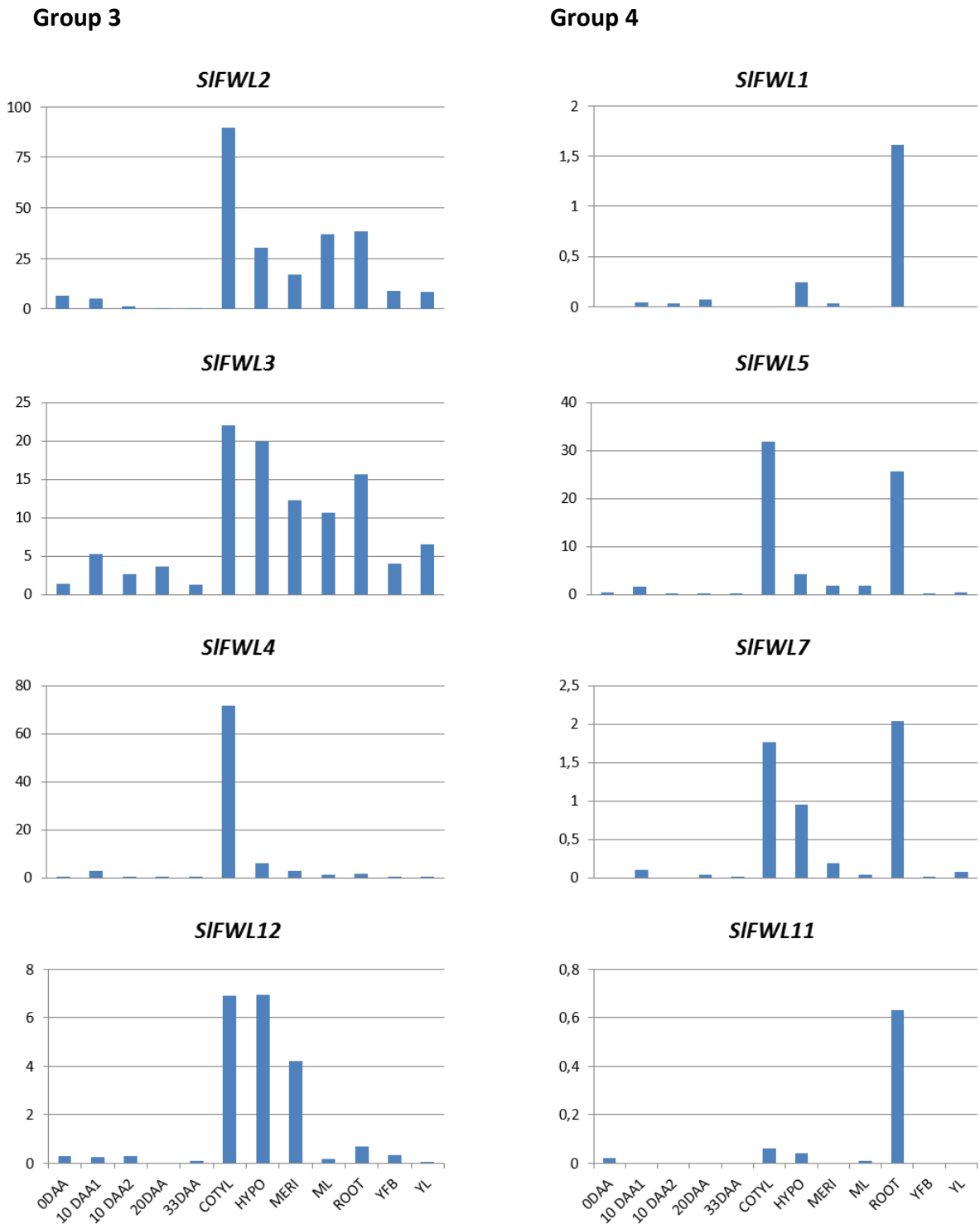

Figure 21: Gene expression patterns of *SlFW2.2* and its homologues in different plant organs and at different stages of fruit development in the *Solanum pimpinellifolium* cv LA1589. The y axis represent the normalized expression (in RPKM) and the x axis the organs and their stage of development. The FWLs genes have been separated in 4 groups according to their higher plant tissue expression. DAA: days post anthesis; 0 DAA: anthesis stage; 10 DAA1 and 10 DAA2: 10 DAA fruit n°1 and n°2; 33 DAA: ripening fruit; Cotyl: cotyledons; Hypo: hypocotyl; Meri: vegetative meristem; ML: mature leaves; Root: whole root; YFB: young flower buds; YL: young leaves.

A careful analysis of these expression patterns did not reveal any similar pattern of expression for all the homologues when compared to that of *SlFW2.2*. However, some of the homologues showed very specific tissue expression.

SlFWL1, *SlFWL5*, *SlFWL7* and*SlFWL11* were strongly expressed in an exclusive or majority manner in the roots (group 4). *SlFWL5* displayed a stronger expression in the roots than in the three other genes. As these proteins share homologies with heavy metal transporters, and according to their expression territory, it is tempting to imagine that these proteins could be also involved in heavy metal transport mechanisms.

Similarly, *SlFWL5* and *SlFWL7* were also expressed in the cotyledons and in the hypocotyl, where *SlFWL2*, *SlFWL3*, *SlFWL4* and *SlFWL12* were also expressed. However these latter 4 genes were also expressed in the vegetative tissues such as the cotyledons, the hypocotyl, the vegetative meristems and the leaves. This pattern of expression led us to separate them from the previous group and to create a new group, namely group 3. These territories of expression could also correspond to a heavy metal transport activity.

Some of these genes presented an interesting exclusive expression within flowers at anthesis: they were assembled in group 2. These genes, namely *SlFWL6*, *SlFWL9*, *SlFWL10* and *SlFWL16*, were strongly and coordinately expressed with *SlFW2.2*. Thus they seemed to be involved in the early control of ovary development.

The other genes showed no specific localization of expression and had a relative high level of expression in the plant in a ubiquitous manner. These genes, namely *SlFWL8, SlFWL13, SlFWL14, SlFWL15* and *SlFWL17*, wereassembled within group 1. Since *SlFW2.2* wasalso expressed everywhere in the plant and even if the expression levels were less important than the other genes from this group, *SlFW2.2* was placed in group 1.

Obviously the localizations of expression cannot give a precise idea of a gene function, but since these proteins belong to the same gene family, we can hypothesize that their function is conserved but distributed all over the plant.

3- Expression of *SlFW2.2* in different organs of the plant

The expression of *SlFW2.2* in Solanum lycopersicum cv WVA106 was then monitored by quantitative RT-PCR (Figure 22) in order to determine if the expression of *SlFW2.2* was detectable all over the plant. It appeared that *SlFW2.2* was only significantly detectable in the roots and in mature leaves. *SlFW2.2* was also noticeably detectable in the carpel before the anthesis stage (9 mm long flower), confirming its role during floral inititation.

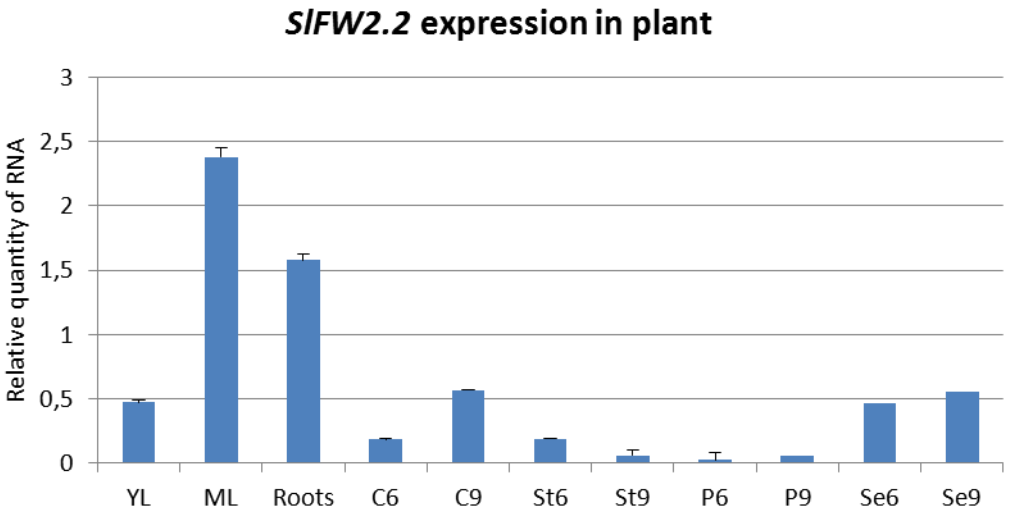

Figure 22: Expression of *SlFW2.2* in *Solanum lycopersicum* cv M82, line TA1143 (large fruit allele), in different organs and in different parts of the flower at two different stages of the flower development. It is noticeable that the higher levels of *FW2.2* expression are detected in the vegetative plant parts. YL: young leaves; ML: mature leaves; Root: whole root; 6: 6 millimeters long flower; 9: 9 millimeters long flower; C: carpel; St: stamen; P: petal; Se: sepal.

As described in Figure 21, RNAseq data obtained from *Solanum pimpinellifolium* cv LA1589 showed that *SlFW2.2* was expressed in the roots and the leaves. We here confirmed using RT-PCR on cDNA generated from different organs of a large fruit allele plant (TA1143) that *SlFW2.2* was also expressed in these organs, suggesting its implication in other developmental processes and in different regulatory processes in other organs than the fruit.

4- Comparison of the homologues genes structure

The gene sequence organization has been studied using the FLAGdb++ tool which can predict the intron/exon composition (Figure 23).

The length of introns was clearly not conserved between all the homologues (not shown in Figure 23).

However, a conservation pattern could be observed for the exons. We can easily notice that in some of the genes there is an iterative alternation of long and short exons (at least twice; group marked in red). *FWL2, 3, 4, 5, 7, 9, 10* and *15* belong to this group with *FWL4* displaying a large 5' extension of the first exon. The group marked in green seems to have undergone a series of deletion events within the first exon, provoking its shortening (*FWL1* and *11*), coupled with a complete deletion of the last exon (*FWL12*) and a 3' extension of the

last exon (*FWL6*). However this group conserves the global organization encountered within the first group (red). The group marked in blue presents a completely disrupted exon organization, which separate them from the previous two groups.

The two *SlMCA* genes (yellow) present a highly conserved structure with each other in both of them, with two big introns followed by five small introns. However this organization is completely different from that of the other FW2.2 homologous genes, which clearly separate them from the *FWL* genes. Similarly, the SOLYC07G020970.1 gene only displays two small introns, the first one being very short. The very different exon composition and organization of these last three genes reinforces the fact that we dismissed them from our study.

Although the organization of exons appeared different within in the *FWL* genes, we can still find a similarity in some of the genes, and the relative exon custody suggests that the majority of these genes may originate from a duplication event.

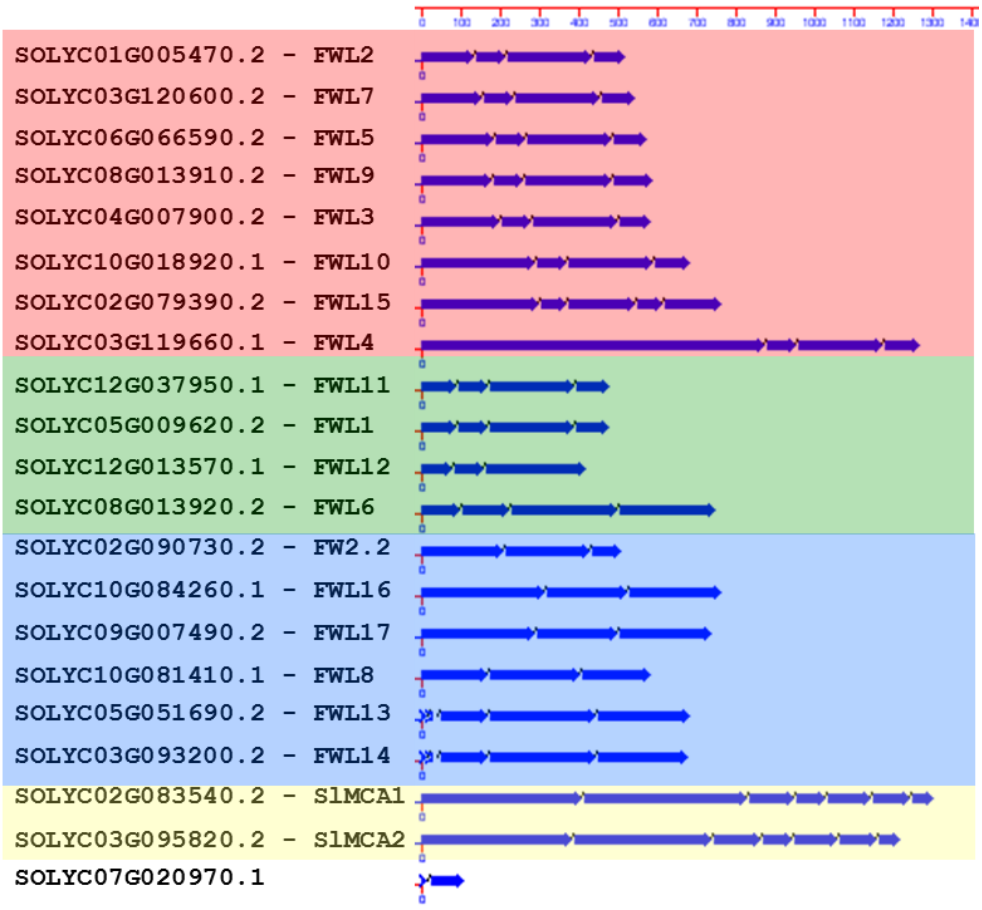

Figure 23: Exon composition of the *SlFW2.2* homologue genes obtained using FLAGdb++. The genes have been seperated in 4 groups, according to their exon length composition. The Gene IDs indicated are the same than described Table 1.

5- Phylogeny

To better understand the evolution of these genes and try to find a clue to the FW2.2 protein function, a phylogenic analysis was necessary. A phylogenic tree has been generated in order to separate the proteins in groups, expecting to find better homologies of function.

The generated tree (Figure 24) was built with 107 plant protein sequences from the work of Guo *et al.* (2010), who found these sequences in publicly available databases. In these 107 proteins, we added the sequences of the newly identified FWLs from FLAGdb++ and the two MCA protein sequences from *Arabidopsis thaliana* to allow a better separation of the protein sequences.

The tree was generated by first aligning the sequences with MUSCLE. It was then cured with Gblocks to identify only the most conserved domains to be then treated by MEGA5 as to generate the phylogenetic tree.

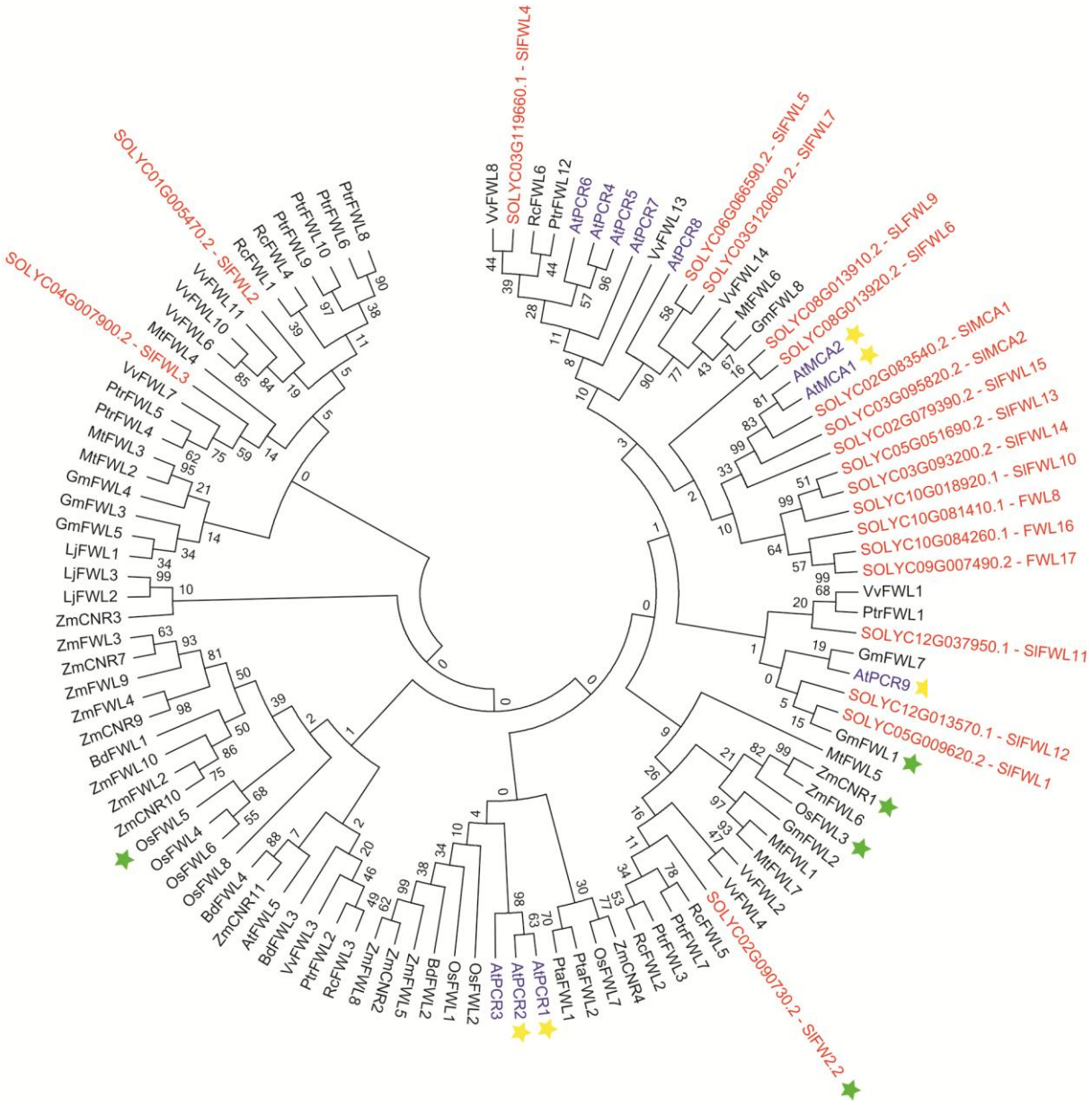

Figure 24: Evolutionary relationship between the tomato FW2.2 and FWLs protein as a part of a large plant protein family. The proteins do not segregate according to their putative function. Red: proteins from *Solanum lycopersicum*; Blue: proteins from *Arabidopsis thaliana*; Green stars: proteins implied in plant and fruit developmental processes; Yellow stars: proteins implied in transport and/or resistance to heavy metal resistance . At: *Arabidopsis thaliana*; Bd: *Brachypodium distachyon*; Gm: *Glycin max*; Lj: *Lotus japonicus*; Mt: *Medicago truncatula*; Os: *Oryza sativa*; Pta: *Pinus taeda*; Ptr: *Populus trichocarpa*; Rc: *Ricinus communis*; Sl: *Solanum lycopersicum*; Vv: *Vitis vinifera*; Zm: *Zea mays*.

The generation of this tree did not allow highlighting any clear separation of FW2.2 from the other proteins. In addition it did not show the existence of any clear function clade. Even the *At*PCRs proteins that were characterized as heavy metal transporter/resistance proteins did not segregate within the same branch. The evolution of protein sequences was

apparently independent and did not allow us to conclude on a possible co-evolution or common function.

Nevertheless it remains clear that FW2.2 has a high sequence similarity with heavy metal resistance proteins: this putative function has now to be investigated.

B. The putative channel function of FW2.2

The phylogenic studies and the previous works performed on the PLAC8 domain-containing proteins suggested that FW2.2 could be such a protein implied in heavy metal transport or resistance processes. Furthermore, the work from Cong and Tanksley (2006) predicted the protein to be localized at the plasmalemme due to the presence of two predicted hydrophobic domains. This cellular localization would make sense if FW2.2 functions as a transporter.

Since we do not know if FW2.2 is a true transporter and if it is a passive or active transporter, we shall refer to as a putative channel.

In order to elucidate the putative channel function of FW2.2, we were first interested in establishing its subcellular localization, as the work from Cong and Tanksley (2006) did not show doubtlessly that FW2.2 localized to the membrane. This analysis became essential in the frame of the study of its potential function and to forecast the different experiments to be performed that could confirm its role.

1- Plant material used for the channel function study

The plant and cells lines used for the experiments described in this part are described in the following table (Table 3).

Table 3: Description of the plant and cell lines used for the study

Plant/cell lines used	Nature of the plant	Transformation type	Use of the lines
M82	Tomato cv M82 undetermined growth - wild type	None	Mineral content measurement
M82-SF	Tomato cv M82 undetermined growth - transgenic line	Stable - insertion of the small fruit allele of Sl*FW2.2*	Mineral content measurement
TA1143	Tomato cv M82 determined growth - wild type	None - NIL for the big fruit allele of *SlFW2.2*	Mineral content measurement
TA1144	Tomato cv M82 determined growth- wild type	None - NIL for the small fruit allele of *SlFW2.2*	Mineral content measurement
Tobacco plant EYFP-FW2.2	*Nicotiana tabacum* - transgenic	Stable - insertion of the *EYFP-FW2.2* construction	Protein localization
Tobacco plant GFP	*Nicotiana tabacum* - transgenic	Stable - insertion of the *GFP* construction	Protein localization
BY2 cell EYFP-FW2.2	*Nicotiana tabacum* - transgenic	Stable - insertion of the *EYFP-FW2.2* construction	Protein localization and mineral content measurement
BY2 cell 3HA-FW2.2	*Nicotiana tabacum* - transgenic	Stable - insertion of the *3HA-FW2.2* construction	Mineral content measurement
BY2 cell GFP	*Nicotiana tabacum* - transgenic	Stable - insertion of the *GFP* construction	Protein localization and mineral content measurement
Arabidopsis plant EYFP-FW2.2	*Arabidopsis thaliana* - transgenic	Transient - insertion of the *EYFP-FW2.2* construction	Protein localization
Arabidopsis plant EYFP-FW2.2	*Arabidopsis thaliana* - transgenic	Stable - insertion of the *EYFP-FW2.2* construction	Growth test on supplemented medium
Arabidopsis plant GFP	*Arabidopsis thaliana* - transgenic	Stable - insertion of the *GFP* construction	Growth test on supplemented medium

2- Subcellular localization of the FW2.2 protein

To investigate the subcellular localization of FW2.2, heterologous transient expression of tomato FW2.2 was performed. Three types of plant materials were used: on the one hand tobacco (*Nicotiana tabacum*) plants and BY2 cultured cells both stably transformed with constructions allowing the overexpression of *FW2.2* fused at its N-terminal part with the *EYFP* coding sequence, and the overexpression of the *GFP* as a control; *Arabidopsis* plantlets that transiently overexpress the EYFP-FW2.2 recombinant protein on the other hand.

a. Microscopic observation of FW2.2 subcellular localization

Using a confocal microscope, the observation of FW2.2 subcellular localization in the leaf epidermis (Figure 25A) and BY2 (Figure 25C) transformed cells has confirmed the fact that FW2.2 is a membrane localized protein. The confocal microscopy allowed us to observe a cell section by section, from its top to its bottom. Actually, the fluorescence observed in the tobacco plants and the BY2 cells overexpressing the EYFP-FW2.2 construction was only localized on the borders of the cells, excluding the nucleus, as visible in the *GFP*-expressing transformants (Figures 25B and 25D). At this point of our observation, we conclude that FW2.2 is localized at or close to the membrane.

Cell plasmolysis of the BY2 cells was then performed to observe the fate of the fluorescence. In isotonic conditions the GFP fluorescence localized close to the membrane. Therefore we can wonder whether it corresponds to a membrane (plasmalemme) localization or to a cytoplasmic localization, since the cytoplasm is flattened against the plasma membrane in these conditions. Under application of a 9% (w/v) NaCl solution, i.e. hypertonic conditions, the vacuole retracted and the fluorescence appeared clearly in the cytoplasm (Figure 25F). Conversely, the plasmolysis of the cells producing the fluorescent EYFP-FW2.2 recombinant protein revealed that the fluorescence followed the plasma membrane (Figure 25E), clearly separated from the cell wall.

What is also interesting is that, in the *EYFP-FW2.2* overexpressors, the fluorescence could also be visible inside the plasmalemme in what looked like some vesicles that localized around the nucleus. We hypothesized that these vesicles were perinuclear vesicles full of folded and functional EYFP-FW2.2 protein ready to be addressed to the membrane.

When the vacuole retracts, it thus provokes a membrane detachment from the cell wall. However, plant cells are known to be linked through plasmodesmatas. These structures allow the communication between the cells and are a specific location where the cell plasma

membranes of the two joined cells are fused. BY2 cells form cellular chains and two adjacent cells inside these chains forms plasmodesmatas. We can imagine that in hypertonic conditions, when the vacuole retracted, it provoked a tension at these locations and the stretching of the membrane. This is what was observed on the plasmolyzed BY2 cells producing the EYFP-FW2.2: we could clearly distinguish strips of fluorescence that stretches from the common cell wall between two adjacent cells to the plasma membrane.

This case has been described for *Nicotiana tabacum* MCA1 and 2 proteins (Kurusu *et al.* 2012) that are calcium intruder proteins and has the specificity to maintain a cell growth in calcium deficiency conditions when they are overexpressed in BY2 cells by the maintenance of a sufficient intracellular calcium concentration. The overexpression of the *Nt*MCA1-GFP and NtMCA2-GFP protein fusions allowed the observation of a punctuated plasma membrane, Hechtian strands (when the cells are plasmolyzed) localization. The Hechtian strands are fibrous structures connecting plasma membrane to cell wall (Buer *et al.* 2000) and localizations on these strands have been described for other ion channels like the *Arabidopsis thaliana* SLAC1 channel (Vahisalu *et al.* 2008). The localizations of the *Nt*MCA1 and 2 proteins have also been detected on the immature cell division plate and the perinuclear membrane vesicles, suggesting their implication in the cell division regulation.

All these informations taken together tally with the FW2.2 protein localization and supposed functions and reinforce the idea that it can both have the role of an ion channel and a cell division regulator.

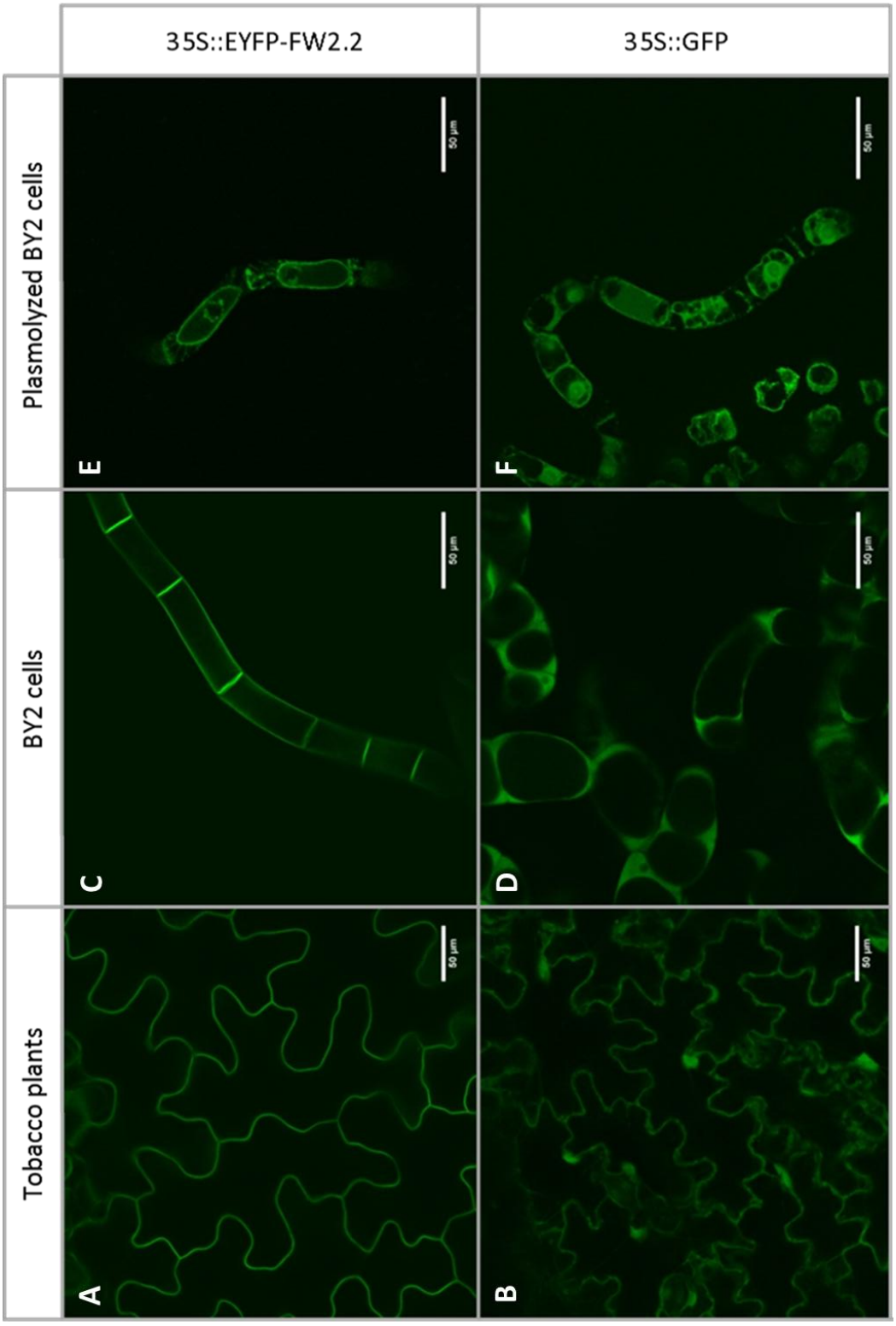

Figure 25: Microscopic observation with a magnification factor of 20 of the transgenic tobacco plants leaf epidermis overexpressing the *EYFP-FW2.2* (A) or the *GFP* (B)gene and BY2 cells overexpressing the same genes (respectively C and D). In an effort to determine the localization of the FW2.2 protein, the BY2 cells expressing the *EYFP-FW2.2* or the *GFP* gene have been plasmolyzed (respectively E and F). The EYFP-FW2.2 fusion protein seems to localize at the plasma membrane compared to the GFP protein that clearly localizes in the cytoplasm.

Using *Arabidopsis* plantlets that transiently overexpress the recombinant EYFP-FW2.2 protein, we noticed that the recombinant EYFP-FW2.2 protein localized according to punctuations all over the membrane, in addition to the already observed localization at the plasma membrane (Figure 26).

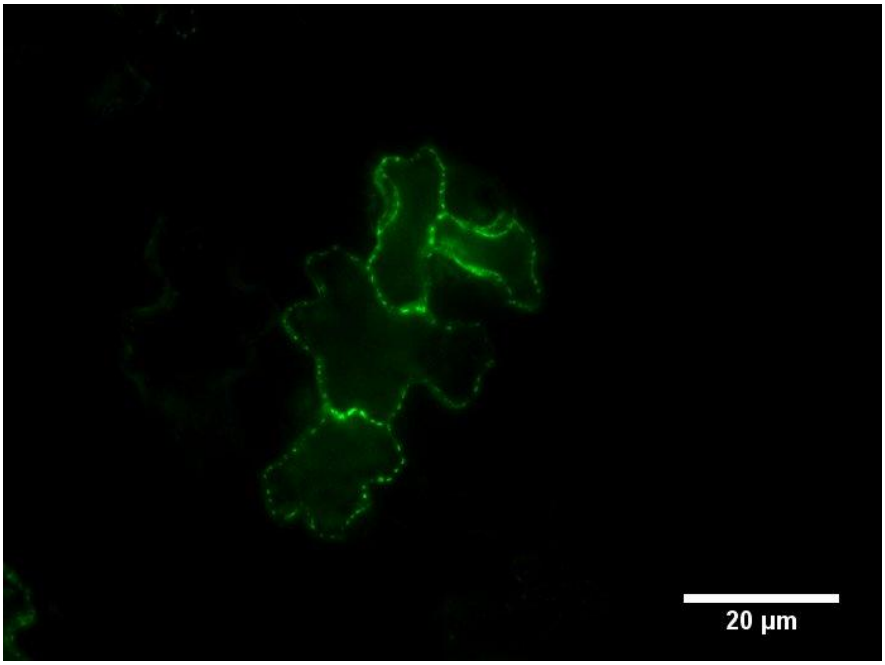

Figure 26: Observation of the EYFP-FW2.2 protein localization in transiently transformed *Arabidopsis* plantlets observed with an epifluorescence microscope with a magnification factor of 40. The fusion protein also seems to localize at the plasma membrane.

This punctuated localization has only been found in the transiently transformed Arabidopsis plant. The recombinant EYFP-FW2.2 protein did not colocalize with co-expressed markers specific of plasmodesmatas (data not shown).

We hypothesized that this punctuated localization could correspond to lipid rafts on the plasma membrane (Mongrand *et al.* 2010), but unfortunately we did not manage to obtain a double transformed cell that overexpress the recombinant protein and a raft marker protein.

b. Western blot on protein extract from Arabidopsis plants

To complete this localization work, we performed a Western blot on total membrane proteins and total soluble proteins from Arabidopsis plants overexpressing the EYFP-FW2.2 recombinant protein, the FW2.2 protein or the GFP protein alone. The EYFP and GFP

proteins were targeting with an anti-GFP antibody, in order to confirm the membrane localization of the protein (Figure 27).

We could observe that the recombinant protein was detectable in the membrane protein fraction (M) of the EYFP-FW2.2 (2) plant and that the GFP was only present in the soluble protein fraction of the GFP1 (1) plant, confirming that FW2.2 is actually localized at the plasma membrane.

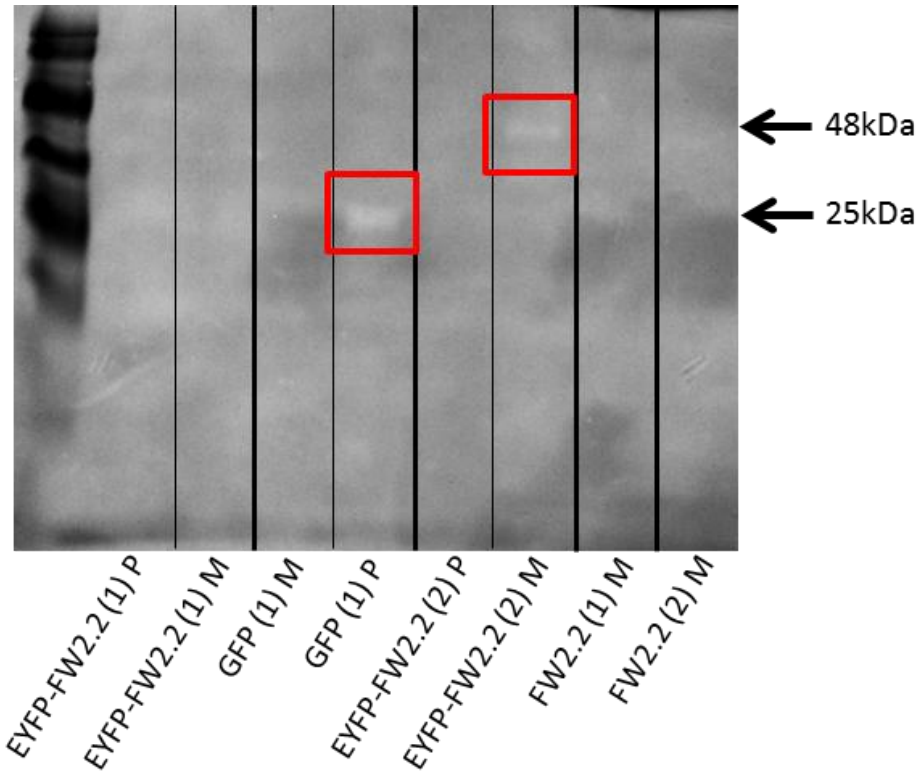

Figure 27: Western blot on the total membrane proteins and the total soluble proteins extracted from *Arabidopsis* plant. The EYFP-FW2.2 fusion protein is only detected in the membrane fraction whereas the GFP protein is only detected in the soluble fraction. P: soluble fraction; M: membrane fraction.

As shown in figure 27, two bands were detected: one of 48 kDa corresponding to the theoretical size of FW2.2 fused with the EYFP and another one of 25 kDa that corresponding to the size of the GFP alone.

The fact that FW2.2 localized at the membrane localization is an argument in favor of a channel function hypothesis. Furthermore the obtained microscopic images confirmed an exclusive plasma membrane localization.

In the other *FW2.2* overexpressing plants (EYFP-FW2.2 (1) and FW2.2 (1) and (2), we did not manage to observe the presence of the protein at the membrane. The absence of

detection of a band in the FW2.2 (1) and (2) plant samples were not surprising since the used total membrane protein extracts only served as negative controls to make sure that the anti-GFP antibody did not result in any unspecific detection. However for the EYFP-FW2.2 (1) plant extracts, we expected to detect the recombinant protein. It is then possible that protein degradation occurred and the amount of the recombinant protein became insufficient to be detected. Indeed the plasma membrane only represents 2 to 5% of the total cell membranes and FW2.2 is localized in this fraction. Protein degradation will impact greatly the total protein concentration and more particularly the plasma membrane proteins, making the detection of the recombinant EYFP-FW2.2 protein almost impossible. There is also the possibility that this transformed plant produce a very low level of FW2.2 protein that makes it difficult to detect using a western blot

2- Accumulation of minerals in the fruit pericarp and the BY2 cells

Like in all plants, tomatoes are able to store inorganic elements within cells. If FW2.2 is an ion channel, it is likely that a difference in mineral content could be detected if the expression of *SlFW2.2* is modulated.

We had the opportunity to work with 4 different lines of tomato plants: a wild type line of *Solanum lycopersicum* cv M82 with an undetermined growth (harboring the large fruit allele that we called M82 on the graphs) and a transgenic line of the same M82 cultivar in which two copies of the small fruit allele with its native promoter had been added by transgenesis (called M82+SF); 2 nearly isogenic lines, sharing the same genetic background and only differing by their *FW2.2* locus, the TA1143 line holding the large fruit allele and the TA1144 line holding the small fruit allele, respectively. The two couples of lines have been studied separately at the same time, each couple cultivated in the same conditions.

In the BFP laboratory, we do not have the competence and suitable equipment to perform such measurements. Therefore we required the help of the USRAVE laboratory (INRA Bordeaux), a service laboratory specialized in the analysis of plant mineral elements. This laboratory has the technical ability to perform these measurements and possesses sample treatment tools such as the ICP-MS (Inductively Coupled Plasma-Mass Spectrometry) and the ICP-OES (Inductively Coupled Plasma Optical Emission Spectrometry) and analysis tools necessary for this study.

a. Total ion content in the wild type and the transgenic line

The fruits used for this mineral content measurement of their pericarp have been harvested at a precise developmental stage on the M82 wild type line harboring the large fruit allele and on the M82 transgenic line harboring the large fruit allele in genetic background, in which two copies of the small fruit allele have been added by transgenesis. To ensure the fruits underwent the same culture conditions, the same stages of development of each line have been harvested the same day.

For this first couple of plants, we harvested fruits at 10, 20, 30 and 40 DAA and the total ion content was measured (see the complete mineral content measurement in appendix 1 and 2).

The results obtained allowed us to compare the content in major elements, such as calcium, iron and magnesium, and in trace elements. It appeared that the wild type line and the transgenic line showed a difference in storage for 3 trace elements during the fruit development (Figure 28).

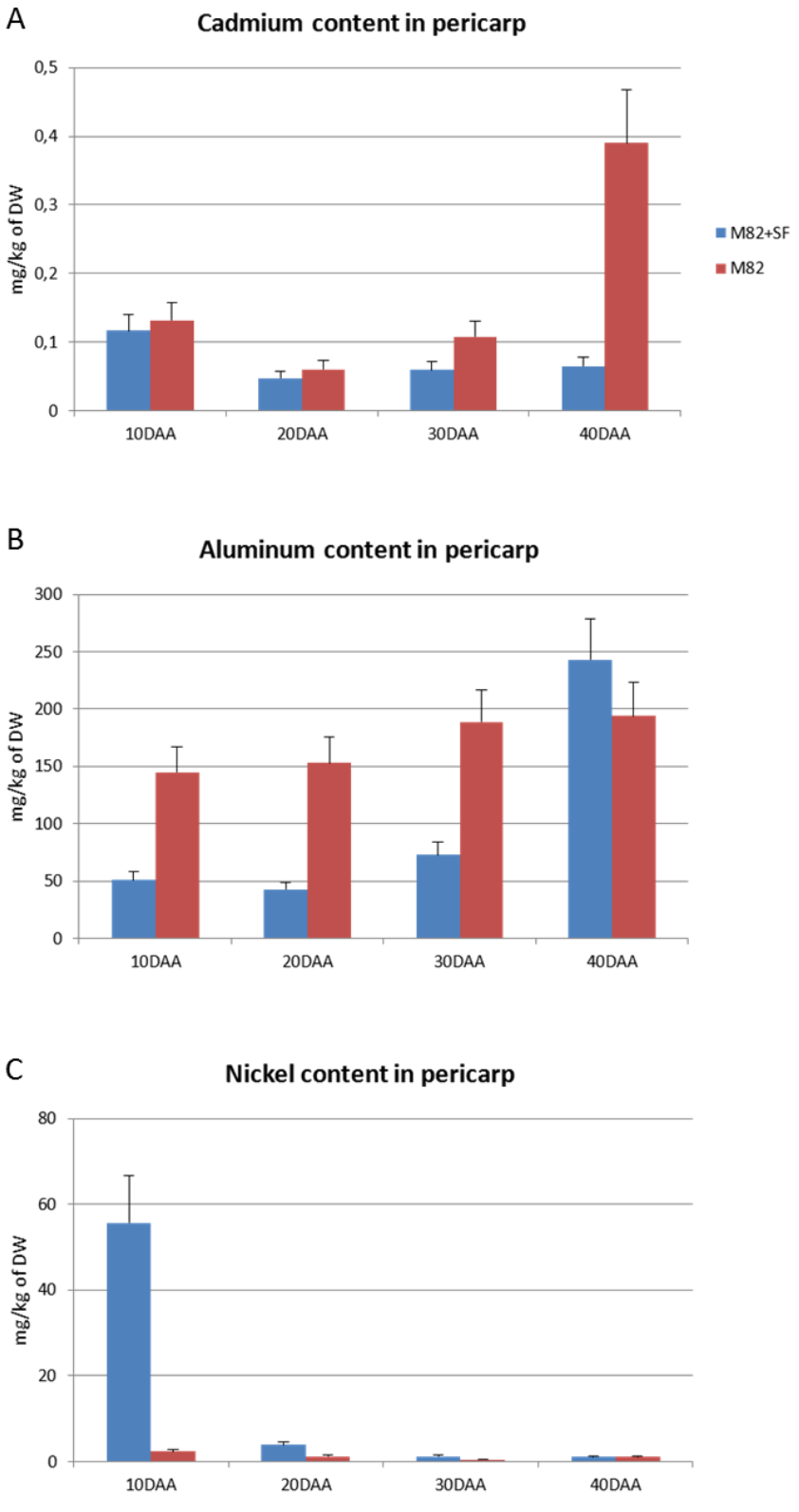

Figure 28: Pericarp content in cadmium (A), aluminum (B) and nickel (C) in the wild type (M82) and the transgenic line M82 holding two copies of the small fruit allele of FW2.2 (M82+SF) during the fruit development. The two lines show a difference of mineral accumulation in the pericarp during the fruit development. The *x* axis indicates the developmental stage (in DAA) and the *y* axis indicates the mineral content in milligrams per kilogram of dry weight (mg/kg of DW).

The two lines showed a difference in mineral accumulation during fruit development. The cadmium accumulation was equivalent for the first three stages of development examined although a little bit higher in the wild type line, and the accumulation increased greatly in the wild type M82 fruit pericarp at 40 DAA. The aluminum content was also different in the two lines: during the three first stages of development, the accumulation was higher in the wild type M82 fruits than in the transgenic M82+SF fruits; then the accumulation of the aluminum increased in the transgenic fruits to reach the accumulation level of the wild type fruits.

There was also a significant accumulation of nickel in the fruits of the transgenic M82+SF line at 10 DAA whereas very low quantities of nickel were measured in the other fruits. However we can see that the accumulation of nickel is still higher in the transgenic M82+SF line than in the wild type M82 line during the fruit development.

As the accumulation of these three elements varied during the tomato fruit development, we wandered whether it could be due to a variation in *FW2.2* expression.

In order to know if there is a correlation between the level of *FW2.2* expression in the two lines and the cadmium, aluminum and nickel contents, we measured the expression levels of *FW2.2* in the same fruit samples that were used for the measurement of total mineral content at the stages of development previously described (Figure 29).

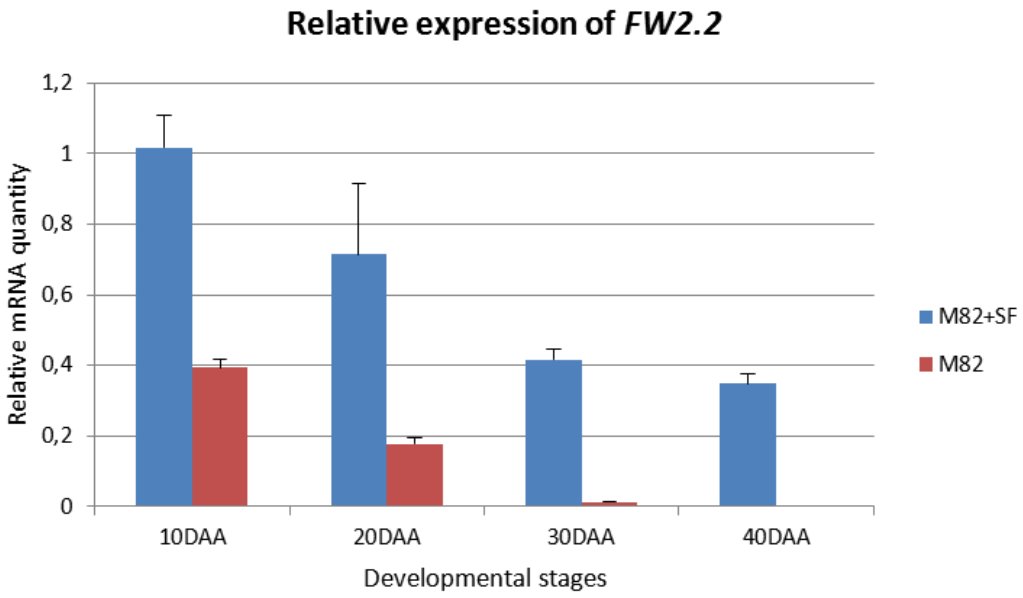

Figure 29: Expression of *FW2.2* in the pericarp of tomato fruits of the wild type M82 and the transgenic M82+SF lines at different stages of the fruit development.

When comparing the expression of *FW2.2* in the fruit pericarp during the fruit development, the content in aluminum and cadmium was inversely correlated with the expression of *FW2.2*: the higher the expression, the lower the accumulation of aluminum and cadmium in the pericarp. The accumulations did not seem to be proportional to the expression of *FW2.2*, but it seemed like the accumulation of these two elements depends upon a minimal threshold of expression under which the aluminum and cadmium are excluded from the fruit pericarp. The inverse correlation found between the accumulation of aluminum and cadmium and the expression of *FW2.2* led us to postulate that, if this channel function is confirmed, the FW2.2 protein may be a cadmium and aluminum exporter.

Concerning the nickel accumulation, it was measured at high quantities in the fruits of the transgenic line at 10 DAA, when the expression of *FW2.2* is at its highest level. This very high accumulation could be due on the one hand, to a minimum threshold of *FW2.2* expression above which there is a massive accumulation of nickel in the fruit pericarp. Indeed we can notice that the nickel accumulation remained higher in the transgenic M82+SF line that present a higher expression of *FW2.2* during the development. On the other hand an artifact in the sample preparation may have provoked a sample contamination with nickel. The visible correlation between the accumulation of aluminum and cadmium and the expression of *FW2.2* led us to postulate that the FW2.2 protein could be a nickel importer contrary to the aluminum and cadmium.

In order to confirm these correlations, a total ion content measurement was also performed using the fruit pericarp from NILs.

b. Total ion content in the nearly isogenic lines TA1143 and TA1144

The total mineral ion content was determined using the two NILs TA1143 and TA1144, which differ in the *FW2.2* allele, in order to confirm the differences of ion content in the previous measurements.

Two stages of fruit development were used because of the observed high difference in *SlFW2.2* expression: namely 15 DAA, where the *SlFW2.2* expression is very high in the TA1144 line and very low in the large fruited TA1143 line, and 30 DAA where both lines present a very low expression level of *SlFW2.2* (Figure 30).

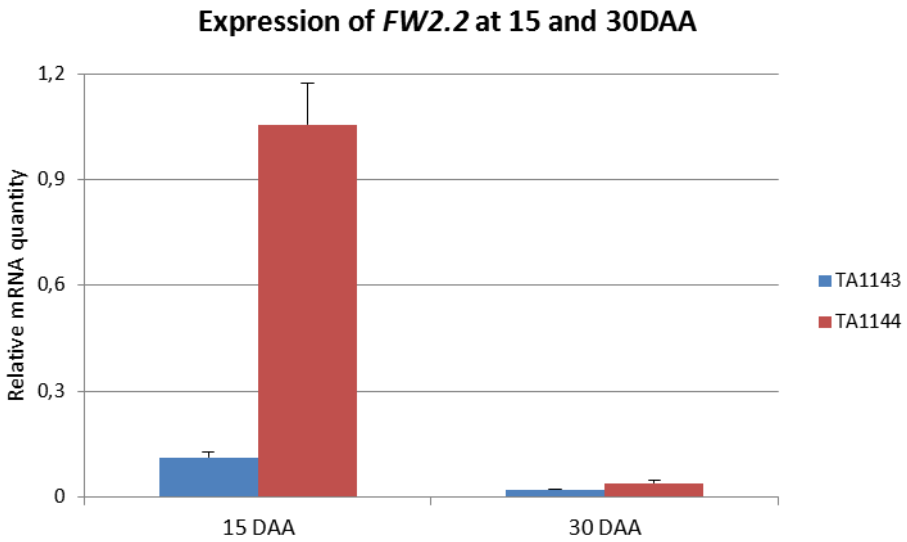

Figure 30: Expression of *FW2.2* in the pericarp of tomato fruits of the two nearly isogenic lines TA1143 (large fruit allele) and TA1144 (small fruit allele) at two stages of the fruit development.

The comparison of the total mineral ion content in the two lines at these two stages of development revealed three interesting differences in the content in zinc, copper and cadmium (Figure 31 - see the complete mineral content measurement in appendix 3).

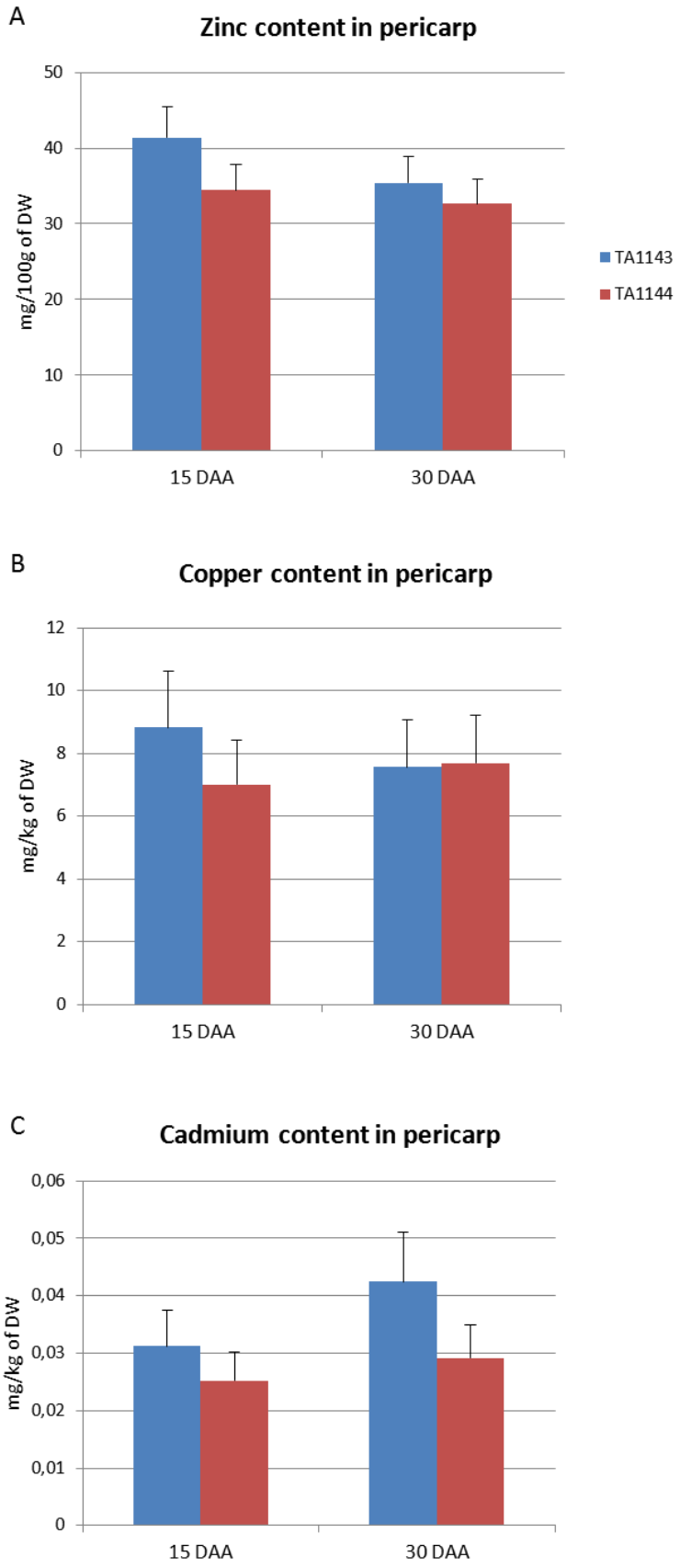

Figure 31: Pericarp content in zinc (A), copper (B) and cadmium (C) in the two NILs TA1143 (large fruit allele) and the TA1144 (small fruit allele) at two stages of the fruit development. The two lines show a difference of mineral accumulation in the pericarp during the fruit development. The *x* axis indicates the developmental

stage (in DAA) and the *y* axis indicates the mineral content in milligrams per kilogram or per 100 grams of dry weight (mg/kg of DW or mg/100g of DW).

Indeed, the zinc was found to accumulate at higher rates in the TA1143 line (large fruit allele) pericarp than in the TA1144 line (small fruit allele) pericarp (Figure 31A). Copper seemed to also accumulate at higher quantities in the large fruited line than in the small fruited line (Figure 31B). The higher levels of accumulation for these two elements in the large fruited line seemed to correlate with lower levels of *FW2.2* expression. However no quantitative correlation was observed, suggesting a minimal threshold of expression before observing a decrease in zinc and copper accumulation.

Interestingly the accumulation of cadmium was different in the two lines (Figure 31C). We previously observed a difference in cadmium accumulation in the M82 and M82+SF lines, correlating with the expression levels of *FW2.2.* In the two NILs, this correlation was also observed: the lower the expression of *FW2.2*, the higher the accumulation of cadmium in the pericarp.

This last observation reinforces the idea that FW2.2 protein could be a cadmium exporter in the cell.

We cannot conclude at present concerning the differences of accumulation for the other elements, but it is not excluded that a single ion transporter may display a transport activity for different elements.

c. Total ion content in the BY2 cells

As the fruits only provide information on the accumulation of mineral elements in the context of different FW2.2 allelic expression levels, we wondered whether the presence of absence of the *FW2.2* gene expression would induce stronger differences in the mineral content.

For this purpose, the total mineral ion content was determined using BY2 cells that overexpress the EYFP-FW2.2 recombinant protein, the 3HA-FW2.2 recombinant protein or the GFP protein alone to reveal differences in mineral accumulation for these lines (Figure 32 - see the complete mineral content measurement in appendix 4).

The expression of *FW2.2* has been tested in the two BY2 cell lines overexpressing the *FW2.2* gene fused with the *EYFP* gene or the *3HA* tagged gene and appeared to be equivalent in both of them (data not shown). In addition, the confocal microscopy observations allowed confirm the presence of the EYFP-FW2.2 recombinant protein inside

the cells, localizing at the membrane (see figure 25). If the EYFP fused protein allows the right localization of the protein, we can postulate that the 3HA-FW2.2 recombinant protein does too localize at the membrane. The line overexpressing the GFP protein was used as a negative transformation control, expected to behave like untransformed wild type cells.

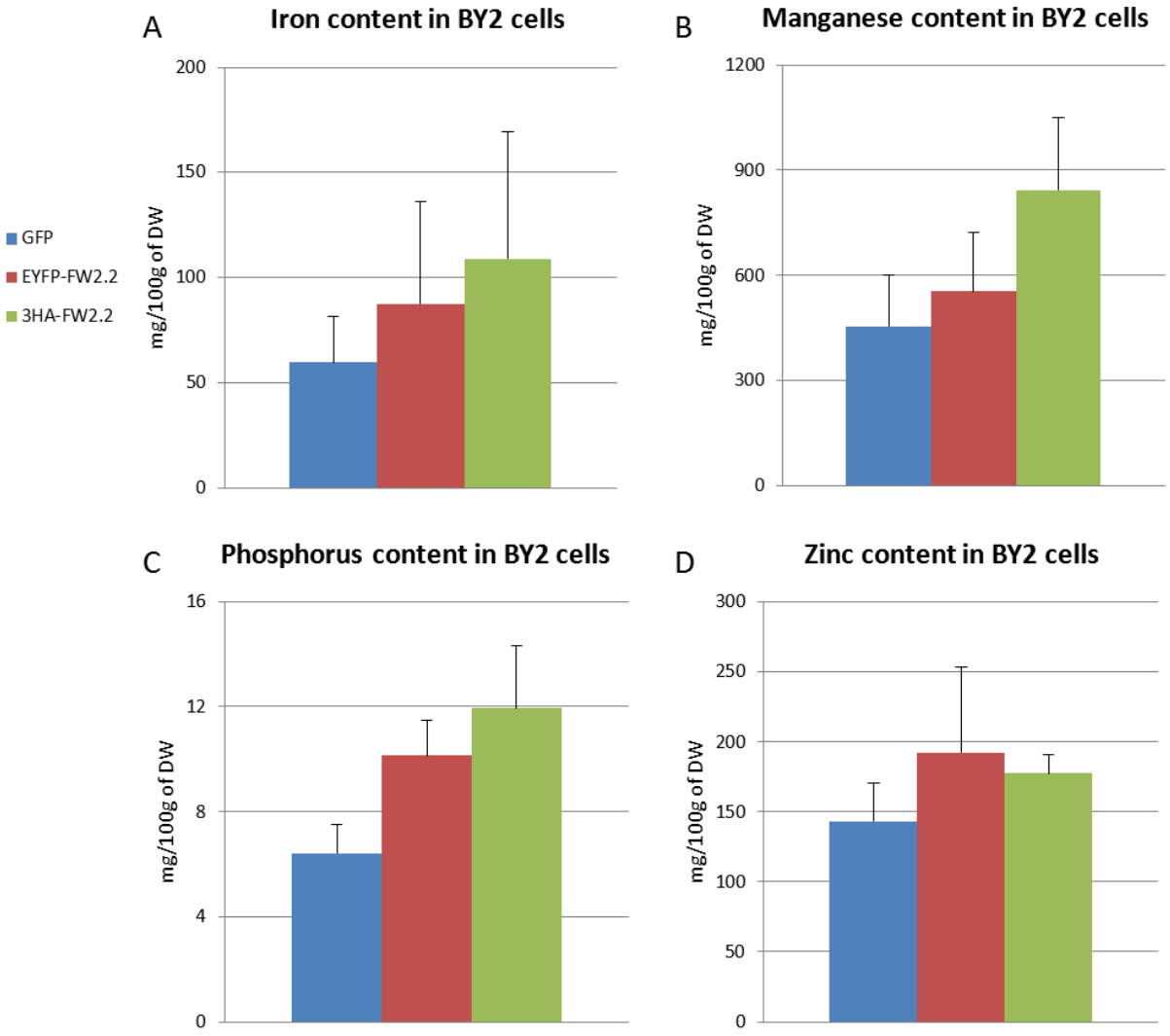

Figure 32: BY2 cells content in total irons (A), manganese (B), phosphorus (C) and zinc (D) in the three BY2 cells lines (indicated with a color code). The cells overexpressing FW2.2 whether fused with the EYFP or the HA tag accumulate higher levels of the 4 elements than the cells overexpressing the GFP protein. The *x* axis indicates the developmental stage (in DAA) and the *y* axis indicates the mineral content in milligrams per 100 grams of dry weight (mg/100g of DW).

The accumulation of iron, manganese, phosphorus and zinc appeared to be increased in the two lines overexpressing the FW2.2 protein whatever the presence of the fused EYFP or the HA tag. Even if the standard error bars may be misleading about the significance of the

observed differences, it clearly appeared that the lines overexpressing the FW2.2 protein accumulated higher levels of these 4 elements.

Ignoring the patterns of accumulation of total irons, manganese and phosphorus in fruits, this experiment suggest simply that the expression of the FW2.2 protein induced the accumulation of these three ion elements.

Concerning zinc, we observed in the NILs that lower levels of *FW2.2* expression led to higher levels of zinc accumulation in the fruit pericarp (Figure 31A). In the transformed BY2 cells, the sole presence of the FW2.2 protein provoked an increased accumulation of zinc (Figure 32D). This different behavior was therefore puzzling.

As FW2.2 was produced in a heterologous system (tobacco BY2 cells), the protein behavior may be consequently completely modified. Additionally, the production of the FW2.2 protein in the BY2 cells has provoked such a change in the cell biology that it could induce an abnormal accumulation of elements that are not supposed to be transported.

In the case of transformed BY2 cells, we cannot conclude clearly on the role of FW2.2 in relation to the mineral element transport. Conversely to the tomato fruits where the mineral content is measured on a tissue, the BY2 cells are individualized and directly in the contact of the external medium. The perturbation of the cell biology may explain that the accumulation of elements showed such dramatic changes.

3- Implication of FW2.2 in the plant resistance to heavy metals

In order to elucidate the FW2.2 protein function, we generated *Arabidopsis thaliana* transformed plants aimed at overexpressing *FW2.2* under the control of the 35S promoter. The obtained plants were confirmed to express the gene and to produce the protein (data not shown).

Song *et al.* (2004; 2010) showed that an overexpression of *AtPCR1* and *AtPCR2*, which encodes for proteins that share a high sequence homology with the FW2.2 protein, in *Arabidopsis* plants conferred to these plants the ability to grow on medium supplemented with cadmium and zinc respectively. The *Arabidopsis* plants overexpressing *FW2.2* were then testedin the same context to obtain similar growth potentials and to observe a putative heavy metal resistance.

The growth tests were performed on media supplemented with zinc or cadmium, because cadmium appeared to have a differential accumulation in the tomato fruit pericarp and both zinc and cadmium are the two heavy metals against which the PCR1 and PCR2 proteins

provide a resistance to overexpressing *Arabidopsis* plants. The plants were grown for 1 week on the medium supplemented or not with heavy metals (Figure 33) and the growth was then monitored.

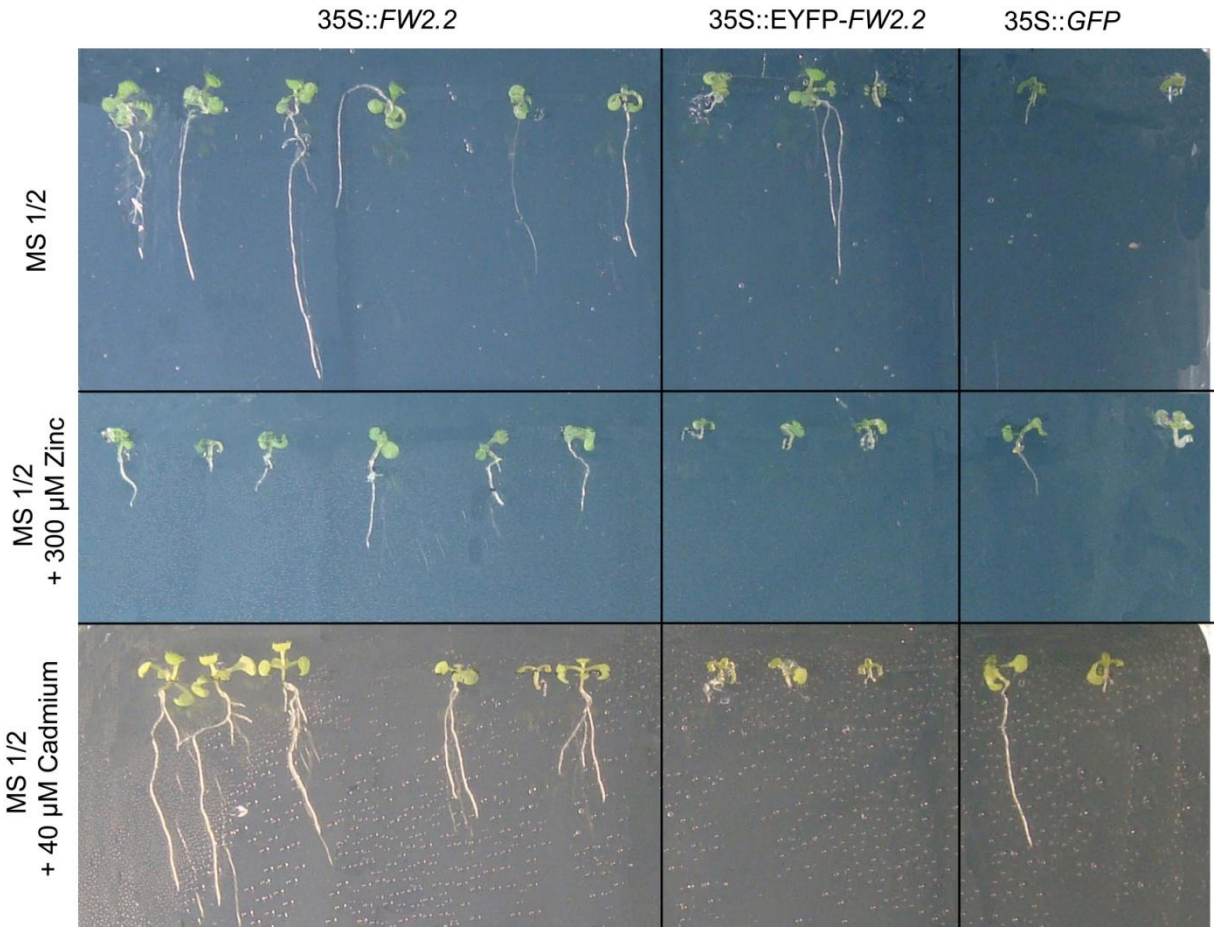

Figure 33: Growth test of *Arabidopsis thaliana* overexpressing the *SlFW2.2* gene or the fusion of the *EYFP* gene with the *SlFW2.2* gene. Plants overexpressing the *GFP* gene were used as a negative control. There is no clear difference of growth between the different plants.

We did not observe a significant growth difference between the transformants overexpressing the *FW2.2* gene alone of the *FW2.2* gene fused with the *EYFP* gene and the negative control (plants overexpressing the *GFP* gene). We noticed that the *GFP* overexpressors showed difficulties to grow on the ½ MS medium. However, if we compare the growth of the *FW2.2* overexpressors and the *GFP* overexpressors, we can see that both plant lines grew better on the medium supplemented with cadmium than the ½ MS medium. This is why we conclude that there was no difference in plant growth.

It may be that FW2.2 does not maintain its original function in *Arabidopsis* plantsbecause it does not find its natural protein partner. In the absence of its protein partners in

Arabidopsis, it may not form a functional channel and therefore may act as a heavy metal resistance protein for the whole plant. For this reason we carried on investigations that could help demonstrating the heavy metal channel function of FW2.2.

4- Experiment of voltage clamp

The voltage clamp technique is used in the electrophysiology field to study the ion currents through the membrane of excitable cells such as neurons or oocytes. This technique consists in holding the cell membrane voltage at a set level and measuring the membrane response. As the cell membrane of excitable cells contains different kinds of channels, some of them being voltage-gated, this allows the manipulation of the membrane voltage independently from the ionic current.

Xenopus laevis oocytes have been injected with RNA transcripts coding for *SlFW2.2*, in order to make the cell produce the FW2.2 protein, and subjected to a voltage clamp experiment in order to measure a channel activity.

The oocytes were injected with the RNAs of interest two days before the experiment and then stung with two electrodes, penetrating in the plasma, the first imposing a voltage and the second measuring the global depolarization in the oocyte.

The oocytes were placed in normal medium and media supplemented with cadmium or zinc in order to look for a modification in depolarization in the presence of heavy metals after the imposition of voltage levels, revealing an ion movement between the extracellular medium and the intracellular medium (Figure 34).

Two controls were used: un-injected oocytes that constituted our negative control and *AtPCR1* RNA injected oocytes that constituted our positive control. The PCR1 protein is indeed supposed to be a cadmium transporter according to Song *et al.* (2004); it was then expected to observe a depolarization modification in the presence of cadmium.

Control conditions : ND96 medium

Uninjected

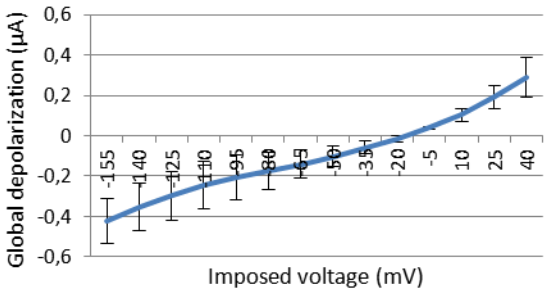

SlFW2.2

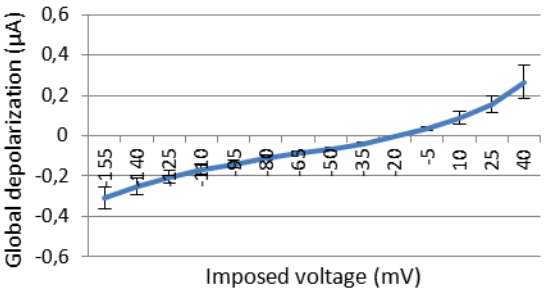

AtPCR1

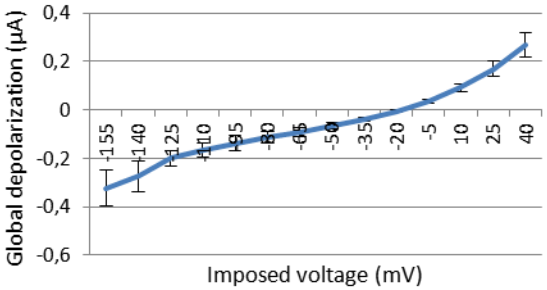

Test condition n°1: ND96 medium supplemented with 1mM Zinc

Uninjected (Zn)

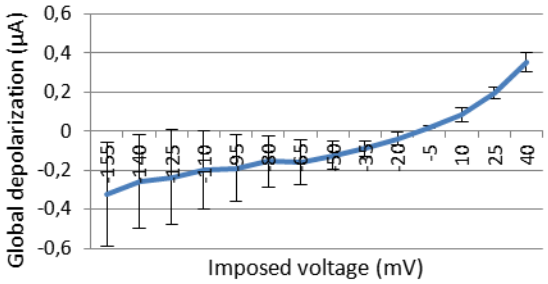

SlFW2.2 (Zn)

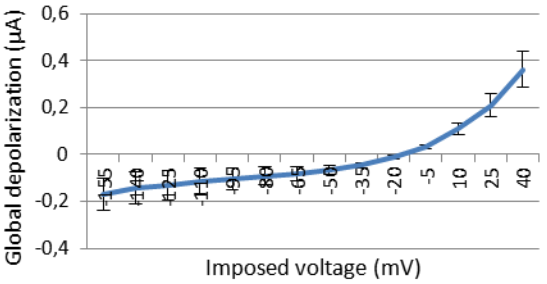

AtPCR1 (Zn)

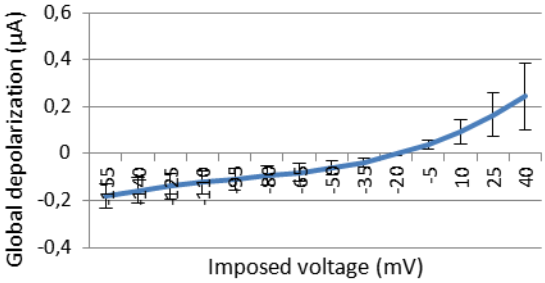

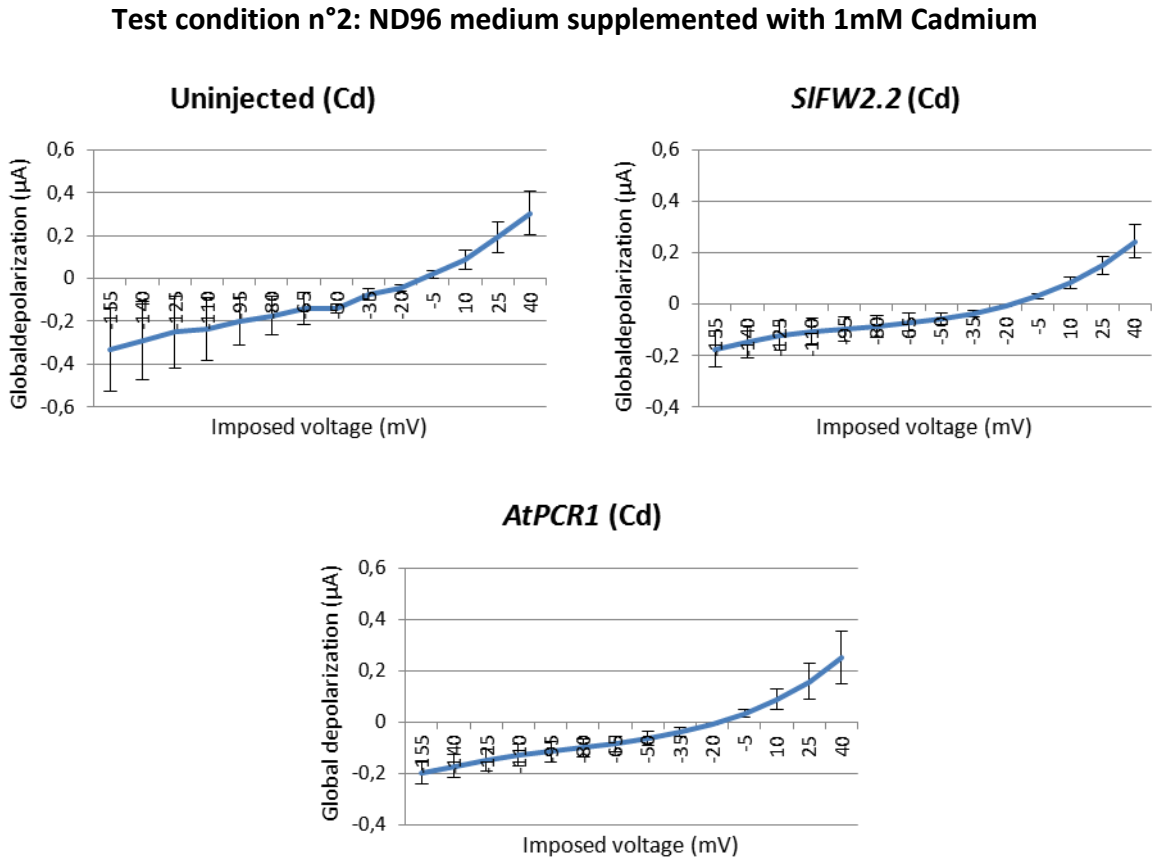

Figure 34: Global oocytes depolarization according to an imposed voltage. For the imposed voltages and the global depolarization measurement, the uninjected or injected oocytes were placed in ND96 medium supplemented or not with 1 mM cadmium (Cd) or zinc (Zn). No visible depolarization has been observed on any of the oocytes. The *x* axis indicates the imposed voltage value (in mV) and the *y* axis indicates the global depolarization value (in µA).

In every conditions tested, the *FW2.2* injected oocytes did not present any abnormal depolarization that could reveal an ion movement.

The membrane depolarization evolution of the oocytes injected with *FW2.2* is similar to the uninjected oocytes membrane and the inversion potential (imposed voltage that corresponds to an absence of membrane depolarization due to an ion movement balance between the two sides of the membrane) always situated around -20mV. A difference in the inversion potential could reveal the presence of a channel that create a significant ion movement and would provoke a shift in the inversion potential, which is here not the case.

However, the oocytes injected with *AtPCR1* RNAs in the presence of cadmium did not reveal any abnormal depolarization as expected from the model, which prevent us to make any conclusion on the experiment.

5- Conclusion regarding the "channel function" hypothesis

In the present state of this study, we have no clear evidence that FW2.2 can be a channel.

FW2.2 is apparently not involved in the cadmium and zinc resistance in tomato as its overexpression does not allow a better growth on medium supplemented with these heavy metals. It is also not involved in the transport of cadmium and zinc since oocytes that are supposed to produce the FW2.2 protein, do not show any change in the depolarization activity in the presence of these heavy metals.

However the PCR1 protein used as a control in this experiment does not seem to be implied in the exclusion of cadmium as though expected.

The accumulation of mineral elements in the tomato fruit pericarp showed some differences for aluminum, cadmium, nickel, zinc and copper content which seemed to be related to the expression levels of *FW2.2*, a cadmium difference of accumulation being observed in both couples of tomato fruit lines.

For this last reason, we shall notdismiss definitely the hypothesis that FW2.2 is a channel as these measurements were performed in tomato, where FW2.2 can find its potential partner(s).

Also it has to be kept in mind that the effect of FW2.2 in *Arabidopsis* and on the depolarization in oocytes was only tested in the presence of cadmium and zinc. These are only two heavy metals in the variety of heavy metals existing and we did not test the growth of the plants or the oocyte depolarization in the presence of aluminum. We can also suppose that FW2.2 can be a channel for other heavy metals rather than cadmium and zinc.

C. Regulation of the development

The work of Cong *et al.* (2002) showed that the difference in expression of the two *FW2.2* alleles provoked a change in the mitotic index inside the tomato fruit pericarp, revealing a higher mitotic activity in the small fruits than in the large fruits in the earlier stages of development. This differential mitotic activity, directly related to the differential expression of *FW2.2* at the onset of fruit development, suggests its implication in the cell cycle control as a mitosis inhibitor.

We showed earlier that FW2.2 is a membrane protein. Therefore the suggestion that the membrane localized FW2.2 can be a regulatory protein for the cell cycle control appeared to be puzzling. To address this question, we made use of the previously generated plant materials that overexpress *FW2.2* and report in the following section some interesting phenotypes.

1- Effect of FW2.2 expression on *Arabidopsis* development

To study the effect of *FW2.2* on plant development, the most appropriate plant materials would be transgenic tomato plants overexpressing the gene in the whole plant. Unfortunately, all previous works done on FW2.2 described the impossibility to stabilize tomato plant transformants that could overexpress the gene.

In order to circumvent this problem, we choose to study the effect of *SlFW2.2* in heterologous organisms with a short life cycle and consequently used *Arabidopsis thaliana* for the whole plant level and BY2 cells for the cellular level.

The first observations done on the *Arabidopsis* leaves and BY2 cells allowed us to observe dramatic phenotypic changes. We tried to understand better the causes of these developmental modifications in the transgenic lines we generated.

The first visible phenotype observed in the *Arabidopsis* transformants was an important plant size reduction (Figure 35A). This plant size reduction has been observed on 84 transformants of the T1 generation, coming from 11 independent transformation events, measured and statistically confirmed to be very significant with a T-test (Figure 35B).

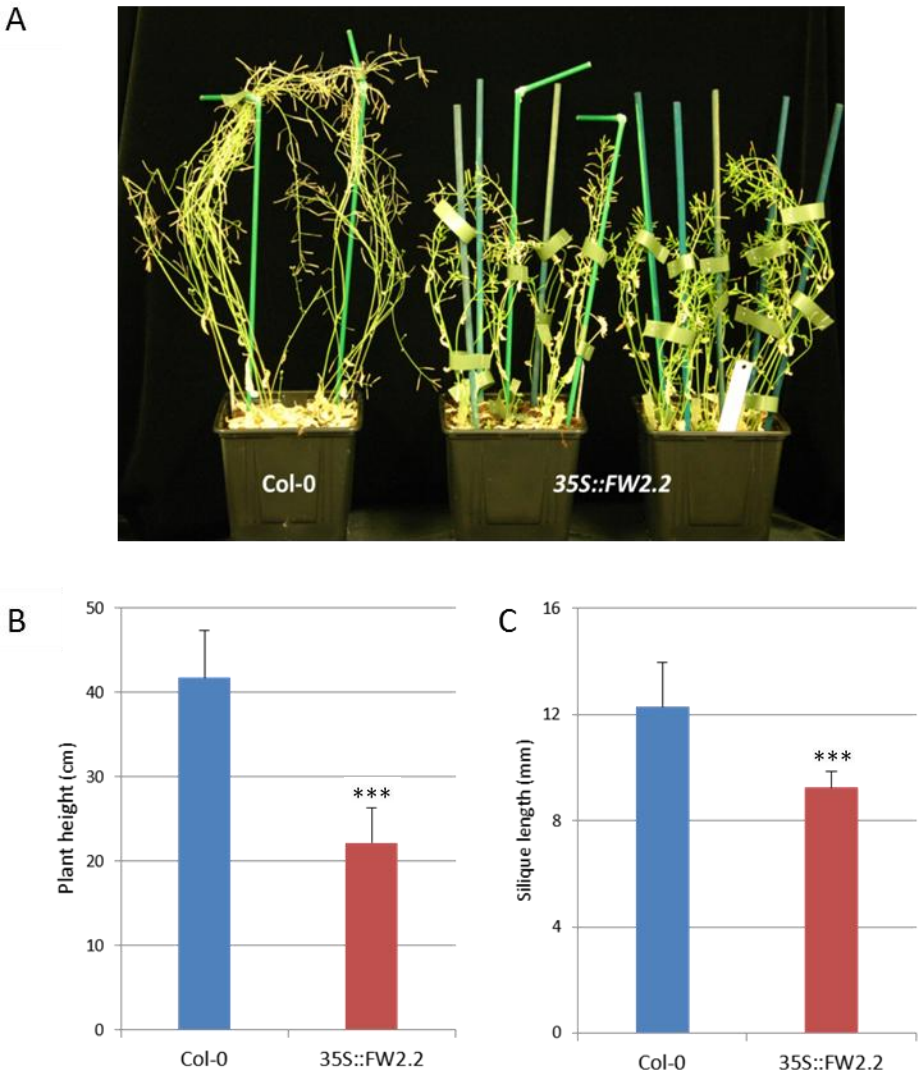

Figure 35: (A), *Arabidopsis thaliana* plants presenting a visible size reduction.(B), plant height and (C), silique length of the transformants overexpressing *FW2.2* under the control of the 35S promoter (35S::FW2.2) compared to wild type plants (Col-0). The measurements were performed on 10 wild type plants and 84 transgenic plants coming from 11 independent transformation events. The p-values obtained from the T- test were both <0.0005.

A significant size reduction was also noticeable for the length of the silique (Figure 30C).

With this dramatic size reduction, we wondered whether the reduction in whole plant and silique size was due to a cell size reduction or a cell number reduction, as described for the tomato fruits with the two different alleles of *FW2.2.*

To answer this question, we observed the *Arabidopsis* leaf epidermis to determine which event was responsible for this phenotype (Figure 36). The leaves of the transformants also displayed a dramatic cell phenotype as the cell size was clearly reduced and the stoma density increased in the *FW2.2* overexpressor (Figure 36B).

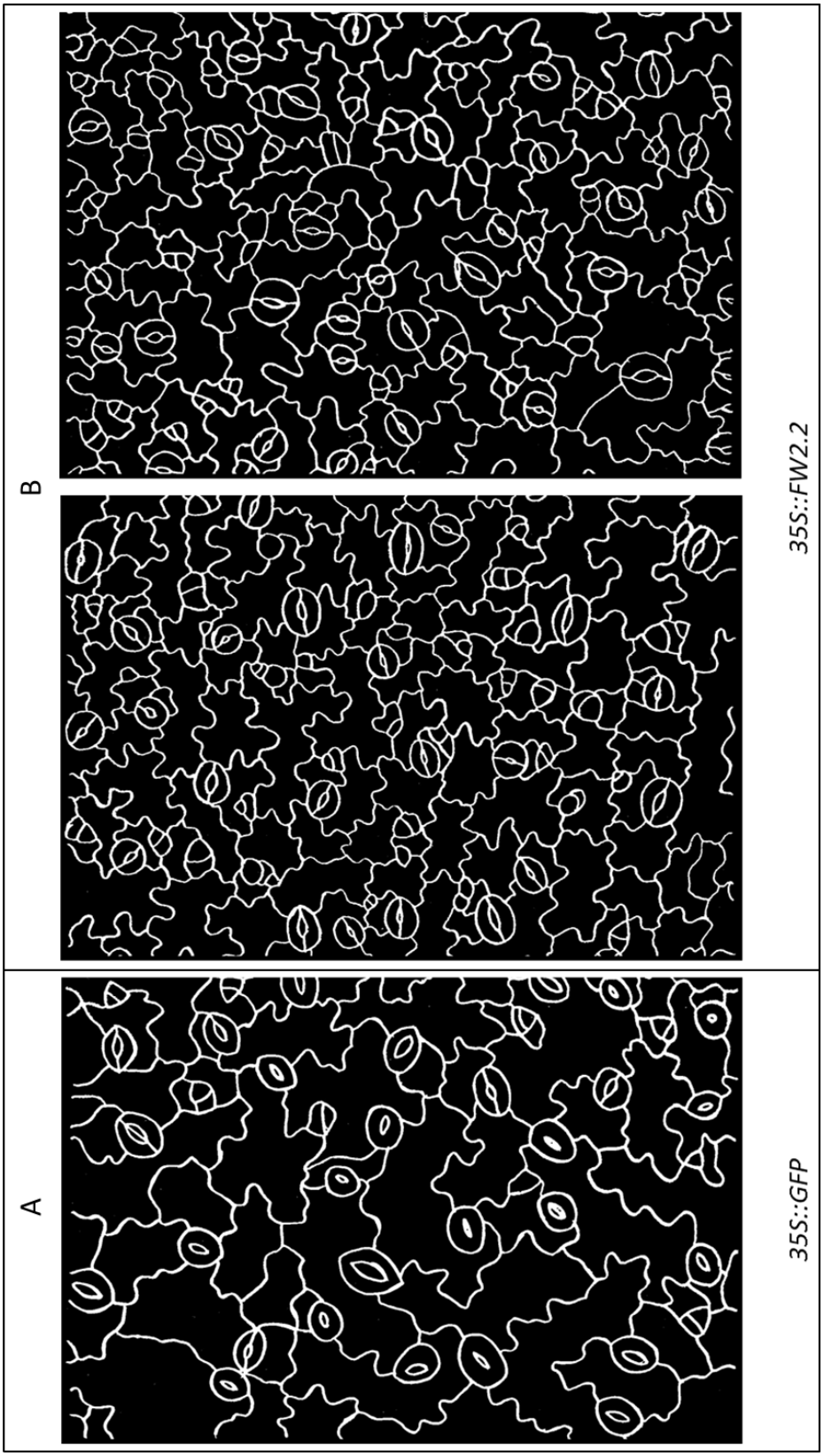

Figure 36: Leaf epidermis cell outline of *Arabidopsis thaliana* plants overexpressing the (A) *GFP* gene (considered as a negative transformation control) or the (B) *FW2.2* gene under the control of the *35S* promoter, observed with a magnification factor of 20. The leaf epidermis cell outlines of the *FW2.2* overexpressor have been obtained from 2 independent plant transformation lines. The transformants leaves display a dramatic cell phenotype with a reduced cell size and an increased stoma density.

The number of cells and stoma per mm² have been measured in the two lines of plants. As the measurement of the mean cell size in the two lines gave results with very high standard deviation, due to an important cell size variation within the epidermis, we could not conclude easily on the observed difference. We then choose to focus on the number of cells and number of stoma per mm² to interpret the changes in cell size in the plants (Figure 37).

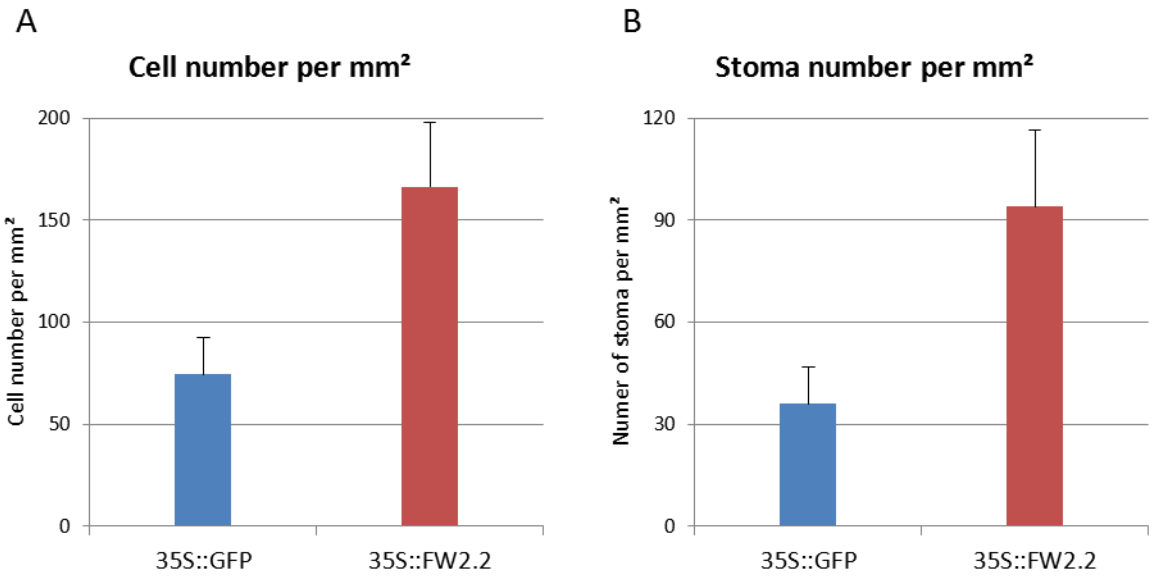

Figure 37: Measurement of the cell number (A) and stoma number (B) per mm² in the *Arabidopsis* transformants leaves. The cell number and stoma number per mm² are both clearly increased in the *FW2.2* overexpressors.

The *FW2.2* transformants displayed twice as much cells per mm² than the negative control transformants (Figure 37A) and almost three times as much stoma per mm² (Figure 37B). The measurements have been performed on 8 *FW2.2* transformed plants coming from 4 independent transformation events and on 2 *GFP* transformed plants coming from 2 independent transformation events.

These measurements correlated with the significant plant size reduction and the visible size reduction of the cells on the leaf epidermis cell outlines. Two hypotheses could be drawn at this stage.

First having in mind that *FW2.2* is an inhibitor of cell mitosis during tomato fruit development, and more broadly a cell number regulator (as named CNR in *Zea mays*; Guo et

al. 2010), we hypothesized that *FW2.2* induces a slower cell cycle in the *Arabidopsis* transformed plants. This effect on the cell cycle could be revealed by a modification in the expression of key genes controlling the cell cycle. As described above, the increased number in cells and stoma is likely to be due to a higher density of cells at the surface of the leaf, according to a similar phenotypic pattern that was described in *Arabidopsis* plants overexpressing *CyclinD3.1* (Dewitte *et al.* 2003) (Figure 38).

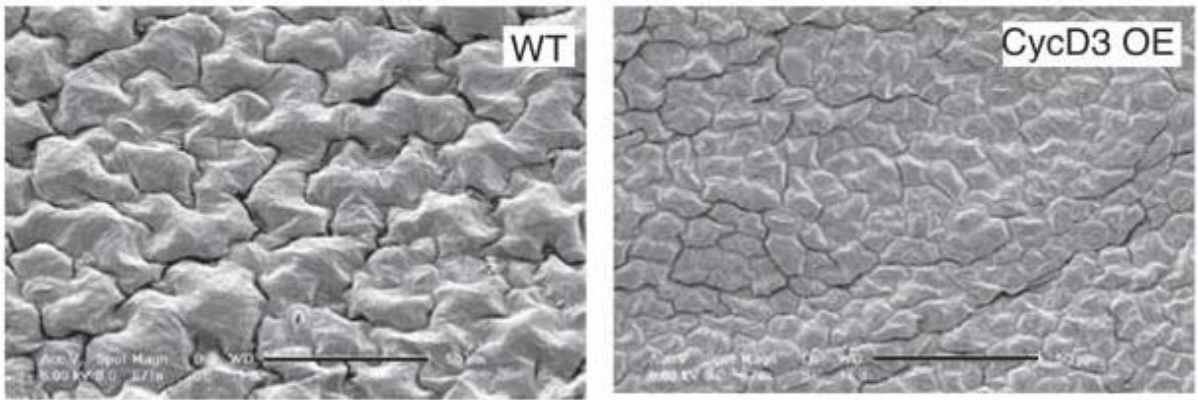

Figure 38: Scanning electron micrographs of the adaxial leaf epidermis of wild-type (WT) and *CyclinD3.1* overexpressor (CycD3 OE) in *Arabidopsis* plants (from Dewitte *et al.* 2003).

Second, similar phenotypes of modified stoma density have been reported in the literature. Actually, several mutants in the brassinosteroid pathway display the same increased number of stoma coupled with a cell size reduction. The *bri1-116* and the *bin2-1Arabidopsis* mutants, respectively affected in the brassinosteroid perception and transduction signals, show an affected stoma proliferation in the epidermis (Kim *et al.* 2012). Therefore, the involvement of hormone, and especially brassinosteroids, in the control of cell proliferation could be the second hypothesis to be tested, in light of the reported literature data in *Arabidopsis* (Hu *et al.* 2000).

To address the first hypothesis, we measured the expression levels of the *CycD3.1* gene in the transformed plants and it appears that there was no noticeable difference between the two lines. Since a precise kinetic study of gene expression related to cell cycle control is complicated to perform and poorly informative using non-synchronized cells, we shall try in a future work to monitor these gene expressions in synchronized cell cultures.

Concerning the second hypothesis, seeds of the *Arabidopsis* trangenic plantswere sawn on medium containing different brassinosteroid derivatives that mimic the effects of the brassinosteroid hormone (brassinolide), activates (bikinin) or inhibits the brassinosteroid signaling pathway (brassinazole). The work is at present in progress.

2- Effect of FW2.2 expression on the development of tobacco BY2 cells

To study the effect of FW2.2 at the cellular level, BY2 cells were transformed with a construct aimed at producing the recombinant FW2.2 protein fused to EYFP protein and with a construct expressing the GFP protein alone. Alike the dramatic effects observed for the *Arabidopsis FW2.2* overexpressingplants, interesting phenotypes were similarly observed in the transformed BY2 cells.

The first observed phenotype was a modification in the cellular shape during the culture cycle. When reaching the plateau phase of development (7-8 days of culture), the transformants overexpressing the EYFP-FW2.2 protein show an elongated shape. We manage to measure the cell length and width in order to render the shape change (Figure 39).

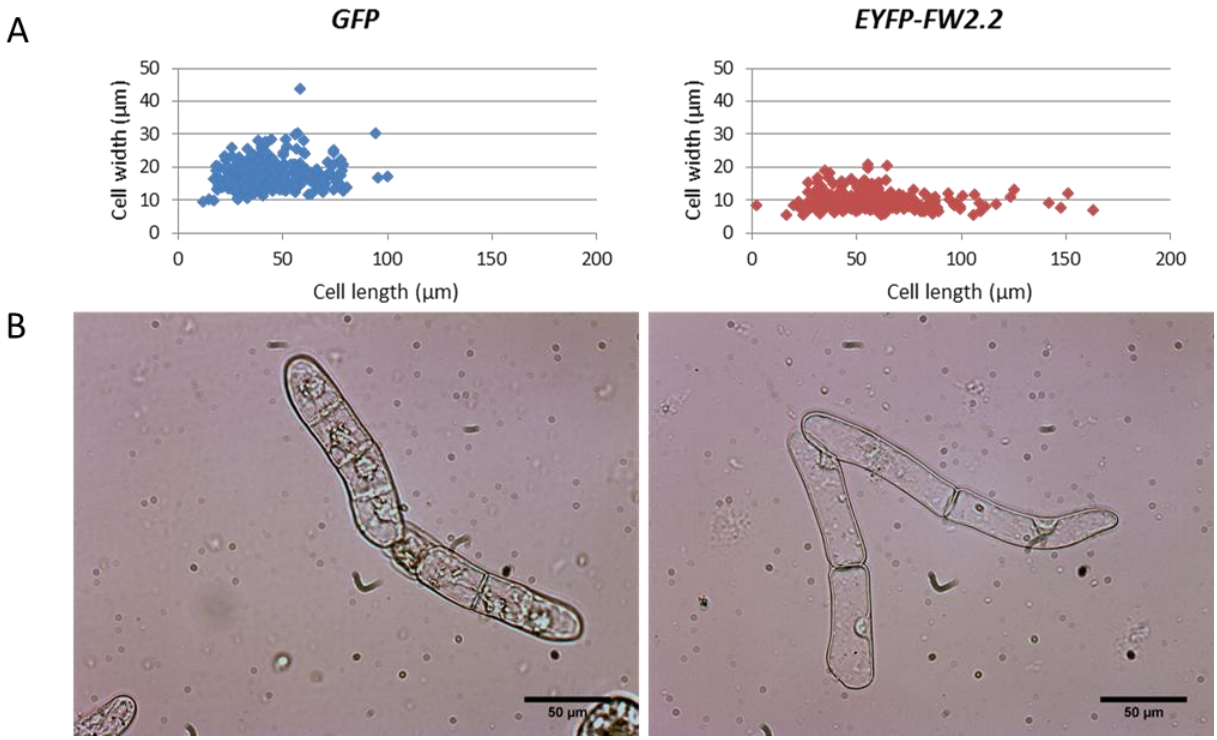

Figure 39: BY2 cell shape in the control cells (GFP) and the cells overexpressing the *FW2.2* gene. A) Scatterplot showing the width to length relationship in both control (*GFP)* and *FW2.2* overexpressing BY2 cells. B) The typical morphologies of cells after 7-8 days of culture are illustrated.

The measurements performed and graphically reported in scatterplot allow a better representation of the shape change in the transformants cells. The comparison of the two scatterplots show that the BY2 cells that overexpress the recombinant EYFP-FW2.2 protein present an increased length compared to that of the cells producing the GFP protein, which also appear to be larger than the EYFP-FW2.2 overexpressing cells. The *EYFP-FW2.2* overexpressors indeed see their cell shape elongate and become thinner during the cell culture cycle.

Interestingly, a similar modification in the shape of BY2 cells has been already described in the literature, as the result of an auxin deprivation (Winicur *et al.* 1998) (Figure 40).

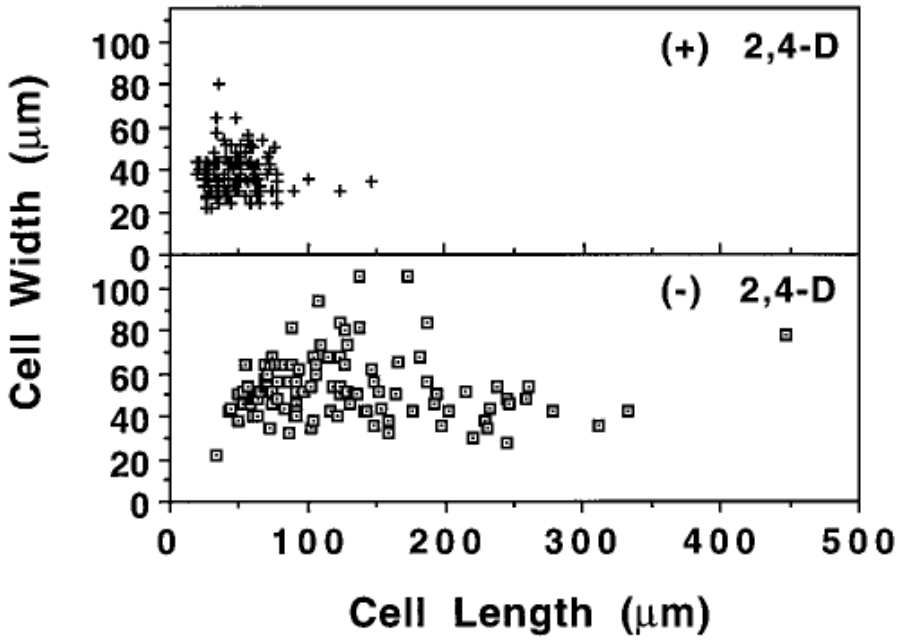

Figure 40: Scatterplot showing the length and width of both control and auxin deprived cells (from Winicur *et al.* 1998). The *FW2.2* overexpressing cells show higher length values and lower width values compared to the control *GFP* overexpressing cells, which reveals an elongated shape.

As we observed a similar shape variation in the BY2 FW2.2 overexpressors, we could wonder whether the FW2.2 overexpressors are less sensitive to auxin than the control cells.

This effect on cell elongation in BY2 cultured cells has been also reported for brassinosteroid. Miyazawa *et al.* (2003) showed that increasing the concentration of brassinolide (a form of brassinosteroid) in the culture medium induced a shorter cell length together with increased cell proliferation. This last observation about cell multiplication is all the more interesting, since the *FW2.2* overexpressing BY2 cells seemed to grow more slowly than the control cells.

Consequently, a kinetic study of cell growth over the culture period was performed as to confirm a lower multiplication rate. Unfortunately, we encountered problems in stabilizing the *FW2.2* transgenic cell culture. At present, we still work at maintaining viable cell cultures during the first subculture cycles before performing growth kinetics on several days. Indeed, the *FW2.2* transgenic cells after 3 subcultures, showed a degeneration to finally completely arrest growth before reaching the saturation plateau, thus totally impairing a kinetic study based on the packed cell volume or on the cell fresh weight per milliliter of culture.

When the matter of cell culture stabilization is solved, we shall keep on exploring the hormonal regulation hypothesis in BY2 cells and also investigating whether a relationship between brassinosteroid and the cell cycle control may occur.

3- Conclusion on the developmental effects of FW2.2

It is very interesting to observe that both *Arabidopsis* and BY2 cells overexpressing *FW2.2* showed phenotypes that seemed to be related to the brassinosteroid regulation or perception. An inhibition of the brassinosteroid pathway could explain both the elongation of the BY2 cells and the increased density in stoma within the *Arabidopsis* leaf epidermis.

In both *Arabidopsis* and BY2 cells, the control of the cell cycle through the brassinosteroid pathway has already been questioned and Hu *et al.* (2000) showed that the brassinosteroids have a positive effect on the mitotic activity through the induction of the *CycD3.1* in *Arabidopsis.* This could explain that both *Arabidopsis* and BY2 cells overexpressing *SlFW2.2* seem to be affected in the cell cycle.

Since FW2.2 is a membrane-localized protein of relatively short size (163 amino acids), a putative implication in hormonal sensing could make sense, but still does not explain how this small protein interferes with the cell cycle regulation.

D. Involvement of FW2.2 in the cell cycle regulation

In this fourth part of the work, we tried to figure out how FW2.2 is able to control the cell cycle and, according to its subcellular (membranous) localization, investigated the protein-protein interaction network FW2.2 may require for its cell cycle regulatory function.

1- Control of the cell cycle

Since FW2.2 is known to be a negative regulator of the mitosis, we hypothesized that the genes implied in the control of the cell cycle must be down or upregulated in the fruits where the *FW2.2* expression during their development could be altered.

We used the two isogenic lines TA1143 and TA1144 differing in the *FW2.2* allele (large-fruited allele versus small-fruited allele) to check the expression of cell cycle regulatory genes, either involved in the canonical cell cycle or the onset of endoreduplication.

The set of genes tested for the expression study includes:

- the *SlCCS52A* gene involved in the onset and regulation of the endoreduplication process (Cebolla *et al.* 1999; Lammens *et al.* 2008; Boudolf *et al*. 2009; Larson-Rabin *et al.* 2009; Mathieu-Rivet *et al.* 2010);
- the *SlCCS52B* gene that is expressed during the cell division phase of early tomato fruit development (likely to be mitosis specific) (Mathieu-Rivet *et al.* 2010a);
- the *SlCDKB1* gene that encodes for a Cyclin Dependent Kinase specific of the G2/M transition (Boudolf *et al.* 2004; Inzé and De Veylder, 2006; Boudolf *et al*. 2009) which is considered as a perfect gene marker for commitment to mitosis, effectively induced during the cell division phase of tomato fruit development (Joubès *et al.* 2001);
- the *SlCK2*β*1* gene encodes a protein supposed to be an in vitro interactor of the FW2.2 protein (Cong and Tanksley, 2006);
- the *SlCycD3.1* gene that encodes a G1/S specific cyclin (Joubès *et al*. 2000; Dewitte *et al.* 2007);
- the *SlIMA* gene that encodes a protein that described as an inhibitor of meristem activity, and likely to be a negative regulator of cell proliferation (Sicard *et al.* 2008);
- the *SlKRP4* genethat belongs to the *KRP* family and encodes a specific CDK/Cyclin complex inhibitor (Nafati *et al*. 2011).

The gene expression studies have been performed using RT-PCR experiments and cDNAs prepared from developing fruits, from anthesis to 30 DAA (Figure 41).

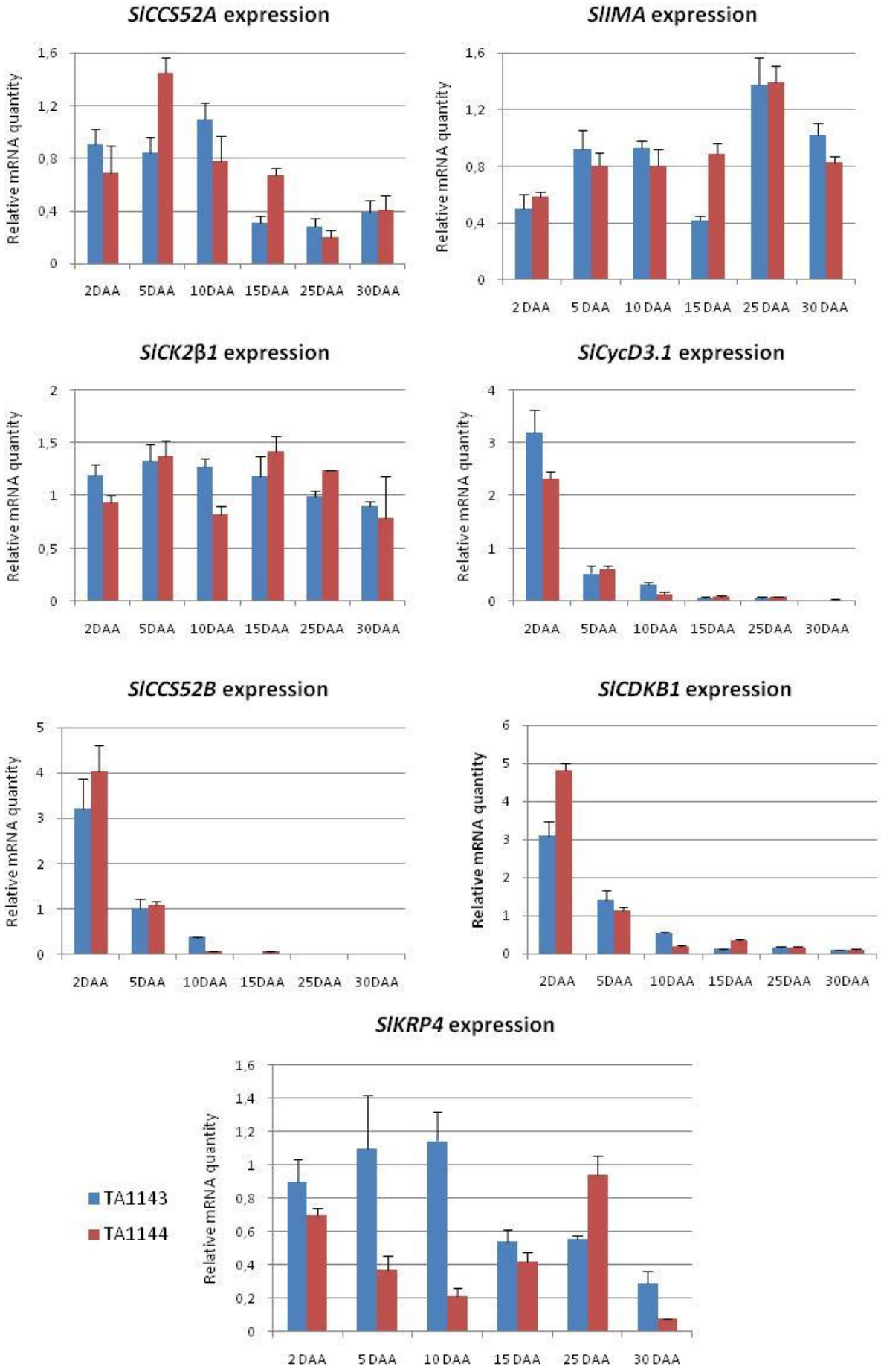
SlCCS52A expression
SlIMA expression
SlCK2β1 expression
SlCycD3.1 expression
SlCCS52B expression
SlCDKB1 expression
SlKRP4 expression
Relative mRNA quantity
2DAA
5DAA
10DAA
15DAA
25DAA
30DAA
TA1143
TA1144

Figure 41: Expression of cell cycle control genes in the TA1143 line (large fruit allele – blue bars) and the TA1144 line (small fruit allele – red bars) during the tomato fruit development. The TA1143 anthesis stage and TA1144 20DAA stage have not been treated. The genes expressions have been measured using RT-PCR and show some differences between the two lines.The *x* axis indicates the developmental stage (in DAA) and the *y* axis indicates the relative mRNA abundance.

As a first observation, no difference in expression level occurred for the *SlCK2β1* gene amongst the two lines. We could not identify any significant and developmentally relevant differences for the expression of *SlIMA* in the two lines.

A significant difference in gene expression for the two lines was observed for the *SlCDKB1* gene, a marker of mitosis. Interestingly, the levels of expression correlated with the mitotic index at 2 DAA that were measured by Cong *et al.* (2002) (see Figure 11 in the Introduction section): the small fruited line TA1144 displayed a higher mitotic activity than the large fruited line TA1143, and clearly the *SlCDKB1* gene was much more expressed accordingly (Figure 41). Although weaker at 5 and 10 DAA, the expression level of *SlCDKB1* in the large fruited TA1143 line is reversed compared to the small fruited TA1144 line: in these developmental stages the expression of *SlCDKB1* is decreasing in both lines but still maintained at a higher level in the large fruited line, where the mitotic activity is also maintained for a longer period than in the small fruited line.

An almost similar pattern of gene expression was observed for the *SlCCS52B* gene which was found to be essentially associated to cell proliferation during tomato fruit development (Mathieu-Rivet *et al*. 2010).

The pattern of gene expression for *SlCycD3.1* seemed opposite to that *SlCDKB1* and *SlCCS52B*: the *SlCycD3.1* expression peaked at 2DAA and was higher in the large fruited line than in the small fruited line. Since *SlCycD3.1* is a marker of the G1/S transition, the peak of expression at 2 DAA was fully associated with the mitotic activity occurring in this early stage of development, and the difference in gene expression among the two lines could reflect a quantitative difference in the number of cells remaining at the G1 phase and ready to commit to S, or already engaged in the subsequent G2 and M phases of the cell cycle.

The *SlCCS52A* gene was used as a marker of the onset of endoreduplication (exit from mitosis and entry into endoreduplication-driven cell expansion; Chevalier *et al*. 2011). Interestingly, the peak of expression of *SlCCS52A* in the large fruited line (TA1143) occurred at 10 DAA, while it occurred in the small fruited line (TA1144), at 5 DAA. These respective patterns of expression were in total agreement with the mitosic activity which lasts longer in the large fruited line (TA1143) (up to 10-12 DAA, Figure 11) than in the small fruited line

(TA1144) (up to 4-5 DAA, Figure 11), thus explaining the differential effects on final fruit size. The last gene expression we tested was that for *SlKRP4*.The *SlKRP4* expression kinetics in the two lines gave striking differences. Indeed, the patterns of *SlKRP4* expression were completely opposite in the two lines. Interestingly, when the *SlKRP4* expression was compared to that of *SlFW2.2*, a clear inverted correlation between the expression of *SlFW2.2* and the expression of *SlKRP4* was observedduring the fruit development (Figure 42). To summarize, when the expression of *FW2.2* is at its lowest in the tomato fruit, the *SlKRP4* expression is at its highest, and conversely.

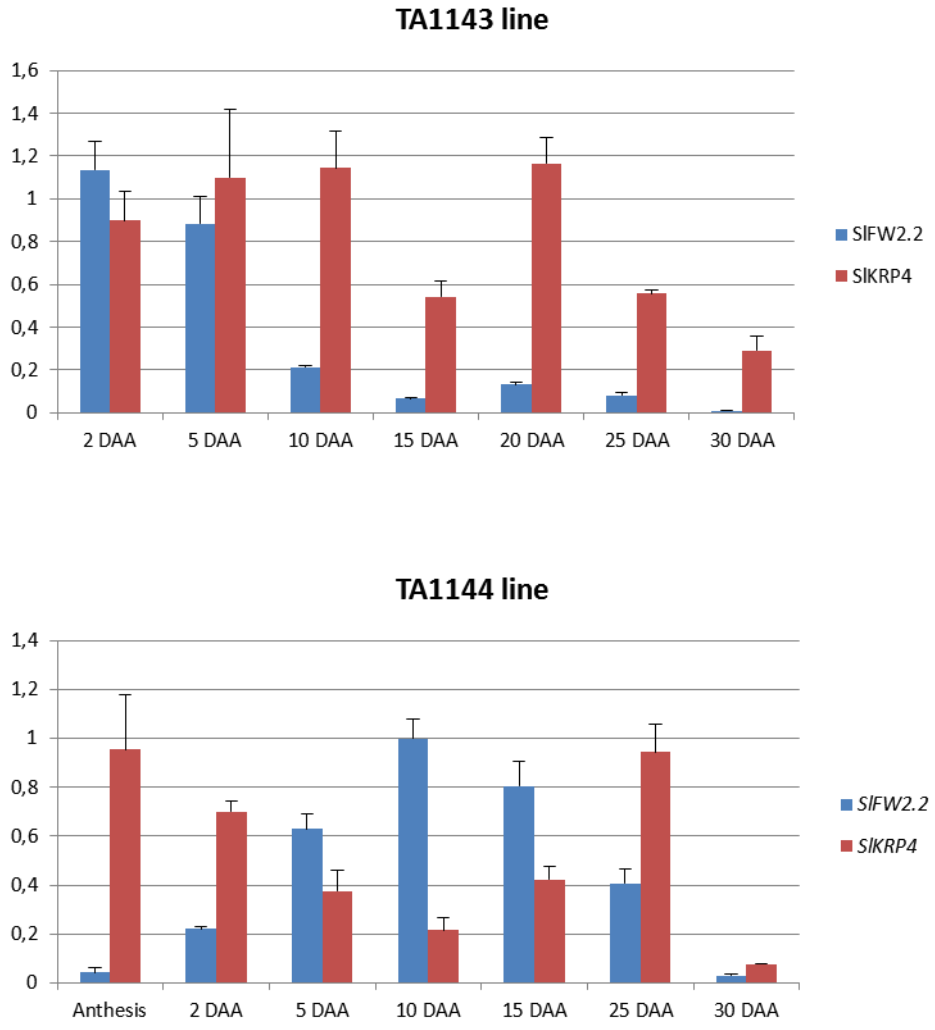

Figure 42: Comparison of the *SlFW2.2* and *SlKRP4* gene expression in the two NILs during the tomato fruit development. The expression of the *SlKRP4* gene is opposite in the two lines. The *x* axis indicates the developmental stage (in DAA) and the *y* axis indicates the relative mRNA abundance.

During tomato fruit growth, both cell proliferation and endoreduplication-driven cell expansion account for the determination of final fruit size (Joubès *et al.* 1999; Cheniclet *et al.* 2005; Chevalier *et al*. 2011). Therefore, it was important to check whether the modifications of cell cycle and endocycle gene expression in the two lines TA1143 and TA1144 correlate with any modification in nuclear DNA content, *i.e.* the endoreduplication level.

The determination of the endoreduplication index in fruit pericarp of the two lines showed that it was higher in the small fruited TA1144 line than in the large fruited TA113 line (Figure 43). From anthesis to 5 DAA, the endoreduplication index was similar, but thereafter clearly increased in the TA1144 line. This increase occurred concomitantly to the peak of mitotic index in the TA1144 line, as well as the peak of *SlCSS52A* gene expression.

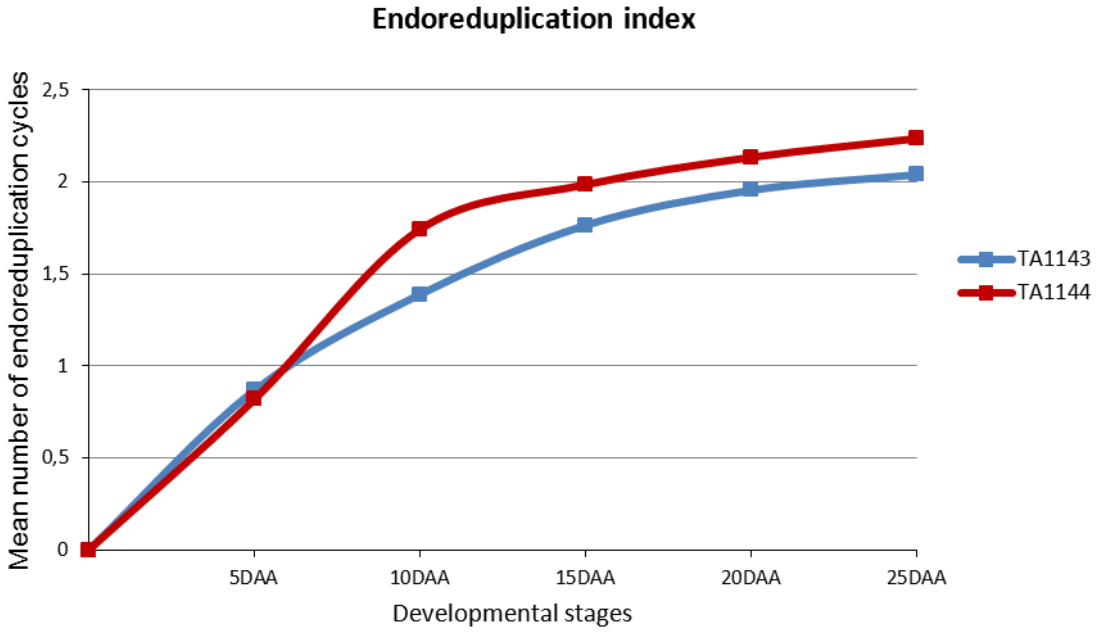

Figure 43: Endoreduplication index in the fruit pericarp of the two lines TA1143 (large fruit allele) and TA1144 (small fruited line). The endoreplication index is a little bit higher in the large fruit at the beginning of the fruit development but then becomes higher in the small fruits after 5 DAA).

Altogether these data are in good agreement with the differential and developmental processes of cell proliferation and endoreduplication occurring in the large fruited TA1143 and small fruited TA1144 lines. There is indeed an interesting correlation between the expression levels of cell cycle and endocycle marker gene, and the mitotic index and endoreduplication index.

In an attempt to integrate all these data with the pattern of *SlFW2.2* geneexpression, we need to recall the basic of the fruit phenotypes differing in TA1143 and TA1144 lines. The "small fruit" phenotype comes from a longer period of expression of the *FW2.2* gene whose function as a negative regulator of cell proliferation therefore restricts cell divisions to an early shorter period of time (with a peak of cell divisions at 4 DAA). On the contrary, the large fruit phenotype comes from a heterochronicity in FW2.2 gene expression which lasts for a shorter period and peaks earlier in TA1143 than in TA1144, resulting in a longer period of cell proliferation, thus providing more cells to build larger fruits.

The patterns of expression for cell cycle control genes in the first stages of fruit development seemed then to correlate pretty well with the expression level of *SlFW2.2* in both lines, not only at the temporal level, but also at a quantitative level. This was particularly evident for the mitosis associated genes *SlCDKB1* and *SlCSS52B*. At a temporal level, the differential peaks of expression for the endoreduplication-specific marker *SlCSS52A* is in accordance with an early mitotic index and hence an early commitment to endoreduplication in the small-fruited TA1144 line when compared to the large-fruited TA1143 line. This correlates with the fact that genes implied during the mitosis process are up-regulated when the expression of *SlFW2.2* is low, for instance at 2 DAA. Thereafter in fruit development, these genes become extinct as *SlFW2.2* expression increases.

The most striking differential expression among the two lines has been observed for *SlKRP4. SlKRP4* belongs to the *Kip-Related Protein (KRP)* gene family which encodes specific Cyclin-Dependent kinase inhibitor (De Veylder *et al*. 2001). In *Arabidopsis thaliana*, KRPs have been shown to be involved in the regulation of mitosis and the commitment to endoreduplication (Verkest *et al.* 2005a; Weinl *et al.* 2005). In tomato, Nafati *et al.* (2011) showed that *SlKRP4* is preferentially expressed in the early fruit development (between antesis and 10 DAA), *i.e.* during the cell division phase. This expression pattern was obtained using the small cherry tomato of the Wva106 cultivar. Interestingly, the pattern of expression for *SlKRP4* which was determined in the small-fruited TA1144 line (Figure 41) is strikingly similar (to the exception of the 25DAA point which may result from an artifact in the RT-PCR experiment). Hence the opposite pattern of *SlKRP4* expression observed in these two lines suggests that it can be the result of an upstream effect exerted by FW2.2, and consequently the difference in temporal expression of *SlKRP4* influences cell proliferation in the course of fruit development.

It has been shown that the SlKRP4 protein localizes within the nucleus (Nafati *et al.* 2010). Again this implies that that there is no supposedly possible physical interaction between FW2.2 and SlKRP4, since the influence of a membrane protein on the *SlKRP4* gene expression is dubious. However the existence of a signaling pathway between the membrane and the nucleus, involving the interaction of FW2.2 with other proteins then transmitting a signal (such as a kinase protein) cannot be excluded.

2- Investigating the FW2.2 interacting protein-protein network

To deeper in the analysis of the potential role of FW2.2 in fruit development, we looked for putative protein interactors of FW2.2.

As a result of a two-hybrid screen, Cong and Tanksley (2006) showed an interaction between FW2.2 and the β regulatory subunit of casein kinase II, namely CKIIβ1. This finding provided an interesting clue to explain the pathway through which FW2.2 may influence the mitotic activity in the tomato fruit pericarp. In this publication, the authors realized two two-hybrid screens using a cDNA library synthesized with mRNAs prepared from 0 to 12 DAA tomato fruits. The first screen has been performed using the full length FW2.2 protein as a bait and resulted in too many interacting candidate clones. The authors then performed a second cDNA library screen using the soluble part of the FW2.2 protein (*i.e.* the C-terminal last 74 amino acids of the protein) free from the two transmembrane domains. Six putatively interesting cDNAs were isolated from this second screen, one of them encoding the CKIIβ1 protein. Further in vitro binding tests confirmed that FW2.2 was only able to interact with the CKIIβ1 protein. If valid, this interaction offers a means to explain how FW2.2 can influence the cell cycle, since reports from the literature indicated that the CKIIβ1 protein may influence plant development and cell cycle control (Espunya *et al*. 1999; Espunya *et al.* 2005; Moreno-Romero *et al.* 2008).

In order to investigate the pathway through which FW2.2 may exert its developmental influence on tomato fruit growth, we looked for candidate proteins able to interact with FW2.2. We expected from this part to decipher the mechanisms by which FW2.2 may influence the cell cycle, confirming and extending the results obtained by Cong and Tanksley (2006), and may participate in the brassinosteroid signal pathway.

a. Confirmation of the CKIIβ1 interaction

To confirm the validity of the interaction of FW2.2 with the CKIIβ1 protein described by Cong and Tanksley (2006), we first performed the two-hybrid technique using the full length FW2.2 protein and the truncated protein, keeping only the soluble C-terminal part. All the attempts to reproduce the previously published results failed systematically.

Since FW2.2 is a membrane-localized protein, the interaction of FW2.2 with CKIIβ1 can be questioned, as the two-hybrid technique is only applicable to soluble proteins. Nevertheless we attempted to reproduce this interaction, using a more suitable technique for membrane proteins, namely the Split-Ubiquitin technique (Stagljar *et al.* 1998; see Materials and Methods section for more details). Again the interaction could not be confirmed, and our efforts to demonstrate it using the Split-Ubiquitin technique also remained unfruitful.

We conclude that the interaction between FW2.2 and the CKIIβ1 protein is actually irrelevant. It may be that the first numerous clones isolated by Cong and Tanksley (2006) after the first screen would only have been false positives. The second screen result is also questionable, as the soluble C-terminal part of the protein was only used as a bait: the interaction was certainly an artefactual result induced by the use of the truncated protein, most probably because the protein fragment used as bait was out of its natural protein context and cannot behave normally leading to abnormal interactions that actually does not exist.

Even though the direct interaction of FW2.2 with CKIIβ1 could not be confirmed, other interactions with one or several proteins may explain the influence of FW2.2 on fruit development and the cell cycle control.

b. Targeted Split-Ubiquitin with the FWL proteins

The FWL proteins display a high degree of homology with the FW2.2 protein sequence. The FW2.2 protein is only 163 amino acids long and thus appears to be very small to form a functional transporter on its own. Therefore, we first hypothesized that the FWL and FW2.2 proteins could participate in protein complexes in order to form a membrane complex and harbor the putative transporter function.

To verify this hypothesis, we performed a targeted Split-Ubiquitin experiment in order to check the ability of the FW2.2 protein to interact with the FWL1 to FWL5 proteins.

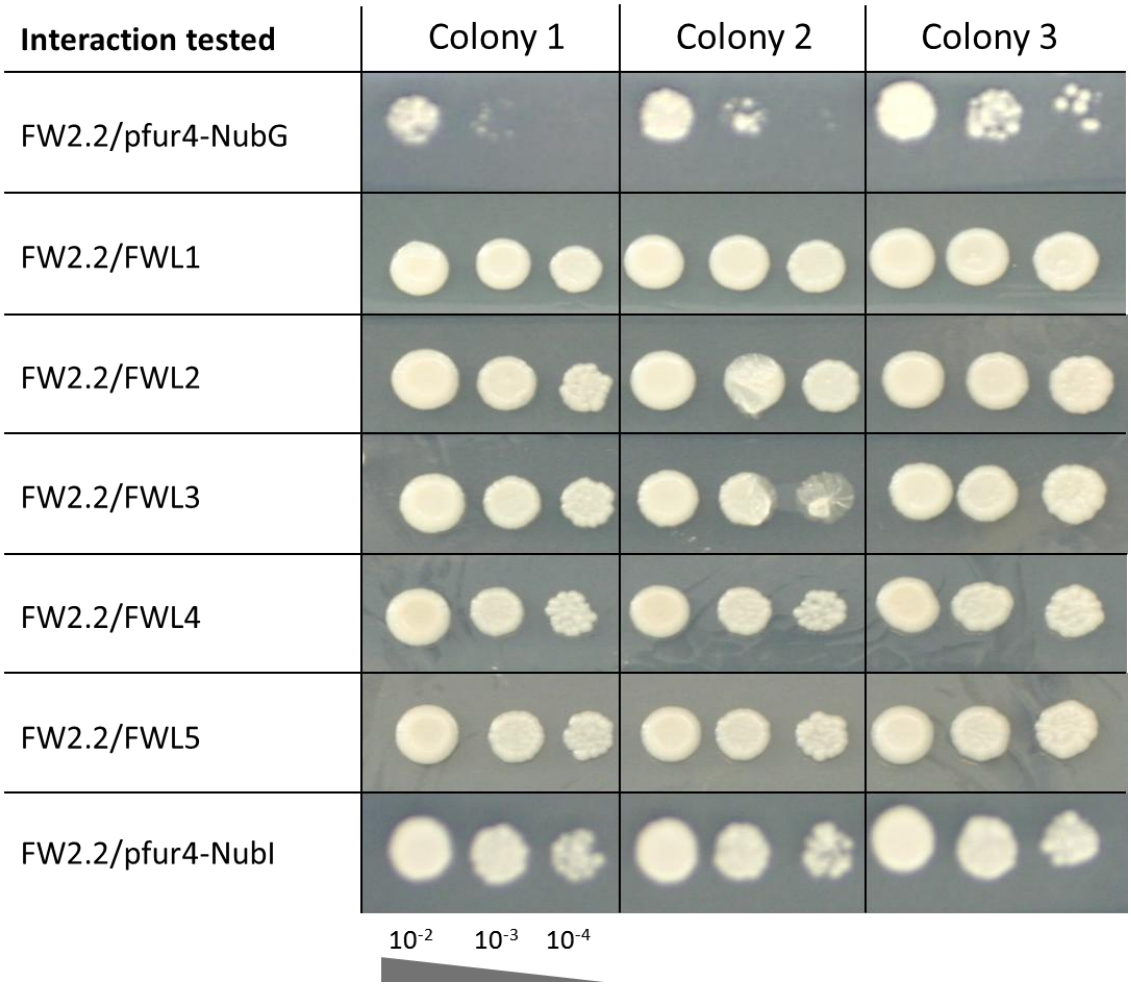

Figure 44: Interaction test between the FW2.2 protein and the FWL protein using the Split-Ubiquitin technique. The yeast cells have been plated on a SD-LTHA medium supplemented with 50mM 3-aminotriazole to test the interaction strength and grown during 3 days. The pfur4 protein is an ER resident membrane protein that serves as a negative control (when fused to the modified N-terminal part of the ubiquitin (NubG) it cannot interact with the C-terminal part of the ubiquitin (Cub)) and as a positive control when fused to the wild-type N-terminal part of the ubiquitin (NubI). Three colonies of each transformation tests have been picked up on the double transformants selection medium (SD-LT) and dropped on the interaction selection medium (SD-LTHA) after having their OD_{590nm} harmonized and being diluted 100 (10^{-2}), 1000 (10^{-3}) and 10000 (10^{-4}) times to be then grown during 3 days.All the FWLs proteins tested seem to interact with FW2.2.

In all tested combinations, the growth of the double transformed yeasts revealed that the reporter genes (HIS3 and ADE2) allowing the synthesis of both histidine and adenine are transcripted. The transcription of these genes reported the reconstitution of a functional ubiquitin due to the interaction of the two parts of the ubiquitin (NubG and Cub). This interaction allowed the liberation of the LexA transcription factor, by proteolysis of the link between the Cub and the LexA. LexA then shifted from the plasma membrane proximity to

the nucleus and activated the transcription of the reporter genes. The N-terminal part of the ubiquitin being modified, it cannot naturally interact with the C-terminal part of the ubiquitin to reconstitute a functional ubiquitin. This is possible only if the proteins that are fused to the two part of the ubiquitin are interacting and force them to enter in close proximity, reconstituting a functional ubiquitin, which provokes the transcription of the two reporter genes.

The addition of 3-aminotriazole (3-AT), which is a competitor of the HIS3 gene product, in the culture medium allowed the selection of the strongest interactions, *i.e.* the interactions that generated the higher levels of HIS3 transcription. Indeed yeast colonies that grow on an interaction selection medium supplemented with 3-AT produce two proteins that interact very strongly.

The double transformation with *FW2.2* and *FWL* genes resulted in yeast colonies that grew very well (the dilution of yeast cells did not impact their growth on the interaction selection medium): it was thus concluded that the FW2.2 protein could interact with the FWL1, 2, 3, 4 and 5 proteins. The negative control also showed some growth but of a very much weaker ability than for the interactions tested.

These interactions have been tested with the FW2.2 protein being fused with the C-terminal part of the ubiquitin (Cub) and the FWL protein fused with the modified N-terminal part of the ubiquitin (NubG). These interactions have thus been tested in only one directed system and will need to be tested in the other direction (FW2.2 fused with NubG and FWL fused with Cub) in order to make sure that the interactions are relevant.

c. cDNA library screen to identify the FW2.2 protein interactor(s)

We then applied the Split-Ubiquitin technique to screen a cDNA library synthesized from mRNAs extracted from 5 DAA TA1143 fruits and 10 and 15 DAA TA1144 fruits. These developmental stages have been chosen because of the relatively high expression of *FW2.2*, putatively ensuring the presence of its potential interactor(s).

A very high number of cDNA clones arose from the screen of the library, even though this screen has been performed on a stringent medium containing 3-aminotriazole (3-AT) at a concentration that allows the theoretical elimination of false positives and the selection of strongest interactions.

About 300 of the resulting cDNAs were then sequenced and none of them seemed to correspond to an expected (logical) interactor that could explain the effect of FW2.2 (Table

4) as each clone have been identified only once. We did not found in the clones sequences the *CKIIβ1* cDNA sequence.

Table 4: Examples of clones isolated with the cDNA library screen. The clone identification has been performed by blasting the sequence obtained after the plasmid sequencing that follows the plasmid extraction from the grown yeast colonies.

Result
40S Ribosome
60S Ribosome
Chloroplastic protein - unknown function - ycf49-like
Zinc Knucle CCHC family protein
PCP-like (pollen coat protein)/Flower specific gamma thionin
Gibberelin regulated family protein
PCP-like (pollen coat protein)/Flower specific gamma thionin
Aminopeptidase
60S Ribosome
60S Ribosome
DSBA oxidoreductase
PCP-like (pollen coat protein)/Flower specific gamma thionin
unknown
ATP synthase
RNA polymerase II
Vacuolar ATP synthase
Osmotin like
Vacuolar ATP synthase
Photosystem II
Ribosome 40S
Adenin phosphoribosyl transferase 1 (APT1)
unknown
Phosphoglycerate/biphosphoglycerate mutase family
Imidazole glycerol phosphate dehydratase
VAMP (vesicle associated membrane protein)
Cytochrome b6f
Glutathione S transferase
Zinc Knucle CCHC family protein
Plastocyanin
Ankyrin repeat family
eIF5A-3
NAD(P)H-quinone oxidoreductase chain 4L
ubiquitin-conjugating enzyme 2 (UBC2)
hypothetical protein - unknown function
Vacuolar ATP synthase 16 kDa proteolipid subunit
putative small nuclear ribonucleoprotein E

oxidoreductase NAD-binding domain-containing protein
adenine phosphoribosyltransferase 1 (APT1)
60S ribosomal protein L13
acyl carrier family protein / ACP family protein, similar to Acyl carrier protein
50S ribosomal protein L15
photosystem II 10 kDa polypeptide
Vacuolar ATP synthase 16 kDa proteolipid subunit
photosystem II reaction center 6.1KD protein
invertase/pectin methylesterase inhibitor family protein
fatty acid desaturase family protein
Vacuolar ATP synthase 16 kDa proteolipid subunit
zinc finger (DNL type) family protein
endoribonuclease L-PSP family protein
amino acid permease family protein
structure-specific recognition protein 1 / high mobility group protein / HMG protein
Ran-binding protein 1a (RanBP1a)
60S ribosomal protein L37 (RPL37C)
pom30 (porin)
protease inhibitor
similar to auxin down-regulated protein ARG10
glycoprotein-like protein
60S ribosomal protein L6 (RPL6A)
photosystem I subunit XI
acyl carrier family protein / ACP family protein
ribulose bisphosphate carboxylase small chain 1A / RuBisCO small subunit 1A
osmotin-like protein
WRKY family transcription factor
stress enhanced protein 2 (SEP2)
cytochrome oxidase subunit 3
octicosapeptide/Phox/Bem1p (PB1)
putative UDP-glucose dehydrogenase 2
ribulose bisphosphate carboxylase small chain 1A / RuBisCO small subunit 1A (RBCS-1A) (ATS1A)
similarity to the PCP (pollen coat protein) gene family

The Split-ubiquitin library screening thus revealed that FW2.2 can interact with a large variety of proteins in a somewhat random manner, even comprising chloroplastic proteins. Since these largely represented proteins may saturate the system, we tested another cDNA library, made from cDNAs prepared from *Arabidopsis* stem peeled epidermis, in order to get rid of all the chloroplastic proteins that could interfere with the system. This last cDNA library had been successfully screened by Bernard *etal.* (2012).

In this second screen, we attempted to verify the behavior of the FW2.2 protein when put in contact with heterologous protein, and check whether it could be able to form as much numerous interactions as previously observed.

The screen of the *Arabidopsis* cDNA library still gave a very high number of clones, even if the 3-AT concentration has been increased, confirming that FW2.2 interacts randomly with various proteins, without any physiological explanation.

The composition of the FW2.2 protein reveals that there is a very high amount of cysteine residues that are certainly important for the protein conformation, but in turn that can also form strong disulfide bonds with many other proteins when taken out of their physiological context.

We could have increased much more the concentrations of 3-AT but, even if it could decrease the number of selected clones, the interactions would not have any physiological relevance with such stringency.

3- Conclusion on the effect of FW2.2 on cell cycle regulation

The involvement of FW2.2 in the control of cell proliferation remains unquestionable as it is clearly a negative regulator of mitosis. However the true commitment to cell cycle regulation remains an enigma, especially in light of its membrane localization.

Following the expression of some cell cycle regulatory genes during the fruit development revealed that FW2.2 could influence the cell cycle through modulating the expression of *SlKRP4*. Unfortunately, the cDNA library screen gave neither convincing clue on the regulation pathway it implies, nor confirmed our hypothesis dealing with the brassinosteroid pathway.

IV

Discussion
Perspectives

IV. Discussion and perspectives

A. Does the conservation of the protein sequences within the FWL protein family in tomato indicate a conservation of protein function?

We here described the identification of 17 homologous proteins to FW2.2 in tomato, which share a high percentage of sequence identity and contain the same PLAC8 domain. These homologous sequences form the FW2.2 family in tomato and were thus named the *FW2.2- like* (FWL) gene family.

Several studies have shown that the complexity of a gene family was produced from four important mechanisms: segmental duplication, tandem duplication, transpositional duplication and genome duplication (Cannon *et al.* 2004; Freeling *et al.* 2009).

The analysis of the exon composition and exon length in these 17 homologue proteins showed that the exon organization was relatively conserved, although groups within this gene family could be defined and differentiated by their exon length arrangements. The differences in the exon length do not seem to correspond to sequence fragment deletions, but rather to a rearrangement in the intron/exon boundaries.

Analyzing the isolated sequences revealed that they all share the PLAC8 domain within which two highly conserved motifs are found. However a more rigorous analysis of the present motifs indicated that the FWLs display the completely conserved or slightly modified CCXXXCPC motif (involved in heavy metal resistance) and the QEYRELK motif (whose function has not been determined). As revealed by a phylogenetic study using the FWLs and a set of homologues identified all over the plant reign, the relative conservation of these motifs could be indicative of the existence of functional groups within the plant FWL gene family. Since all FW2.2 homologues present a relatively conserved intron/exon gene structure, it is suggested that all these sequences derived from the same ancestor and that the gene evolution provoked sequence changes putatively in relation with the specialization of protein function.

A treatment of the aligned sequences with the Gblocks tool confirmed that the most conserved domain within all the proteins consisted in the major part of the PLAC8 domain, suggesting a low level of divergence between all the homologues used for the alignments.

However the situation seems to be much more complicated as the the constructed phylogenic tree could not allow any clear separation into protein clades. The so-called conserved proteins appeared to be actually highly divergent proteins with insignificant mutations within the most conserved parts of the protein sequence. We therefore concluded that this might be due to a high sequence divergence with the appearance of mutations that do not correlate with, but do affect the evolution of the protein function.

All the phylogenetic studies made at present did not give any clues relative to the FW2.2 function and did not clearly and doubtlessly separated FW2.2 from proteins implied in the heavy metal transport.

Another FW2.2 homologue from *Brassica juncea*, named *Bj*PCR1 because of its very high sequence homology with the *At*PCR1 and *At*PCR2 proteins, has been isolated and shown as well to contain the PLAC8 domain,(Song *et al.* 2011). The CCXXXXCPC motif, demonstrated to be involved in the cadmium resistance role of the AtPCR1 protein, is indeed present in the sequence of *Bj*PCR1. As a consequence, it was expected that *Bj*PCR1 could play a role in mediating cadmium resistance to transformed yeasts. In fact, this appeared to be wrong as *Bj*PCR1 was shown to facilitate the radial transport of calcium in the roots (Song *et al.* 2011). However, a hybrid construct consisting in the N-terminal part of the *At*PCR1 protein fused to the C-terminal part of *Bj*PCR1 was able to confer cadmium resistance to transformed yeasts. In addition, the substitution of one single amino acid residue in the sequence of *Bj*PCR1 resulted in a protein that conferred cadmium resistance to transformed yeasts and provoked a decrease in the cadmium content within the yeast cells.

This study highlights the fact that the function of the PLAC8 domain-containing protein family does not probably reside in the CCXXXXCPC motif or derived motif, but is rather supported by the N-terminal part of the PLAC8 motif.

A new phylogenetic analysis of all the protein sequences was performed using Gblocks. The Gblocks alignment tool eliminates poorly aligned positions and divergent regions that do not make an evolution sense from a protein alignment so that it becomes more suitable for phylogenetic analysis. This sequence cleaning with a previous C-terminal part suppression of the PLAC8 domain (the only part that has been conserved for the tree generation in Figure 24) or the generation of a tree with the N-terminal part of all the PLAC8 domain-containing

proteinscould maybe help in understanding the evolution of the homologue sequences and allowing the separation of functional clades.

The RNAseq data retrieved from the Sol Genomics Network allowed separate these homologues into 4 different groups of genes according to their tissular expression, which could be indicative of common functional properties according to the localization expression. It implies that some of these FWLs can be fruit or organ size regulators on different plant organs, the same way FW2.2 influences fruit size.

In future works, the implication of the FWLs in the fruit size control could be investigated by QTL association mapping, in order to know if some of the homologues are fruit size regulators alike FW2.2 or occupy other function in plant development.

We cannot exclude the idea that the FWLs can display the same developmental effects than FW2.2 on plant organs. This has already been described in rice for two homologues of FW2.2, namely *Os*FWL3 and *Os*FWL5, controlling the glume size and the leaf size respectively (Xu *et al.* 2013).

We also keep in mind that *At*PCR1 and *At*PCR2have a similar function as heavy metal transporters but their respective localization of gene expression is very different: the *AtPCR1* gene is exclusively expressed under a cadmium induction in the shoot parts of the plant, whereas the *AtPCR2* gene is expressed in both shoot and roots and upregulated in the presence of cadmium (Song *et al.* 2004 and 2010). The *At*PCR1 protein fulfills a cadmium transporter role in the shoot whereas the *At*PCR2 protein fulfills a zinc transporter role in the whole plant, except in the stem and flowers. These two proteins are effective transporters, excluding two different kinds of heavy metals and acting in different localization within the plant.

The fact that the tissue localization of the FWL is different does not exclude the possibility that their expression localization can change or that it can be up- or downregulated in response to a heavy metal treatment. This could be easily tested by growing tomato plants under a heavy metal treatment and look for a change in FWL gene expression to establish a clue about their putative function.

B. Does FW2.2 play a role in mineral ion transport?

We managed to show that FW2.2 is a membrane protein, in light of the hypothesis that it can be a transmembrane channel.

The first observations performed on *Arabidopsis* plantlets revealed that the protein seemed to be at the plasma membrane (which has been then confirmed) and interestingly showed a punctuated localization that did not colocalize with protein markers for plasmodesmatas. It was suggested that this punctuated localization could correspond to lipid rafts (with unsuccessful observation and confirmation in BY2 cells or tobacco plants). Lipid rafts are very active microdomains within the plasma membrane known to be implied in many transduction signal processes (Mongrand *et al.* 2010). If it is further confirmed that the FW2.2 protein localizes in lipid rafts, this specific localization would suggest a role for FW2.2 in signal transduction pathways.

FW2.2 shows sequence homologies with the *At*PCRs and the *Om*FCR proteins that are directly implied in heavy metal resistance. Additionally the CCXXXXCPC motif which ensures this function is slightly modified (CLXXXXCPC) in FW2.2. Taken together these observations suggest that the function of FW2.2 could be related to a heavy metal or ion transport activity. Unfortunately all our efforts to confirm this hypothesis remained unsuccessful as we did not provide the irrefutable proof that FW2.2 is a protein directly involved in heavy metal transport.

However, the measurements of mineral ion contents performed on the fruits from the M82+SF transgenic line holding two additional copies of the small fruit allele of *FW2.2* compared *to* M82 wild type line, and, and on the fruits of the two nearly isogenic lines TA1143 and TA1144, both showed a difference in the cadmium accumulation. This raised the question on how the mineral ion content can be that different in the tomato fruit.

A voltage clamp experiment using oocytes that are expressing the FW2.2 protein and in the presence of cadmium did not allow demonstrate this transport. The voltage clamp technique give clear patterns of depolarization in the case of channels with an intense activity creating a significant ion movement between the two sides of the membrane that provokes in turn a change in the natural membrane polarization. No abnormal

depolarization was observed in the case of FW2.2, thus revealing that there was no significant ion movement between the two sides of the membrane.

However we cannot exclude the fact that FW2.2 can provoke any ion movement: it may be just not revealed in such a small time span and the conditions of our experiments. FW2.2 can be a passive transporter that induces a slow ion movement, not strong enough to provoke a membrane depolarization. If it is a passive transporter, a change in the mineral content can be then measurable within the oocytes.

To confirm the absence of a clear membrane depolarization and determine whether *SlFW2.2* mRNA-injected oocytes present higher or lower heavy metal content than the controls, we plan to realize an uptake measurement. With or without a transport system, the heavy metals can diffuse through the membrane and accumulate within the cytoplasm. These uptake measurements will allow us to compare the mineral content of the oocytes producing the SlFW2.2 protein or AtPCR1 in the presence of different incubation media.

We propose to perform as well functional complementation experiments. Indeed, *Arabidopsis* knock-out mutants for the *AtPCR1* and *AtPCR2* genes are available and could be used to perform such a functional complementation of these mutants by inserting a copy of the *SlFW2.2* gene through transgenesis. For instance, the *pcr2* mutant presents a higher sensitivity to zinc than the wild type. This functional complementation experiment will have the aim to look for a better growth of the FW2.2-transformed *pcr1* and *pcr2* mutants on media supplemented with cadmium and zinc respectively. Hence we should confirm the implication of FW2.2 in a heavy metal transport system, although not demonstrating ultimately the role of a transporter itself.

The fact that FW2.2 is a 164 amino acid-long protein excludes the idea that it can form a size-sufficient structure allowing the fitting out of a pore, then allowing the ion passage between the two sides of the membrane. To form such a structure that has a sufficient size to transport ions or create an ion flux, we hypothesize that FW2.2 interacts with other proteins or is able to self-multimerize to constitute this appropriate structure. To identify the putative interactors, an adapted protocol for the Split-Ubiquitin technique or efficient pull-down experiments using membrane protein extracts have to be established.

If we manage to confirm that FW2.2 interacts with other proteins, this could explain the fact that no difference in growth was observed for the *Arabidopsis FW2.2*-overexpressing plants in the presence of cadmium or zinc. Hence the overexpressed FW2.2 protein in this

heterologous system may not meet its natural (species specific?) partners to ensure the formation of a functional transporter.

In another voltage-clamp experiment, we could work at investigating whether the isolated interactors have the ability to form a functional pore inside the membrane that allows a significant ion movement.

C. How does FW2.2 regulate the plant and/or fruit development?

The study of *Arabidopsis* plants and BY2 cells overexpressing the *SlFW2.2* gene revealed the appearance of phenotypes that seem to be related to hormone signaling.

Indeed, smaller cells and an increased stoma density characterized the leaf epidermis of the *Arabidopsis* plants overexpressing *SlFW2.2*. Cultured BY2 cell lines overexpressing the *SlFW2.2* gene showed a change in cellular shape, with elongated cells compared to control cells.

These two phenotypes observed for *Arabidopsis* plantsand BY2 cells resembled to that observed in brassinosteroid signal pathway mutants and in brassinosteroid deprived BY2 cells respectively (Kim *et al.* 2012; Miyazawa *et al.* 2003).

Kim *et al.* (2012) recently proposed a model which connects the regulation of cell growth through the brassinosteroids and the stomatal production pathway (Figure 45).

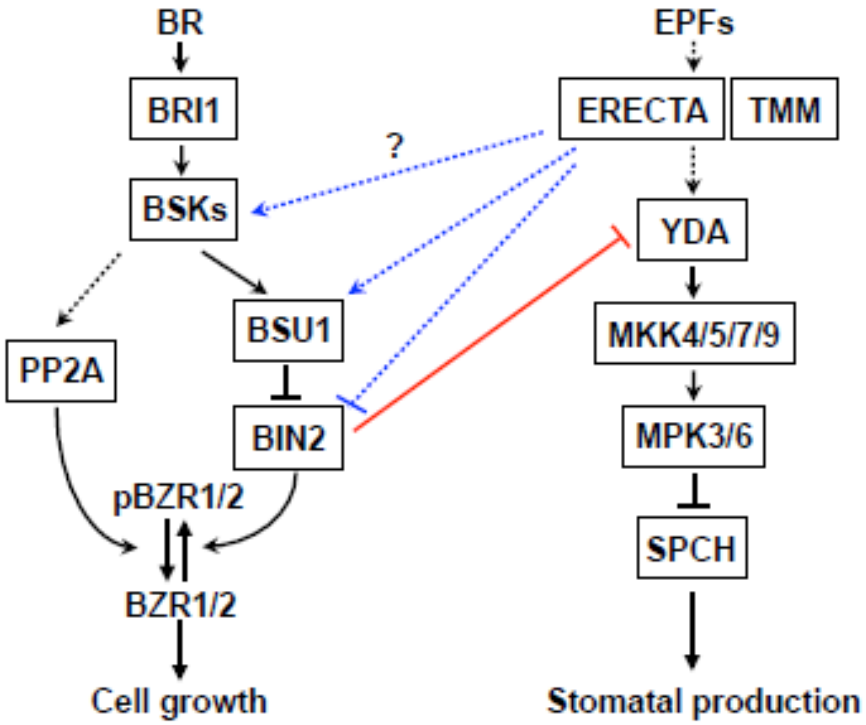

Figure 45: Proposed model for the interplay between the regulation of cell growth through brassinosteroids and the stomatal production pathway (from Kim *et al.* 2012). See details in the text.

Under normal hormonal conditions, brassinosteroids bind to the extracellular domain of the membrane-bound receptor kinase BRI1 (Brassinosteroid Insensitive 1) which activates an intracellular signal transduction pathway mediated by the protein kinase BSK1 and the protein phosphatase BSU1 that inactivates the BIN2 kinase. The BZR1/2 transcription factors then act as activators of the genes implied in the brassinosteroid signal response, ultimately stimulating cell growth.

In parallel, upon hormonal and environmental factors as well as intrinsic developmental programs, the stomatal production pathway also implies a kinase cascade that results in the inhibition of the SPCH (Speechless) transcription factor that activates genes involved in the stomatal differentiation.

Under low brassinosteroid concentration, the BSU1 protein phosphatase is no more activated and thus does not inhibit the BIN2 kinase targeting the phosphorylation of BZR1. The downstream genes involved in cell growth are consequently no more activated and the plants display smaller cells. According to the pathway interconnection and under the same conditionof low brassinosteroid concentration, the BIN2 kinase still stands in its active form;

it then phosphorylates the YDA (Yoda) kinase which becomes inactive and therefore does not activate the downstream kinase cascade that usually inhibits the SPCH transcription factor. If SPCH is functional, it then activates the genes involved in the stomatal production and plants display a higher stomatal density.

The phenotypes observed with the *Arabidopsis* plants and BY2 cells overexpressing *SlFW2.2* are in good agreement with this model: for instance the Arabidopsis *FW2.2* overexpressors showed an increased stomatal density and a reduced pavement cell size. Therefore this phenotype makes us think that FW2.2 could play a role in the brassinosteroid sensing, the brassinosteroid transduction signal or the brassinosteroid biosynthesis pathway.

The phenotype associated to small cell size has been also described in plants overexpressing the *CycD3.1* gene. However the plants overexpressing the *SlFW2.2* gene do not show an increased *CycD3.1* expression. In developing plants cells do not divide or differentiate synchronously and therefore the expression of cell cycle genes is then complicated to investigate at the cellular level. BY2 cells overexpressing the *SlFW2.2* gene could be used in a synchronization experiment, as to compare the effects on cell cycle regulation in the presence or absence of *SlFW2.2.*

Brassinosteroids play well defined roles in cell division and cell elongation (Azpiroz et al. 1998; Hu et al. 2000). In addition brassinosteroids also control the balance between proliferation and cell fate specification (Kuppusamy et al. 2009), as well as cell differentiation such as stomatal differentiation (Kim et al. 2012).

Chemical tools are available to be used for deciphering the role of FW2.2 in the brassinosteroid signal pathway. Molecules such as epibrassinolide can mimic the brassinosteroid effect and can allow determining if FW2.2 impacts the plant sensitivity to this hormone by lowering the brassinosteroid binding on the BRI1 receptor for instance. The bikinin, a GSK3-like kinase inhibitor (BIN2 is a GSK3-like kinase), mimics the effect of the brassinosteroid hormone by shunting the upstream kinase cascade and consequently the receptor activation; bikinincan help us determining if FW2.2 acts on the signal transduction by inhibiting the upstream kinase cascade that usually leads to the inactivation of the BIN2 kinase and the switch to the brassinosteroid responses. The brassinazole is a brassinosteroid biosynthesis inhibitor and plants treated with this molecule show a brassinosteroid depletion phenotype. If the treatment of plants overexpressing *SlFW2.2* with

brassinazoleshows a reinforced stoma phenotype, this will mean that FW2.2 is not involved in the brassinosteroid biosynthesis as it will be still responsible for the increased stomatal number phenotype.

Using these effectors could help in addressing the proposed hypothesis for a role of FW2.2 in brassinosteroid regulatory pathway. Experiments aimed at growing *Arabidopsis* plants overexpressing the *SlFW2.2* gene on media supplemented with the molecules described above could be performed; then the effects on the stomatal density and cell size could be monitored.

If epibrassinolide restores the wild type phenotype, it means that the FW2.2 overexpressing plants are affected in the brassinosteroid sensitivity. If the phenotype is not rescued, it implies that the signal transduction is not transmitted to activate the responses to a brassinosteroid application and that FW2.2 is responsible of the brassinosteroid signal transduction inhibition.

In this case, the signal sensing could be shunted and the brassinosteroid pathway could be directly activated by the application of bikinin which can inhibit the BIN2 kinase and activate the brassinosteroid gene response. If no phenotypic change occurs with the application of bikinin, it may be possible that FW2.2 does not act on the kinase cascade activation but rather acts directly on the regulation of transcription factors. The GSK3-like kinase activity of BIN2 could also be assayed in complement of the growth test using bikinin, in order to quantify the BIN2 kinase activity and to determine if there is a change in this activity that could reveal a modification in the transduction signal pathway.

The application of brassinazole, an inhibitor of the brassinosteroid biosynthesis, could allow determining whether the FW2.2control occurs on the brassinosteroid biosynthesis: the absence of any phenotypic change in the *SlFW2.2* overexpressors would be expected when a brassinazole treatment is applied. Such an observation coupled with a phenotype recovery in the presence of bikinin will confirm this hypothesis.

All the growth tests on supplemented media with these effectors will be coupled with gene expression analyses especially for those involved in the response to brassinosteroid, in order to identify which genes are up or downregulated. For these gene expression analyses, genes involved in the stomatal differentiation, such as MUTE and SPCH that are transcription factors required for the stomatal differentiation signal pathway, will be included. As well, the expression of cell cycle genes involved in cell proliferation such as *AtCycD3.1* and

*AtCCS52B*will be monitored. Investigating the pattern of *AtCycD3.1* expression in the plants overexpressing *SlFW2.2* could be very interesting since *AtCycD3.1* is upregulated under a brassinosteroid stimulus and since the overexpression of *AtCycD3.1* was shown to induce cell proliferation in the *Arabidopsis* leaf epidermis (Hu et al. 2000). As the role of the brassinosteroid seems to be very wide and involved in different mechanisms such as cell expansion (Nemhauser *et al.* 2004) and cell division (Hu *et al.* 2000), it would be interesting to monitor the *AtCycD3.1* gene expression in plants overexpressing *SlFW2.2* In order to determine if there is a correlation between the expressions of *SlFW2.2* and *AtCycD3.1*.The synchronization issue in plants could prevent us from observing a direct correlation between the *SlFW2.2* and *AtCycD3.1* expression levels. To circumvent this problem, the BY2 cell cultures that overexpress the *SlFW2.2* could be a valuable tool as they can be easily synchronized.

All of the above described experiments could be performed using BY2 cultured cells with a particular attention given to the observation of cell shape changes according to the applied treatment. Since BY2 cells overexpressing *SlFW2.2* appeared to grow more slowly than control cells, we hypothesized that they may be affected in the process of cell cycle control. To address this hypothesis, BY2 cultured cells could be synchronized using aphidicolin (which blocks cells during the M phase) in order to observe the effects on cell cycle progression in the BY2 cell line overexpressing *SlFW2.2* compared to untransformed cells. According to this hypothesis we expect that the duration of the G1 phase is longer in the BY2 *SlFW2.2* overexpressor line. This synchronization will also allow compare the expression of cell cycle regulatory genes (especially CycD3.1 as a marker of the G1 phase) in order to investigate whether the overexpression of FW2.2 does influence or not the cell cycle progression.

Establishing a link between the two stated functional hypotheses for the putative role of FW2.2, *i.e.* the mineral ion transporter- and the brassinosteroid pathway hypothesis, is not obvious. This putative dual function of FW2.2 seems to be difficult to integrate.

However, a recent study from Villiers *et al.* (2012) proposed the existence in *Arabidopsis thaliana* of an interaction between the brassinosteroid pathway and cadmium response pathway. This study showed that a reduced brassinosteroid level enhances the plant tolerance to cadmium. Interestingly, this study correlates with the observations made on the *ArabidopsisSlFW2.2* overexpressing plants that seem to have a reduced brassinosteroid

transduction signal pathway. If these plants present a better heavy metal tolerance, we could relate this tolerance with a weakened brassinosteroid signal pathway.

D. How does FW2.2 regulate the cell cycle and to which protein network does it participate?

From the early characterization of *FW2.2* by Steve Tanksley and co-workers, FW2.2 was described as a negative regulator of the mitosis process. However the connection of FW2.2 with the regulation of the cell cycle remained totally elusive. The cell cycle progression from one phase to another is controlled by the level of CDK/Cyclin complex activity (De Veylder et al., 2011). Above a certain threshold of CDK/Cyclin activity, cells can switch off the mitotic cycle during the G2 phase, thus shunting the M phase, to commit to the endoreduplication cycle.

The effects of FW2.2 on the cell cycle regulation were investigated with the aim to determine which genes were up- or downregulated by FW2.2 to provoke an inhibition of the cell cycle.

The expression of cell cycle regulatory genes was apparently only slightly perturbed, and did not seem to be under the direct effect of FW2.2, but rather correlated with the activity of cell division or with the switch to an endoreduplicative process due to the inhibition of mitoses.

The data obtained for the differential expression for *SlKRP4* in the two lines TA1143 and TA1144 were the most spectacular. *SlKRP4* was originally isolated by Nafati *et al.* (2011). These authors showed that *SlKRP4* was preferentially expressed from anthesis to 5 DAA during the fruit development of the cherry tomato Wva106 cultivar, *i.e.* when the activity of cell divisions is very intense. The three other genes encoding tomato KRPs isolated so far (Nafati *et al.* 2011) display very specific expression patterns during tomato fruit development, suggesting different functional and physiological roles. For instance, *SlKRP3* has been shown to be preferentially expressed in the latest stages of fruit development, when cell enlargement and endoreduplication account mostly for the control of fruit growth. The pattern of expression of SlKRP4 (high expression in the earliest stages) thus reflects the

specific involvement of SlKRP4 in the control of mitosis, most probably by targeting specifically mitosis-associated CDK/Cyclin complexes (necessary for G1/S or G2/M transition) rather than endoreduplication-associated complexes.

Hence the kinetic of *SlKRP4* expression in Wva106 was very similar to that for *SlKRP4* in the TA1144 line harboring the small fruit allele, in accordance with the presence of the small fruit allele in the Wva106 cultivar. In the large fruit allele line TA1143, the kinetic of expression of *SlKRP4* is completely opposite to that in the TA1144 line. Interestingly, an inverse correlation between *SlKRP4* and *FW2.2* gene expression was clearly observed: the higher the level of *FW2.2* expression, the lower the level of *SlKRP4* expression, and conversely.This observation is in agreement with the role of negative regulator of cell divisions during fruit development assigned to FW2.2, and the involvement of *SlKRP4* in the control of cell cycle phase transitions.

Since their pattern of expression is inverted, it is suggested that SlFW2.2 could control the regulation of *SlKRP4*. Cong and Tanksley (2006) found that the FW2.2 protein can interact with the CKIIβ1 protein, which is required for the progression through the G1/S and the G2/M cell cycle phase transitions in *Saccharomyces cerevisiae* (Hanna *et al.* 1995). The interaction between FW2.2 and the CKIIβ1 protein could be indicative of the regulatory pathway involved in the cell cycle control. According to this scheme, we can imagine that a low level of FW2.2 protein induces a low level of interaction with the CKIIβ1 and allows the progression through the cell cycle, inducing an increased expression of the *SlKRP4* gene.

To understand how such a regulation of FW2.2 on the *SlKRP4* gene expression can occur, we tried to reproduce the interaction between FW2.2 and CKIIβ1. Our aim was to re-isolate the interacting CKIIβ1 protein and also proteins putatively involved in the brassinosteroid signal pathway. However our attempts were unsuccessful, most probably because Cong and Tanksley used an inappropriate system (the two-hybrid technique) for membrane proteins. Therefore, we did it again using a more appropriate technique, the Split-Ubiquitin technique, to screen the tomato fruit cDNA library. Unfortunately this experiment did not provide any positive result. This was mainly due to the intrinsic structure of the FW2.2 protein: FW2.2 is a very small membrane protein with a high composition in cysteine residues, which provoked the arising of a very high number of clones. In all these sequenced clones we could not identify the cDNA coding for CKIIβ1.

The Split-Ubiquitin system seems to be difficult to calibrate in order to analyze the protein interactions with the FW2.2 protein, even if all the controls performed before screening the cDNA library appeared to be encouraging.

Pull down experiments could have been performed with the identified proteins after sequencing the cDNAs. However such an experiment would require hydrophilic conditions that cannot be suitable with the protein folding of FW2.2 as a membrane protein, and again it would generate aspecific interactions with a very high number of proteins. . Detergents could be used to limit the number of interactions, but this type of experiments needs to be finely tuned.

If it appears that this technique is functional and give interesting results, they will have to be confirmed using another technique such as the Bimolecular Fluorescence Complementation (BiFC) or a targeted Split-Ubiquitin.

On its own, it is difficult to assume that FW2.2 could act as a transporter across the membrane because of the small size of the protein. We then hypothesized that FW2.2 could multimerize, and eventually form multicomplexes with the FWL proteins that share a high degree of sequence homology with FW2.2. We then addressed the ability of FWL1 to FWL5 to interact with FW2.2 using the Split-Ubiquitin and it appeared that all of them could associate with FW2.2. Obviously these data have to be confirmed, but it is encouraging as the observed phenotype of very strong growth is indicative of strong interactions. Therefore the targeted Split-Ubiquitin experiment is truly functional in our hands.

We wondered why the Split-Ubiquitin experiment using the cDNA library screen did not work properly. In the process of setting the technique, the tests that were run before applying the technique showed that observed interactions came from autoactivation in yeasts. This autoactivation corresponds to a percentage of growth under selection sometimes close to 10% (measured as the rate between the number of colonies growing on an interaction selection medium and the number of colonies growing on a double transformation selection medium). This phenomenon of autoactivation is due to the fact that the bait FW2.2 protein is not entirely addressed to the plasma membrane and can form aggregates in the cytoplasm (already described in the work of Song *et al.* 2004) that could produce aspecific interactions. According to the manufacturer's recommendations this high percentage of autoactivation is considered as acceptable, but it introduces a large number of

false positives that raise the number of colonies growing on the interaction selection medium in the case of a large scale transformation. As a result, the screening of candidate clones is largely hampered after the growth of colonies. In the case of a targeted Split-Ubiquitin, each double transformation is performed independently; the growth ability can be then tested under the different selection media and in comparison to negative control tests, which makes the screen between a false and a positive interaction much easier to establish. Table 5 illustrates the percentages of growth under selective media obtained in the targeted Split-Ubiquitin experiment aimed at testing the interaction between FW2.2 and FWLs.

Table 5: Targeted Split-Ubiquitin to reveal the interactions between FW2.2 and the FWLs.The growth ability under selection media is represented by the number of colonies obtained after a yeast double transformation, and expressed as the growth percentage (nb of colonies on SD-LWHA / nb of colonies on SD-LWH). The yeasts are bearing the bait plasmid pBT3-SUC (containing the *SlFW2.2* coding sequence) and the prey plasmid pPR3-N (containing one of the *SlFWL* coding sequence). The transformation combination indicated in blue correspond to the interactions tested and the interactions indicated in orange to the negative controls.

Transformation	SD-LWH	SD-LWHA + 20mM 3-AT	Growth percentage
pBT3-SUC-FW2.2 / pPR3-SUC-FWL1	103	100	97.1%
pBT3-SUC-empty / pPR3-SUC-FWL1	110	1	0.9%
pBT3-SUC-FW2.2 / pPR3-SUC-FWL2	91	33	36.3%
pBT3-SUC- empty / pPR3-SUC-FWL2	110	1	0.9%
pBT3-SUC-FW2.2 / pPR3-SUC-FWL3	90	81	90%
pBT3-SUC-empty / pPR3-SUC-FWL3	107	1	0.9%
pBT3-SUC-FW2.2 / pPR3-SUC-FWL4	128	27	21.1%
pBT3-SUC-empty / pPR3-SUC-FWL4	100	6	6%
pBT3-SUC-FW2.2 / pPR3-SUC-FWL5	158	77	48.7%
pBT3-SUC-empty / pPR3-SUC-FWL5	171	0	0%
pBT3-SUC-FW2.2 / pPR3-SUC-empty	167	4	2.3%

Since the FWLs are supposed to share the same function as FW2.2, the membrane localization and positive result obtained with the Split-Ubiquitin system suggest the formation of a potential channel associate with the transporter function.

We should also keep in mind that FW2.2 may be implied in the brassinosteroid signal transduction pathway that requires interactions with protein kinases. The pull-down technique could also help us identify the putative interactors implied in this pathway.

E. General conclusion

So far the functional role of FW2.2 during tomato fruit development is still an enigma as it remains unidentified.

This study generated interesting insights on the effect of FW2.2 on development at the level of whole plant and cell growth, and raised hypotheses to be addressed: FW2.2 can be both a heavy metal transporter and a protein implied in the brassinosteroid sensing or transduction signal.

The fact that this protein belongs to a large protein family present in every plant species studied so far indicates that it has an essential role in the plant development. The absence of clear loss-of-function mutants or transgenic plants supports this assertion.

The role of FW2.2 has been related to the evolution of fruit size during domestication; the potential implication of FW2.2 in heavy metal resistance or the brassinosteroid signal transduction pathway suggests that FW2.2 is essential in the adaptation to environment and more specifically in abiotic stresses.

This hypothesis would make sense in the frame of the cell cycle control: plant development leads to the production of seeds for a further plant generation and preservation of the species. Under a stress condition, only essential processes are conserved, including fruit development to ensure a normal seed production and dispersal.

Fruit development involves a first phase of very active cell divisions that contribute to fruit enlargement and a second phase that amplifies fruit growth via the endoreduplication-associated cell expansion Cell division and endoreduplication require regulatory proteins that control the progression through the cell cycle and represent more or less energy consuming cellular processes of. Organ growth by cell divisions implies reorganization of the

cell microtubule architecture, membrane and cell wall synthesis, and is thus very costly in energy. Organ growth by endoreduplication-associated cell expansion appears less costly. Under stress conditions, the energy expenses are lowered; as a consequence, one can easily imagine that processes of adaptive value have been selected during evolution. For instance, the cell division phase during fruit development has been shortened to give place to a sooner cell expansion and endoreduplication phase, in order to fasten growth and therefore ensure the proper seed development and dispersal. Interestingly, Bourdon et al. (2010, Progress in Botany) clearly demonstrated that fleshy fruits requiring a long period of growth prior to reach maturation never encountered the endoreduplication process, while fleshy fruits of shorter period of growth always develop according to endoreduplication-induced cell expansion: this was particularly true for Solanaceae species such as pepper, potato and tomato, which are originally endemic from the Andean mountains and submitted to adverse growth conditions, such as altitude and UV irradiation. Accordingly the UVB irradiation stress has been demonstrated to induce endoreduplication (Hase et al., 2006; Adachi et al., 2011).

In the tomato evolutionary and domestication context, the functional hypothesis of FW2.2 being a mineral ion transporter as discussed in this work is of particular interest. Indeed, the small-fruited allele is considered to be the ancestral allele and the large-fruited allele the domesticated allele. The small-fruited allele is found in the ancestor varieties of tomato characterized by very small fruits of few grams in weight, that grow in the Andean mountain region known to be of volcanic geology. Volcanic regions are naturally characterized by the presence of soils enriched in heavy metals. The ancestral varieties of tomato were thus growing in naturally heavy metal “contaminated” regions. In this context, the evolution and selection of *SlFW2.2* alleles may simply reflect the plant adaptation to environmental changes that has accompanied the domestication. As a result, the domestication of tomato then allowed the arising of the domesticated allele of *SlFW2.2* when tomato were selected, cultivated and adapted in plain regions that are less contaminated in heavy metals.

The nature of the *SlFW2.2* alleleswould thus reflect the adaptive system adopted by the tomato species to overcome the developmental issues related to the presence of heavy metals. The selective pressure would then maintain the existence of the small-fruited allele which was then modified in its expression chronicity once the selective pressure was

lowered as domestication occurred. A new allele appeared with mutations that did not affect the survival of plants and conferred the large fruit trait that had been selected by human domestication.

V

Material and Methods

V. Material and methods

A. Biological material

1- Plant material

a- Tomato lines

In our studies we used two nearly isogenic lines, the TA1143 line (*Solanum lycopersicum* [Mill.] cv. M82) containing the domesticated large fruit allele at the *fw2.2* locus and the TA1144 line (*Solanum lycopersicum* [Mill.] cv. M82) containing a 0.8 cM *Solanum pennellii* introgression harboring the small fruit allele at *fw2.2* locus (Eshed and Zamir, 1995).

We also used the wild type TA1620, TA1621, TA1622 and TA1623 lines (*Solanum lycopersicum* [Mill.] cv. TA496 – large fruit allele) and the transgenic TA1616 and TA1618 lines arising from the self-pollination of the fw71 line containing the 15 kbp *Solanum pennellii* chromosome 2 portion harboring *fw2.2* (*Solanum lycopersicum* [Mill.] cv. TA496) (Frary *et al.*, 2000). Transgenic plants were selected in axenic conditions on MS medium (Murashige and Skoog, Duchefa Biochemie BV) supplemented with 50 µg/mLmL kanamycin. The decontamination of seeds was performed using 3.2% sodium hypochloride for 15 min and washed 5 times with sterile milliQ water.

The plants were grown in a greenhouse under a thermoperiod of 25°C/20°C and a photoperiod of 14h/10h (day/night). When an experiment planified required the comparison of two stages of development from two different lines, the fruits coming from the two lines were harvested the same day in order to get rid of the environmental variations.

All these lines have been kindly provided by Yimin Xu from Cornell University.

b- *Arabidopsis thaliana* lines

Arabidopsis thaliana ecotype Columbia-0 plants were grown in axenic conditions on half-strength MS medium under a 22°C/18°C thermoperiod and a photoperiod of 16h/8h (day/night) in an *in vitro* culture room and transferred to soil with vermiculite in a culture room when after 15 to 30 days. The decontamination of seeds was performed with 4.8% sodium hypochloride and 1% Triton X-100 during 10 min and washed 5 times with sterile

milliQ water. Transgenic plants were selected on MS ½ medium supplemented with 50 µg/mL kanamycin.

PSB-L(*Arabidopsis thaliana* ecotype Landsberg erecta) suspension cells were grown under a 22°C/18°C thermoperiod and a photoperiod of 16h/8h (day/night), on modified solid MS medium (MS including vitamin supplemented with 30 g/L sucrose, 0.5 mg/L 1-naphtaleneacetic acid and 50 µg/L kinetin, pH 5.7). The cells grown on solid medium were subcultured every three weeks. Cell cultures were started with a piece of callus dissolved in 5 mL modified liquid MS medium, placed on a rotary shaker (120 rpm) in the same photo- and thermoperiod during 4 days and then subcultured in 50 mL modified MS liquid medium. The liquid culture were then subcultured every 7 days by transferring 2 mL of stationary phase cells in 50 mL final volume of fresh modified liquid MS medium in a 250 mL flask under shaking. Transgenic cell lines were selected on modified MS medium supplemented with 50 µg/mL kanamycin.

c- Tobacco lines

Nicotiana tabacum cv. Petit Havana SR1 were grown in axenic conditions on MS medium under a thermoperiod 22°C/18°C and a photoperiod of 16h/8h (day/night) in an *in vitro* culture room and transferred to soil with vermiculite in a greenhouse under a thermoperiod 25°C/20°C and a photoperiod of 14h/10h (day/night) after 15 to 30 days old. The decontamination of seeds was performed with 4.8% sodium hypochloride and 1% Triton X-100 during 10 min and washed 5 times with sterile milliQ water.

Nicotiana tabacum cv. BY2 suspension cells were grow in the dark at 25°C on modified solid MS medium (MS basal salt supplemented with 0.2 g/L KH2PO4, 2.5 mg/L thiamine, 50 mg/L myo-inositol, 30 g/L sucrose, and 0.2 mg/L of 2,4 dichlorophenoxyacetic acid, pH 5.8). The cells grown on solid medium were subcultured every three weeks. The liquid cultures were started with a piece of callus dissolved in 5mL modified liquid MS medium, placed on a rotary shaker (110 rpm) in the dark during 4 days and then subcultured in 50 mL modified MS liquid medium. The liquid culture were then subcultured every 7 days by transferring 5 mL of stationary phase cells in 50 mL final volume of fresh modified liquid MS medium in a 250 mL shake flask under shaking.

2- Bacterial and yeast strains

a- Bacterial strains for plasmid cloning and propagation

The *Escherichia coli* strain TOP10 strain (F- *mcr*A Δ(*mrr-hsd*RMS-*mcr*BC) ϕ80*lac*ZΔM15 Δ*lac*X74 deoR *rec*A1 *ara*D139 Δ(*ara-leu*)7697 *gal*U *gal*K *rps*L (Str^R) *end*A1 *nup*G) was used for cloning and propagating recombined plasmids obtained from classic ligation or from Gateway® technology (Invitrogen).

The *Escherichia coli* strain DB3.1 (F- *gyr*A462 *end*A1 *gln*V44 Δ(sr1-*rec*A) *mcr*B *mrrhsd*S20 (rB-, mB-) *ara*14 *gal*K2 *lac*Y1 *pro*A2 *rps*L20(Smr) *xyl*-5 λ- *leumtl*1) was used for propagating ccdB containing Gateway® plasmids.

The bacteria were grown in LB medium (Duchefa Biochemie BV) at 37°C for about 16 h either for plasmid cloning of propagation with the appropriate concentrations of antibiotic.

b- Bacterial strains for plant transformation

Agrobaterium tumefaciens strains LBA4404 and GV3101 were used to generate stable transgenic tobacco plants, *Arabidopsis thaliana* plants, BY2 cells and PSB-L cells, and to perform transient *Arabidopsis thaliana* cotyledon transformation. These two strains harbor the disarmed Ti plasmid that allows the transfer of the transgene in plant genomic DNA.

The bacteria were grown in 2YT medium (16 g/L Bactotryptone, 10 g/L Bacto yeast extract, 5 g/L NaCl, 0.4 g/L MgSO4, 2 g/L glucose) with the appropriate concentrations of antibiotics.

c- Yeast strains

The *Saccharomyces cerevisiae* strain THY.AP4 (*MATa ura3 leu2 lexA::lacZ::trp1 lexA::HIS3 lexA::ADE2*) was used to perform the split-ubiquitin technique, in targeted and untargeted assays.

The *Saccharomyces cerevisiae* strain MAV203 (*MAT*α*leu2-3,112 trp1-901 his3*Δ*200 ade2-101 gal4*Δ*gal80*Δ*SPAL10*::*URA*3 *GAL1*::*lacZ HIS*3$_{\text{UAS}GAL1}$::*HIS*3@*LYS*2, *can1*^{R}*cyh2*^{R}) was used to perform the two-hybrid technique.

These two strains were grown in YPAD medium at 30°C for 17h with shaking when preparing liquid culture, or for 48h when plated on solid medium. When co-transformed,

yeasts were grown in SD-LW medium at 30°C for 24h with shaking when preparing liquid culture, or for 48h when plated on solid medium.

3- Plasmids

a- Entry vectors

The pDONR201 (Invitrogen) was used as an entry vector for cloning DNA fragment flanked with the attB1 and attB2 sequences allowing a recombination using the Gateway® technology. The pDONR201 contains the bacterial cassette allowing the selection of bacteria that contains the recombinated plasmid only and a kanamycin selection.

The pE6C and pE6N vectors were used as entry vectors to clone DNA fragment by enzyme digestion in order to generate a C-terminus or N-terminus fusion with the EYFP coding sequence. The same way, the pE2C and pE2N vectors were used to generate a C-terminus or N-terminus fusion with the 3xHA coding sequence and the pE3C and pE3N vectors were used to generate a C-terminus or N-terminus fusion with the 6xMyc coding sequence. These vectors were then used for cloning DNA fragments in destination vectors with the Gateway® technology.

b- Destination vectors used for plant stable transformation

The pK2GW7 plasmid was used as a destination vector to integrate a DNA fragment. The recombinated vector was then used as a stable and transient transformation vector for *Arabidopsis thaliana* plants. This vector was also used for stable transformation of tobacco plants, BY2 cells and PSB-L cells. This vector is prepared with the Gateway® technology and is selected with spectinomycin when inserted in bacteria. The transformation cassette held by the plasmid confers kanamycin resistance to transformed plants.

c- Destination vectors used for split-ubiquitin experiments

The pBT3-SUC plasmid (Dualsystems Biotech), which carries a signal sequence derived from the *Saccharomyces cerevisiae* invertase gene (SUC2) to ensure the proper insertion of our bait into yeast membrane, was used to produce the protein of interest fused with the C-terminal part of the ubiquitin, fused itself to the LexA transcription factor. The produced fusion protein constitutes the “bait” protein. This plasmid also contains the sequence of the

LEU2 auxotrophic marker that confers to the transformed yeast the capacity to grow on a leucin-lacking medium and the kanamycin resistance gene for bacterial selection. The DNA fragment of interest has been inserted by SfiI double digestion.

The pPR3-N plasmid (Dualsystems Biotech) was used to produce the protein of interest fused with the N-terminal part of the ubiquitin, which constitutes the "prey" protein. This plasmid also contains the sequence of the TRP1 auxotrophic marker that confers to the transformed yeast the capacity to grow on a tryptophan-lacking medium and the ampicillin resistance gene for bacterial selection. The DNA fragment of interest has been inserted by SfiI double digestion.

B. Nucleic acid manipulation

1- Nucleic acid extraction

a- DNA extraction

i. Plant genomic DNA extraction

For the extraction of genomic DNA, fresh samples (leaf or cells) were homogenized in DNAzol® (Invitrogen) with ceramic beads (Matrix-Green, MP Biomedicals) using a FastPrep 24 (MP Biomedicals) at maximum speed for 20 s, twice. The sample preparation is at the rate of 50 mg of fresh material per 200 µL of DNAzol®. The sample was then incubated at room temperature for 5 min with shaking to ensure the complete dissociation of nucleoproteic complexes. 200 µL of chloroform are added and the sample is shaked for 20 sec using the FastPrep and incubated at room temperature for 5 min with shaking. Samples are centrifuged at 12000 *g* for 20 min and the aqueous phase (upper phase) is carefully transferred in a fresh tube. 150 µL of 100% ethanol is added and the sample is mixed. After a 5 min incubation at room temperature, the sample is centrifuged at 12000 *g* for 4 min. The supernatant is discarded and replaced by 150 µL of a mix of a 1mL DNAzol® and 0.75 mL 100% ethanol. The sample is mixed and incubated at room temperature for 5 min to be then centrifuged at 5000 *g* for 4 min. The supernatant is discarded and replaced by 150 µL of

100% ethanol in order to wash the pellet. After a 5 min centrifugation at 5000 *g*, the pellet is dried for 10 min under vacuum. The pellet is then resuspended by adding 40 µL of nuclease-free Milli-Q water and slowly pipetting.

ii. Bacterial plasmid extraction

Plasmid DNA is extracted using the High Purity Plasmid Miniprep Kit (CliniSciences) according to the protocol provided by the supplier. Plasmids are eluted in 40 µL nuclease-free Milli-Q water.

iii. Yeast plasmid extraction

Following a cDNA library screen using the Split-Ubiquitin technique, a plasmid extraction is performed in order to identify the interacting clone. Yeasts have a polysaccharide wall that protects them from the physicochemical stresses. This wall prevents the functioning of classic plasmid extraction kits. To cope with this problem, we performed a quick polysaccharide wall digestion before performing a classic plasmid extraction.

600µL of a 24h yeast liquid culture are centrifuged and resuspended in 200 µL sterile mQ water. The suspension is then mixed with 8 µL Glucanex solution and placed at 37°C for 30 min prior to enzymatic digestion and the generation of spheroplasts (yeast cells without polysaccharide wall). After the digestion step, the spheroplasts are centrifuged for 10 min at 2000 *g*, the supernatant is discarded and the classic plasmid extraction can start.

b- RNA extraction

Liquid nitrogen frozen ground samples are homogenized in TRIzol® reagent (Invitrogen) using the FastPrep 24 (MP Biomedicals) at maximum speed for 20 s, twice, at the rate of 1 mL of TRIzol® per 50 to 100 mg powdered sample. 200 µL of chloroform are added to each sample to be mixed again with the FastPrep 24 at maximum speed for 20 s. The samples are incubated at room temperature for 3 min and then centrifuged at 12000 *g*, at 4°C, for 10 min. The aqueous phase (upper phase) is carefully removed and added to 500 µL of isopropanol in a fresh tube. After vortexing, the samples are incubated at room temperature for 10 min and then centrifuged at 12000 *g*, at 4°C, for 10 min. The supernatant is discarded and the pellet washed with 1 mL 100% ethanol. After vortexing and a 5 min centrifugation at 7500 *g* and 4°C, the supernatant is discarded and the pellet gently dried for 5 min in a fume

cupboard. The RNA pellets are resuspended in 40 µL nuclease-free Milli-Q water by gently pipetting with RNase-free tips.

Contaminant genomic DNA is removed by using the RQ1 RNase-Free DNase (Promega). 1 µg RNA is mixed with 1 µL RQ1 DNase and 1 µL RQ1 DNase buffer in a 10 µL final volume. The mix is incubated at 37°C for 1h and the reaction stopped by adding 1 µL of RQ1 DNase Stop Solution and incubating the mix at 65°C for 10 min.

2- Nucleic acid treatment

a- Reverse transcription

After checking the absence of genomic DNA contamination, mRNAs are subjected to a reverse transcription reaction in order to synthesize their complementary DNA (cDNA). 0.5 to 1 µg RNA is mixed with 1 µL iScript reverse transcriptase and 4 µL of 5X iScript reaction mix in 20 µL final volume. The stabilization of the RNA/random primer structure is obtained after 5 min at 25°C, then the synthesis step is performed at 42°C for 30 min and the enzyme is inactivated at 85°C for 5 min.

b- PCR reactions and conditions

i. Routine PCR

The PCRs performed to check the presence of an insert or the expression of a gene are prepared in 25 µL final volume, with 0.2 mM dNTP, 0.2 µM of each primer, 5 µL of 10X Green GoTaq® reaction buffer (1.5 mM final concentration of $MgCl_2$) and 0.625 unit of GoTaq® (Promega).

ii. PCR for cloning

The PCRs performed to clone DNA fragments are prepared in 50 µL final volume, with 0.2 mM dNTP, 0.5 µM of each primer, 10 µL of 5X iProof HF Buffer (1.5 mM final concentration of $MgCl_2$) and 1 unit of iProof(Biorad).

iii. PCR conditions

The PCR were performed on Veriti® 96 Well Thermal Cycler (Applied Biosystems) according to a DNA fragment size, primer composition and enzyme adapted program. A denaturation step is first imposed at 94°C (GoTaq®) or 98°C (iProof) during 5 min then the PCR reaction undergoes an amplification step comprising a denaturation step at 94 or 98°C for 20 s, a hybridization step for 20s at a temperature depending on the primer composition and an elongation steps at 72°C for a period depending on the length of the fragment to be amplified. The PCR program ends up with a final elongation step of 5 min at 72°C. The amount of PCR product can be qualitatively estimated after an agarose gel electrophoresis.

Table 5: List of the primer used to obtain the coding sequences of *FW2.2* and the *FW2.2-likes* and to clone them in plasmids

Primer name	**Primer sequence**
GATEFW22-5	GGGGACAAGTTTGTACAAAAAAGCAGGCTACATGTATCAAACGGTAGG
GATEFW22-3	GGGGACCACTTTGTACAAGAAAGCTGGGTCTCACCTGGTCATGCCTGCATG
GATEFWL1-5	GGGGACAAGTTTGTACAAAAAAGCAGGCTACATGACTACAAAAAATTGG
GATEFWL1-3	GGGGACCACTTTGTACAAGAAAGCTGGGTCTTAACGAGTCATGGAAGATG
GATEFWL2-5	GGGGACAAGTTTGTACAAAAAAGCAGGCTACATGAACCCCTCAGCTCAACCAG
GATEFWL2-3	GGGGACCACTTTGTACAAGAAAGCTGGGTCTTATCGAGTCATTCCTCCTTG
GATEFWL3-5	GGGGACAAGTTTGTACAAAAAAGCAGGCTACATGAAATCTTCAACAATTTC
GATEFWL3-3	GGGGACCACTTTGTACAAGAAAGCTGGGTCTTATCTATTCATTCCACCTTC
GATEFWL4-5	GGGGACAAGTTTGTACAAAAAAGCAGGCTACATGGGTATGGGACAATAC
GATEFWL4-3	GGGGACCACTTTGTACAAGAAAGCTGGGTCTCAGCCCATCATGGCTTG
GATEFWL5-5	GGGGACAAGTTTGTACAAAAAAGCAGGCTACATGGGAAGAGTTGAAGCAAAC
GATEFWL5-3	GGGGACCACTTTGTACAAGAAAGCTGGGTCTTACATTGACATGGATTGTAC
GATEFWL6-5	GGGGACAAGTTTGTACAAAAAAGCAGGCTACATGAACTCGAATGGGTATAAC
GATEFWL6-3	GGGGACCACTTTGTACAAGAAAGCTGGGTCTTATCTTTTCATGGCTTCTTG
GATEFWL1NSREV	GGGGACCACTTTGTACAAGAAAGCTGGGTCTAAACGAGTCATGGAAGATG
GATEFWL2NSREV	GGGGACCACTTTGTACAAGAAAGCTGGGTCTAATCGAGTCATTCCTCCTTG
GATEFWL3NSREV	GGGGACCACTTTGTACAAGAAAGCTGGGTCTAATCTATTCATTCCACCTTC
GATEFWL4NSREV	GGGGACCACTTTGTACAAGAAAGCTGGGTCTAAGCCCATCATGGCTTG
GATEFWL5NSREV	GGGGACCACTTTGTACAAGAAAGCTGGGTCTAACATTGACATGGATTGTAC
GATEFWL6NSREV	GGGGACCACTTTGTACAAGAAAGCTGGGTCTAATCTTTTCATGGCTTCTTG
SPLITFWL1-pBTSUC-5	ATTAACAAGGCCATTACGGCCATGGCAGCTAAAGGACATG
SPLITFWL1-pBTSUC-3	AACTGATTGGCCGAGGCGGCCCCACGAGTCATGGAAGATGTAG
SPLITFWL2-pBTSUC-5	ATTAACAAGGCCATTACGGCCATGAACCCCTCAGCTCAAC

SPLITFWL2-pBTSUC-3	AACTGATTGGCCGAGGCGGCCCCTCGAGTCATTCCTCCTTGAAC
SPLITFWL3-pBTSUC-5	ATTAACAAGGCCATTACGGCCATGAAATCTTCAACAATTTC
SPLITFWL3-pBTSUC-3	AACTGATTGGCCGAGGCGGCCCCTCTATTCATTCCACCTTCAAC
SPLITFWL4-pBTSUC-5	ATTAACAAGGCCATTACGGCCATGGGTATGGGACAATACCAAC
SPLITFWL4-pBTSUC-3	AACTGATTGGCCGAGGCGGCCCCGCCCATCATGGCTTGGTGAAC
SPLITFWL5-pBTSUC-5	ATTAACAAGGCCATTACGGCCATGGGAAGAGTTGAAGCAAAC
SPLITFWL5-pBTSUC-3	AACTGATTGGCCGAGGCGGCCCCCATTGACATGGATTGTACTTG
SPLITFWL6-pBTSUC-5	ATTAACAAGGCCATTACGGCCATGTATCCTCTCATGAACTC
SPLITFWL6-pBTSUC-3	AACTGATTGGCCGAGGCGGCCCCTCTTTTCATGGCTTCTTGAAC
BamH1FW22FOR	GGGGGATCCATGTATCAAACGGTAGGATATAATC
Not1FW22REV	GGGGCGGCCGCCCTGGTCATGCCTGCATG

c- Nucleic acid electrophoresis

The PCR products, DNA fragments following a plasmid digestion or RNA were analyzed using agarose gel electrophoresis in non-denaturing conditions. The gel is prepared by melting 1% (w/v) agarose (SeaKem® LE Agarose, Lonza) in 0.5X TAE buffer (20 mM Tris-HCl pH 8, 0.5 mM Na_2EDTA, 2.5 mM Sodium Acetate, pH 8) and adding 1/50000 (v/v) DNA intercalating GelGreen (Biotium). The samples are mixed with 0.2 volume of 6X DNA Loading Dye Solution (Euromedex) and loaded on an agarose gel to be run for 20 min at 100 V. The gel is finally visualized under UV light using the GelDoc EZ instrument and the ImageLab software (Biorad).

d- Real Time PCR (RT-PCR)

The RT-PCR was performed in order to evaluate the accumulation of gene transcripts in given developmental stages or organs. This technique requires the use of an intercalating agent, the SYBR Green molecule, whose fluorescence is emitted at a 520 nm after a 497 nm excitation when intercalated between the two strands of a DNA fragment, proportionally to the DNA amount present in the reaction mix. The SYBR® Green fluorescence is measured at the end of each PCR cycle.

The RT-PCR reaction mix was prepared with 10 µL of the SYBR® Green containing GoTaq® qPCR Mastermix (Promega), 0.2 µM of each primer and 3 µL of cDNA 1:30 dilution. For each sample, 3 reaction mixes are prepared in order to eliminate the pipetting errors. The mixes

are placed on a 96 well-plate (Hard-Shell PCR Plates, Biorad) and the amplifications performed on the CFX 96 Real Time System (Biorad).

The primer efficiency was verified before every RT-PCR assay by performing a classic PCR on a DNA or cDNA sample in order to generate a large amount of specific DNA fragment amplified with the couple of primer to be tested. The DNA fragment is then purified using the Wizard® SV Gel and PCR Clean-Up System (Promega) and serially diluted from 10^{-3} to 10^{-8}, which will consist in the calibration curve. These standards are tested in RT-PCR in order to determine the PCR efficiency that should range between 95 and 105%.

The primers are designed to overlap two exon-intron junctions, in order to get rid of any genomic DNA trace, and to usually generate 100-200 base pair DNA fragment.

The RT-PCR program starts with a 95°C denaturation step for 3 min followed by 40 cycles of a 95°C denaturation step during 15 s and 60°C primer hybridization during 20 s and DNA elongation step. In order to verify the PCR product uniqueness, the 40 cycles are followed by a 0.5°C temperature increase every 5 s and a fluorescence measurement at the end of each increase stage. These final steps allow the generation of a melting curves that directly depends on the DNA fragment nucleic acid composition and length.

Table 6: List of the primer used for Real-Time PCR on tomato and *Arabidopsisthaliana* and tobacco

Primer name	Organism	Primer sequence
SlQFW22FOR	*Solanum lycopersicum*	GGAACAACTTCATGTGGGAG
SlQFW22REV	*Solanum lycopersicum*	TCTTCCAGATCATATTGCCC
SlQActinFOR	*Solanum lycopersicum*	GGACTCTGGTGATGGTGTTAG
SlQActinREV	*Solanum lycopersicum*	CCGTTCAGCAGTAGTGGTG
SlQeiF4AFOR	*Solanum lycopersicum*	AGTGGACGATTTGGAAGGAAG
SlQEiF4AREV	*Solanum lycopersicum*	GCTTCCTCGATTACGACGTTG
SlQLEGUMINFOR	*Solanum lycopersicum*	CCCTGTCCTTAACTGGCTCC
SlQLEGUMINREV	*Solanum lycopersicum*	GCCACTATAGCATTGTTGTAGAGG
SlQCK2Beta1FOR	*Solanum lycopersicum*	TACTAATGGAAAGGATCATCGC
SlQCK2Beta1REV	*Solanum lycopersicum*	TTTCAGATTCTGCATCAGAGC
SlQFWL1FOR	*Solanum lycopersicum*	GAGCGGATCCATCTATAGGG
SlQFWL1REV	*Solanum lycopersicum*	ACGAGTCATGGAAGATGTAGG
SlQFWL2FOR	*Solanum lycopersicum*	GGAGTTCAAGGAGGAATGAC
SlQFWL2REV	*Solanum lycopersicum*	ATTATCCACTAGCCAATGTCAC
SlQFWL3FOR	*Solanum lycopersicum*	GAGATGCATTTAGTTGAACG
SlQFWL3REV	*Solanum lycopersicum*	CTATTCATTCCACCTTCAACTG
SlQFWL4FOR	*Solanum lycopersicum*	GCAGTTACAACAAGCTATGG
SlQFWL4REV	*Solanum lycopersicum*	GGGAATTACAAATCGCAAAGG
SlQFWL5FOR	*Solanum lycopersicum*	TGTTTGATTTGAGGTTGTGG
SlQFWL5REV	*Solanum lycopersicum*	AGTTCAAACAACTAACACAGCC
SlQFWL6FOR	*Solanum lycopersicum*	TAACCAACTACACCTAATGCTG
SlQFWL6REV	*Solanum lycopersicum*	CAAGAAGGTAATCAAGTGGA
AtQCYCD3;1FOR	*Arabidopsis thaliana*	GCAAGTTGATCCCTTTGACC
AtQCYCD3;1REV	*Arabidopsis thaliana*	CAGCTTGGACTGTTCAACGA
AtQCYCA1;1FOR	*Arabidopsis thaliana*	GGCTAAGAAGCGACCTGATG
AtQCYCA1;1REV	*Arabidopsis thaliana*	TACAAGCCACACCAAGCAAC
AtQCYCB2;3FOR	*Arabidopsis thaliana*	TAAACCACCTGTGCATCGAC
AtQCYCB2;3REV	*Arabidopsis thaliana*	ATCTCCTCCAGCATTGCTTC
AtQCDKB1;1FOR	*Arabidopsis thaliana*	CGATTACTCTGCGTCGAACA
AtQCDKB1;1REV	*Arabidopsis thaliana*	TATGACAATGCGCAACACCT
AtQCCS52A1FOR	*Arabidopsis thaliana*	TTATGTGATCTCGGAGCTGAGGAT
AtQCCS52A1REV	*Arabidopsis thaliana*	CCCATATCTGAACTTTCCCGGTA
AtQRBRFOR	*Arabidopsis thaliana*	CAAGTGGCTCAGGACTGTCA
AtQRBRREV	*Arabidopsis thaliana*	TCCATCAGGTCAACAGCTTG
AtQACT2FOR	*Arabidopsis thaliana*	GGCTCCTCTTAACCCAAAGGC
AtQACT2REV	*Arabidopsis thaliana*	CACACCATCACCAGAATCCAGC
NtQEF1AFOR	*Nicotiana tabacum*	GCTGTGAGGGACATGCGTCAAA

NtQEF1AREV	*Nicotiana tabacum*	GTAGTAGATATCGCGAGTACCACCA
NtQPCNAFOR	*Nicotiana tabacum*	TCTTTGACTTTTGCCCTGAGA
NtQPCNAREV	*Nicotiana tabacum*	GCCCATCTCAGCAATCTTGT
NtQCYCB1.2FOR	*Nicotiana tabacum*	GGCTGCATCATCATCAAGTG
NtQCYCB1.2REV	*Nicotiana tabacum*	CATGTGGCACCTTTGACAAC
NtQCYCA1.1FOR	*Nicotiana tabacum*	TGCCCCTCCAACAATACCTGT
NtQCYCA1.1REV	*Nicotiana tabacum*	CGAAGCATCGTTGAAATGAA
NtQCDKBFOR	*Nicotiana tabacum*	CTATGGTACAGAGCTCCTG
NtQCDKBREV	*Nicotiana tabacum*	GCATTAGAAGCAACCTCAG
NtQCYCDFOR	*Nicotiana tabacum*	GAACTCATATCAGAAGTGCTGCCA
NtQCYCDREV	*Nicotiana tabacum*	CTGCCAACTGCAACCACC
NtQTUBFOR	*Nicotiana tabacum*	CCAGACGGCTCATAGGGTTA
NtQTUBREV	*Nicotiana tabacum*	GCAAACGTTGGATGATTCCT
NtQWBC1FOR	*Nicotiana tabacum*	ATCTCACGTAGCCGGAGCA
NtQWBC1REV	*Nicotiana tabacum*	TTTGTTCTGGTGGACGGGAT
NtQGSP1FOR	*Nicotiana tabacum*	TGGAAACTTTAGGGTCCTTACTAC
NtQGSP1REV	*Nicotiana tabacum*	CAAGCCTTGTAGTGAGCATCTG

3- DNA cloning

a- Classic cloning (digestion-ligation)

i. DNA fragment generation

The first step of a classic cloning starts with the generation of the DNA fragment to be cloned. In this aim, a PCR using a gene specific pair of primers with adapter sequences that will allow flanking the DNA sequence with enzyme cutting sites.

The PCR performed uses the iProof (Biorad) DNA polymerase. The first step is a denaturation step at 98°C during 3 min. The second step consists in 5 cycles of a denaturation step at 98°C for 20 s, a primer annealing at 55°C for 20 s and a 15s/kbp elongation step at 72°C. The annealing temperature is set low to force the primers to anneal on the right sequence. The third step also consists in the same 5 previous cycles, except that the annealing temperature is arisen to 60°C, to make the primers more specific and avoid unspecific annealing. The fourth step is a 35 cycle of 98°C for 20 s, 68°C for 20 s and a 15 s/kbp elongation at 72°C. This step is set to allow the multiplication of DNA fragment. The last step is a 5 min elongation step at 72°C.

The PCR product length, relative quantity and uniqueness are verified by migration on agarose gel. After this verification, the DNA fragment obtained is purified using the Wizard® SV Gel and PCR Clean-Up System (Promega) and quantified by spectrometry using the Nanovue (GE Healthcare Life Sciences).

ii. DNA fragment and plasmid digestion

200 ng of DNA fragment and 2 µg of plasmid are digested with the appropriate enzymes in order to generate sticky ends. The DNA fragment and the plasmid are separately mixed with a mix containing the restriction enzyme(s) and the appropriate buffer.The digestion is run for 1 h at 37°C for the NotI or BamHI enzymes (Promega - used for the digestion of the pE2, 3 or 6 C and N plasmids) or 50°C for the SfiI enzyme (Promega - used for the digestion of the pBT3-SUC and pPR3N Split-Ubiquitin plasmids).

After the end of the digestion step, the DNA fragment and the plasmid are purified using the following protocol. The reaction volume is arisen to 200 µL by TE buffer (10 mM Tris-hydroxymethyl aminomethane and 1 mM EDTA pH 8) addition and mixed with 200 µL of

phenol/chloroform/isoamyl acid (25:24:1). The mix is vortexed and incubated at room temperature for 2 min and then centrifuged for 5 min at 13000 *g*. The aqueous phase is carefully removed and 180 µL of chloroform are added. The mix is vortexed and centrifuged at 13000 *g* for 5 min. These two steps allow the reaction interruption and protein precipitation. The aqueous phase is carefully taken and transferred to a fresh tube containing 1/10 volume of 3 M sodium acetate to be then shaken. 6/10 volume of isopropanol is added and the mix is vortexed and centrifugated at 13000 *g* for 30 min at 4°C. This step allows the DNA precipitation. The supernatant is discarded and the pellet washed with 200 µL of 70% ethanol and gentle pipetting. After a 15 min centrifugation at 13000 *g* and 4°C, the supernatant is discarded and the pellet dried with vacuum for 5 min and resuspended in 10 µL TE buffer pH 8. The purified digestion products are quantified by spectrometry using the Nanovue.

iii. Ligation and bacteria transformation

The ligation mix is prepared with specific quantities of insert and plasmid. These quantities are calculated using the following formula:

$$\text{Quantity of insert} = \frac{\text{Quantity of vector x Insert lenght}}{\text{Vector lenght}} \text{ x molar ratio of } \frac{\text{Insert}}{\text{Vector}}$$

The insert and plasmid are mixed with 0.5 µL of T4 DNA Ligase (Thermo Scientific) and 2 µL of T4 DNA Ligase buffer in a 20 µL final volume. The ligation is performed for a minimum of 5 h at room temperature and stopped by heating the mix at 65°C during 10 min.

The bacteria transformation is set by mixing 1 µL of ligation reaction and 40 µL of electro-competent *E. coli* bacteria thawed on ice. The mixture is placed in an electroporation cuvette (1 mm gap – Cell Projects) and subjected to an electric shock at 1.8 kV during 4-5 ms. The bacteria are immediately re-suspended in 1 mL of LB medium and incubated during 30-45 min at 37°C with shaking. A fraction is spread on solid LB medium with the appropriate selection antibiotic and grown at 37°C over night.

b- Gateway® system

This system allows the rapid cloning of DNA fragment in Gateway®-compatible plasmid and is based on the lambda phage ability to recognize specific attachment sites (attB on *E. coli* chromosome and attP on the lambda phage DNA and attL and attR when inserted in *E. coli* genomic DNA) for a recombination. The recombination system is described in figure 45:

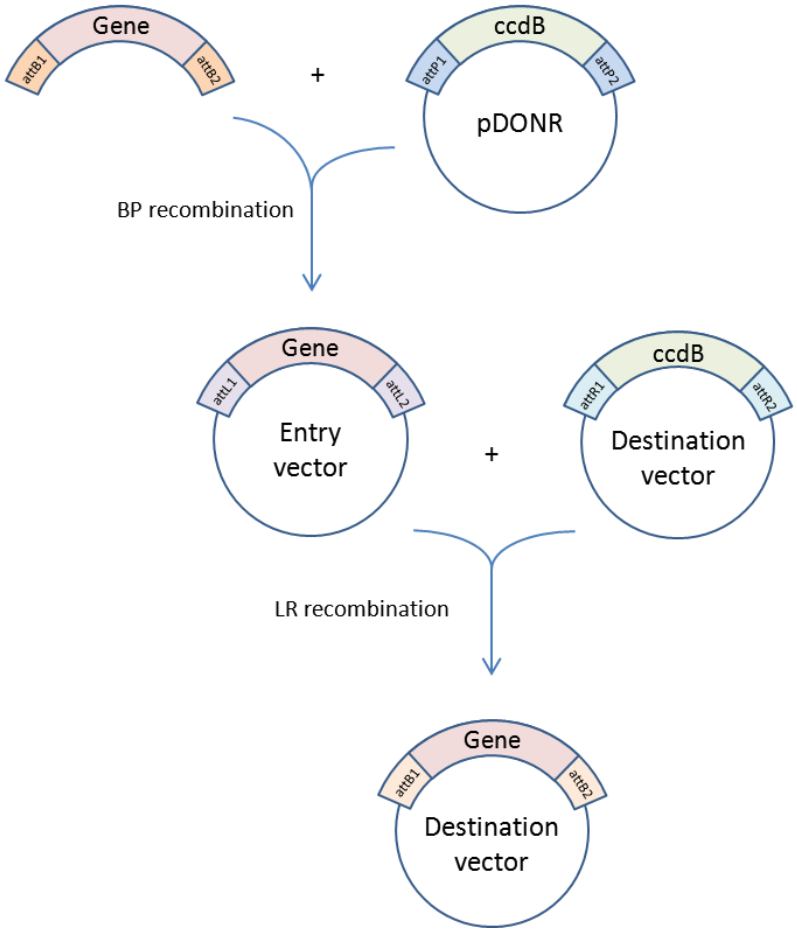

Figure 45: Principle of the Gateway ® system.

i. Insert preparation

The DNA fragment of interest is first amplified from cDNA samples in order to flank it with the attB1/attB2 sequences using specific adapter primers and a modified PCR program (the same then described in section 2-3.1.1).

Once the PCR is over, the PCR product length, relative quantity and uniqueness are verified by migration on agarose gel and then purified using the Wizard® SV Gel and PCR Clean-Up System and quantified with the Nanovue.

ii. Cloning into entry vector and destination vector

The DNA fragment cloning into entry vector is performed using the Gateway® system in a half reaction mix. 150 ng of DNA fragment flanked with the attB1/attB2 sequences are mixed with 75 ng of entry plasmid (usually the pDONR201) and 1 µL of BP clonase enzyme (Invitrogen) in a 5 µL final volume (by adding TE buffer). The recombination reaction is run during a minimum of 5 h and the reaction stopped with the addition of 0.5 µL of Proteinase K at 37°C for 10 min. 1 µL of the recombination mix is used to transform electrocompetent *E. coli* bacteria by electroporation, as described in section 2-3.1.3.

The recombination between the entry vector and the destination vector is also performed using the Gateway® system in a half reaction mix. 75 ng of the recombined entry vector are mixed with 75 ng of destination vector and 1 µL of LR clonase enzyme (Invitrogen) in a 5 µL final volume (by adding TE buffer). The recombination reaction is run for a minimum of 3 h and the reaction stopped with the addition of 0.5 µL of Proteinase K at 37°C for 10 min. 1 µL of the recombination mix is used to transform electro-competent *E. coli* bacteria by electroporation, as described in section 2-3.1.3.

The persistence of the ccdB gene in the non-recombined plasmids allows the selection of the bacteria that only have incorporated the recombined plasmid, as the ccdB gene encodes for a DNA Gyrase inhibitor that constitutes a poison.

c- cDNA library generation

5DAA fruit pericarp of the TA1143 line and 10 and 15DAA fruits pericarp of the TA1144 line were used to perform an RNA extraction using the TRIzol® reagent with the adapted protocol and undergone the quality checks (PCR on RNA, agarose electrophoresis, quantification). The extracted RNAs were used to synthesize cDNA in order to be inserted in a split ubiquitin expression vector.

The cDNA synthesis is performed using the MINT-Universal cDNA synthesis kit (Evrogen), according to the provided "cDNA preparation protocol-II ".

The cDNA synthesized are then inserted in the pPR3N plasmid according to the EasyClone cDNA Library Construction Kit protocol (Dualsystems Biotech).

4- DNA sequencing

The DNA sequencing was performed by Beckman Coulter Genomics, using the Sanger technique.

Table 7: List of the primer used for the DNA sequencing:

Primer name	Primer sequence
AttB1	ACAAGTTTGTACAAAAAAGCAGGCT
AttB2	ACCACTTTGTACAAGAAAGCTGGGT
AttL1	CGCGTTAACGCTAGCATGGATCTC
AttL2	CATCAGAGATTTTGAGACAC
SK primer	CGCTCTAGAACTAGTGGATC
pBTSUC FOR	TTTCTGCACAATATTTCAAGC
pBTSUC REV	CTTGACGAAAATCTGCATGG
pPR3N FOR	GTCGAAAATTCAAGACAAGG
pPR3N REV	AAGCGTGACATAACTAATTA
N-YFP FOR	GTAAACGGCCACAAGTTCAG
N-YFP REV	GTCGTCCTTGAAGAAGATGGT
C-YFP FOR	GACCACTACCAGCAGAACAC
C-YFP REV	TAGCTCAGGTAGTGGTTGTC

C. Protein interaction screen : Split-Ubiquitin on cDNA library

1- Split-ubiquitin transformation

a- Targeted split-ubiquitin

A cDNA library screen using the split-ubiquitin technique has been performed in order to identify the potential FW2.2 interactors.

This technique has been first described by Stagljar (1998) and is based on the two hybrid technique, adapted to membrane proteins. Yeasts are transformed with two plasmids. The first plasmid, the pBT3-SUC plasmid (see section 1-3.3) encodes the “bait” protein fused with the C-terminal part of the ubiquitin itself fused with the LexA transcription factor and the second plasmid; the pPR3-N plasmid (see section 1-3.3) encodes the “prey” protein fused with the N-terminal part of the ubiquitin. The double plasmid yeast transformation allows them to grow on a leucin and tryptophan lacking medium. If the prey and bait proteins interact the two parts of the ubiquitin are put in a close vicinity and a functional ubiquitin is reconstituted. Ubiquitin specific proteases are then required to cut the link between the bait and prey proteins and the two parts of the ubiquitin which leads to the delivery of the LexA transcription factor in the cytoplasm and its shift to the nucleus. This provokes the expression of reporter genes that allow the growth of the transformed yeasts on a histidine and adenine lacking medium (see Figure 46).

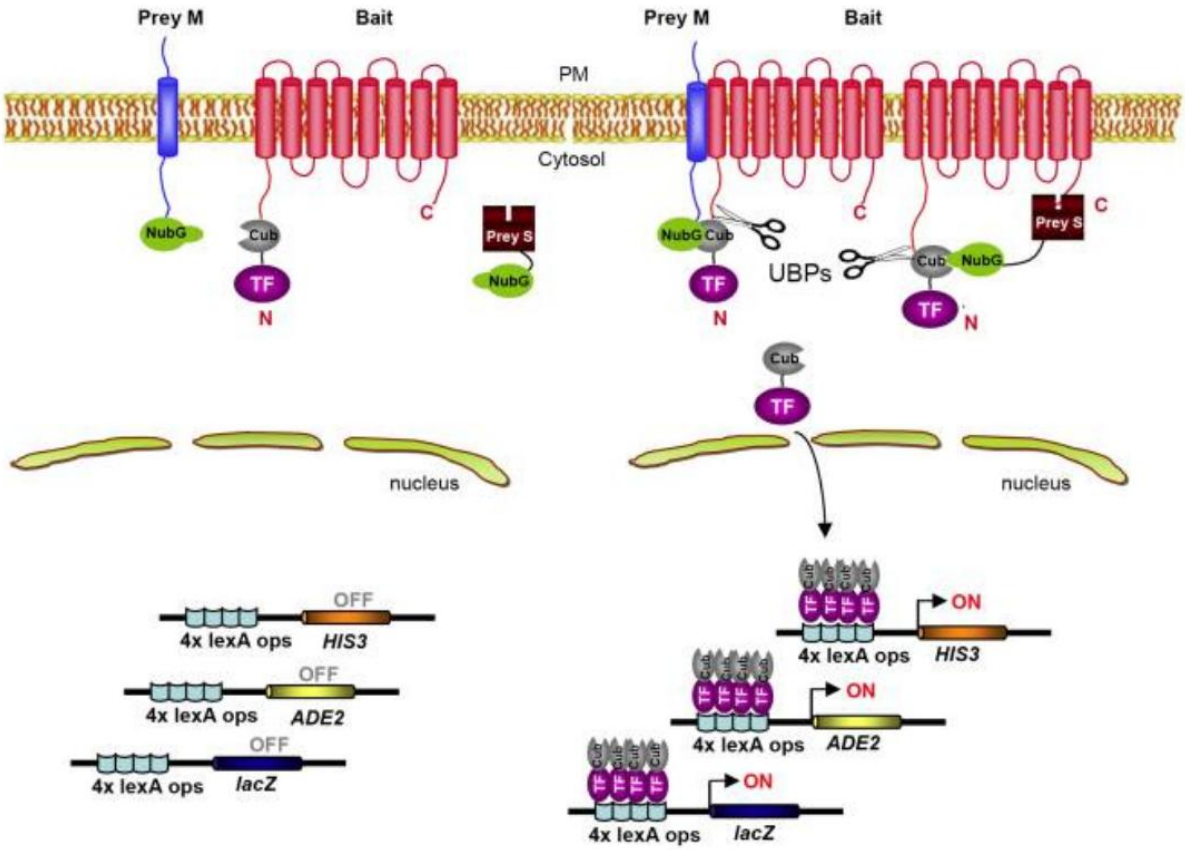

Figure 46: Principle of the Split-ubiquitin system (from Gisler *et al.* 2008).

To perform a double yeast transformation, 3-5 THY.AP4 yeast colonies are diluted in 10 mL of YPAD medium and cultured under shaking at 30°C, the day before the transformation. The morning before the transformation, the cell concentration of the liquid culture is measured using a Malassez counting chamber and a final volume of 50 mL of YPAD is inoculated with $2.5x10^8$ cells and placed at 30°C until the cell concentration reaches $2x10^7$ cells/mL (4-5 h). The yeasts are then centrifuged at 1000 *g* for 5 min and washed with 25 mL of sterile milliQ water. After 5 min centrifugation at 1000 *g* the cell pellet is re-suspended in 3 mL of 0.1 M lithium acetate and incubated for 15 min at 30°C. The yeasts are centrifuged at 1000 *g* for 5 min and the supernatant replaced by 2.4 mL of polyethylene glycol 3500 50%, 360 µL of 1 M lithium acetate, 500 µL of denatured salmon sperm DNA at 2mg/mL and 280 µL of sterile milliQ water. An aliquot of 354 µL is taken and mixed with 3 µL of each plasmid. The mixture incubated at 30°C for 30 min and then placed at 42°C for 20 min with vigorous shaking every 5 min. The yeasts are then centrifuged for 5 min at 700 *g* and resuspended in

460 µL of sterile milliQ water. 150 µL of the suspension are plated on SD-LT, SD-LTH and SD-STHA supplemented with 20 mM 3AT. The plates are placed at 30°C until the appearance of colonies (2-3 days).

b- cDNA screen split-ubiquitin

The technique is slightly modified to screen a tomato cDNA library in order to identify the FW2.2 interactors and is performed using the "DSY Yeast Transformation Kit" (Dualsystems Biotech) according to the supplier's protocol.

The first step of the screen consists in the yeast simple transformation with the "bait" plasmid (pBT3-SUC containing the coding sequence of FW2.2) using the previous protocol.

When transformed yeast colonies have grown, the second step is performed according to the Dualsystems Biotech high-efficiency library scale transformation protocol (P01003) using 7µg of the cDNA library prepared.

After the transformation, yeasts are suspended in a total 9.6 mL of 0.9% NaCl and plated at the rate of 300 µL per 15 cm diameter plate of SD-LTHA medium with 20 mM 3-AT. The 32 plates prepared are placed at 30°C for 3-4 days.

2- Clone extraction and identification

The colonies that have grown after the transformation are picked up and struck on a SD-LWHA medium with a higher concentration of 3-AT (25 mM). If the struck colonies still grow, they are then grown in 600 µL liquid SD-LT overnight at 30°C, shaking.

The plasmid extraction is performed according to the section 2-1.1.3, and once the plasmids extracted, the sequencing has been performed by Cogenics using Sanger technique.

The sequences are identified using the BLAST tool of SGN (http://solgenomics.net/tools/blast/index.pl)against the "SGN tomato combined - WGS, BAC and unigene sequences" sequence set.

D. Stable and transient transformation

1- *Arabidopsis thaliana* transgenesis

a- Plants stable transformation

Arabidopsis thaliana ecotype Columbia (Col-0) plants were transformed using the floral dip technique according to Clough and Bent (1998).

Agrobacterium tumefaciens strain GV3101 containing the plasmid holding the DNA of interest were grown in 2YT overnight and then diluted to reach an OD_{600nm} of 0.8 in ½MS with 5% sucrose.

The bacterial solution prepared is gently put using a pipette on the flower bud, apexes and open flowers in order to create a sticking drop.

This manipulation is repeated until the end of the plant flowering. The seeds are then collected and screened on an appropriate medium.

b- Plants transient transformation

Sterile *Arabidopsis thaliana* ecotype Columbia (Col-0) seeds are sown on 4 ml of solid ½ MS medium covered with a sterile filter, in a 6 well plate (as described on the figure 47 below). The plate is placed in the dark at 4°C for 2 days to make the seeds undergo a stratification step.

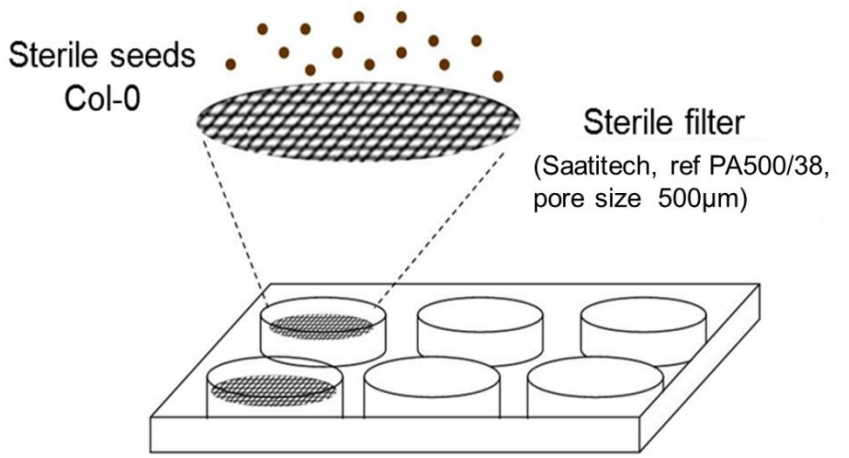

Figure 47: *Arabidopsis* seeds sowing for a transient transformation.

After this step of stratification the plate is transferred in a culture room, t=22/18°C, D=16h/N=8h, for 4 days to let the plants develop their cotyledons.

When the plants are grown, an *Agrobacterium tumefaciens* strain GV3101 culture containing the plasmid holding the DNA of interest is prepared in order to obtain a 4ml aliquot at an OD_{600nm} of 2 in ½ MS with 200 µM acetosynringone.

The plantlets are gently covered with the 4 mL of culture and placed under a vacuum for twice 1 minute. The *Agrobacterium* culture is then gently removed and the plate is placed in the culture room for 3 days before observation.

c- *Arabidopsis* cells stable transformation

PSB-L(*Arabidopsis thaliana* ecotype Landsberg erecta) suspension cells were grown for 4 days in MSMO medium before transformation using GV3101 *Agrobacterium* strain. The PSB-L culture is resuspended in 10 mL of MSMO medium after a 4000 rpm centrifuge during 15 minutes. The resuspended cell culture is distributed in a 6 well plate at the rate of 3 mL of culture per well.

The culture of *Agrobacterium* strain GV3101 containing the DNA of interest is washed 3 times in 10 mL of MSMO the first time, then enough MSMO medium in order to obtain an OD_{600nm} of 1, twice, at 4000 rpm for 15 minutes.

The PSB-L cells are then mixed with 0, 100 µL and 200 µL of *Agrobacterium* culture with 200 µM of acetosyringone. The coculture mix is placed at 25°C for 2 days, shaking.

After the coculture step, the PSB-L cells are washed from *Agrobacterium* with 37 mL of MSMO with 250 µg/mL of Timentin and 50 µg/mL of Kanamycin, and an 800 rpm centrifuge for 5 minutes. After discarding the maximum of supernatant, 2 ml of cell suspension are plated on MSMO petri dishes with 250 µg/ml of Timentin and 50 µg/mL of Kanamycin and placed at 25°C in culture room, until the appearance of calluses. These calluses are then picked up and struck on a new plate of MSMO with antibiotics to grow them and verify their transformation.

2- BY2 cells transgenesis

100 mL of a 4 days BY2 cell culture are used to perform a cell transformation. The cells are washed in 40 mL of MS# (modified MS – 4,4 g/L MS basal salt, 30 g/L sucrose, 0.2 g/L

KH_2PO_4, 2.5 mg/L thiamine, 50 mg/L myo-inositol, 1,8 g/L glucose, 0.2 mg/L 2,4D) with a 700 rpm centrifuge during 5 minutes and resuspended to reach a volume of 25 mL with 200 µM of acetosyringone. An *Agrobacterium* culture is pelleted with a 3000 rpm centrifuge and resuspended in 1 mL of MS# to an OD_{600nm} of 1.

4 mL of the BY2 cells suspension are dispatched in a 6 well plate and mixed with 0, 10, 20, 50, 100 and 200 µL of *Agrobacterium* suspension. The coculture mix is then placed in the dark for 48h at 25°C, without shaking.

After the coculture step, the cells are washed 3 times from the bacteria by harvesting the cells, adding 10 mL of MS with 100 µg/mL of kanamycin and 250 µg/mL of timentin and centrifuging them during 5 minutes at 700 rpm. The supernatant is discarded after every centrifuge and the cells are finally resuspended in a final volume of 3 mL to be then plated on MS 1% agar and 100 µg/mL of kanamycin and 250 µg/mL of timentin by gently shaking the petri dishes. The plates are placed 3 to 4 weeks in the dark at 25°C, until the appearance of calluses. These calluses are then picked up and struck on a new plate of MS with antibiotics to grow them and verify their transformation.

E. Protein study

1- Protein extraction

Flash frozen tobacco leaves crushed using a Dangoumo or fresh PSB-L or BY2 cells cleared from their culture medium were used to extract total membrane protein. 150 mg of the leaves powders obtained or the pelleted cells were mixed with 1mL of extraction buffer (6,06 g/L Tris pH 7.5, 102.7 g/L sucrose, 8,75 g/L NaCl, 1 g/L potassium acetate, 1,85 g/L EDTA, 1 mM PMSF and 3% v/v protease inhibitor cocktail). Ceramic beads (Matrix-Green, MP Biomedicals) were added to the cells to ensure a better homogenization and functioning of the extraction buffer. The mixing was performed using the FastPrep 24 (MP Biomedicals) at maximum speed for 40 seconds, 3 times. The samples are then centrifugated at 10000 *g* for 10 minutes at 4°C. The supernatant is carefully harvested and centrifugated at 100000 *g* for 1h at 4°C. Once the centrifugation is over, the supernatant is taken and constitutes the

soluble proteins, whereas the pellet is resuspended in 50 µL of the extraction buffer by pipetting and constitutes the total membrane proteins.

The protein concentration is measured using the Bradford technique (1976) referring to a solution of bovine serum albumin (BSA) as a standard.

2- Analysis

a- Monodimentional electrophoresis in denaturing conditions

The proteins extracted were analyzed by monodimentional electrophoresis in denaturing conditions described by Laemmli (1970). The gel is prepared in two separated steps.

The first step allows the preparation of the running gel, which allows separating the proteins according to their size, constituted by 10 to 15% (w/v) of acrylamide, 0,3 to 0,5 bis-acrylamide, 375 mM of Tris HCl pH 8.8; 0,1% (w/v) SDS; 2 mM (Na2)EDTA; 0,5% (w/v) ammonium persulfate and 0,05% (w/v) TEMED.

The second step consists in the preparation of the concentration gel, which allows bringing all the proteins at the same point before being separated according to their size. This gel is constituted by 5,4% (w/v) of acrylamide, 0,18% (w/v) of bis-acrylamide, 125 mM of Tris HCl pH 6.8; 0,1% (w/v) SDS; 2mM (Na2)EDTA; 0,5% (w/v) ammonium persulfate and 0,05% (w/v) TEMED.

The gel prepared is placed in a migration buffer (25 mM Tris, 1 mM (Na2)EDTA, 196 mM glycine and 0,1% (w/v) SDS). 20 µg of protein are mixed with the 3rd of their volume of a loading buffer (80 mM Tris HCl pH 6,8; 2% (w/v) SDS; 17% (v/v) glycerol; 0,05% (w/v) bromophenol blue and 3% (w/v) DTT) and heated at 95°C for 5 minutes to be then placed on the gel. A 5µl protein ladder (Spectra Multicolor Broad Range Protein Ladder – ThermoScientific) sample is also placed on the gel to further evaluate the protein size. The migration occurs at a voltage of 100V during 1h.

b- Western blot

i. Protein electrotransfer on PVDF membrane

The proteins are transferred on a water-wet PVDF membrane using the iBlot™ system (Gel Transfer Stacks – Invitrogen), according to the manufacturer's recommendations. The transfer occurs during 7 minutes at 20V.

ii. Protein immunodetection on PVDF membrane

The "WesternDot™ 625 Goat anti-rabbit or mouse Western Blot" (Invitrogen) kit has been used to immunodetect the proteins on the membrane, according to the manufacturer's recommendations. We used rabbit anti-GFP antibodies (Torrey Pines Biolabs) diluted to 1/1000th as a primary antibody and a goat anti-rabbit antibody, coupled to biotin diluted to 1/2000th as a secondary antibody and the Qdot® nanocrystals 625 streptavidin conjugate at 1/2000th as signal. After washing, the membrane is revealed using the Biorad GelDoc EZ system with a transilluminator tray detecting a 625nm signal.

c- Microscopic analysis

The detection of the fluorescent proteins in tobacco and *Arabidopsis* plants and cells presence was observed using the Nikon Eclipse E800 epifluorescence microscope.

The localization of the fluorescent proteins in tobacco and *Arabidopsis* plants and cells was observed using the Leica TSC SP2 confocal laser scanning microscope.

The EYFP and the GFP proteins were visualized using a GFP filter (excitation: 514 nm, emission: from 460 to 500nm).

The BY2 cells plasmolysis has been performed by dissolving a piece of BY2 cells callus in a drop of 5% NaCl solution (w/v). The observation of the plasmolyzed cells is performed instantly after mixing the cells and the NaCl solution.

The epidermis cell outlines of the transformed *Arabidopsis thaliana* have been draw after taking a picture of the leaf epidermis surface under an optical microscope. The images obtained were converted to 8 bit images that serve to cell size measurement using the ImageJ software.

The BY2 cell sizes were also measured using ImageJ.

3- Voltage-clamp

a- Medium preparation

The ND96 medium (96mM NaCl, 2mM KCl, 1,8 mM $MgCl_2$, 2 mM $CaCl_2$, 10 mM HEPES, 2,5 mM Sodium pyruvate, 50 µg/ml Gentamycine, pH 6,5) was prepared and separated in 100 mL aliquots in which $CdCl_2$ (cadmium chloride) and $ZnCl_2$ (zinc chloride) have been added to a final concentration of 1mM.

b- cDNA preparation and oocytes injection

The *AtPCR1* and *SlFW2.2* coding sequences have been inserted in the pGEMGWC plasmid and linearized using the NheI enzyme (Promega) in order to proceed to the in vitro transcription using the SP6 in vitro transcription kit (Promega), according to the manufacturer's protocol, precipitated at -20°C with lithium chloride, centrifugated at 15000 rpm during 15 minutes at 4°C, washed with 1 mL ethanol at 70% to be then again centrifugated at 15000 rpm during 15 minutes at 4°C and being resuspended in 22µl of nuclease free water.

The *Xenopus* oocytes, taken the day before and incubated in regular ND96 medium in the dark at 20°C over night, are injected with 50 nL of *AtPCR1* or *SlFW2.2* cDNAs (24 oocytes have been used for each cDNA injection) using a stretched glass capillary tube and a Nanoinjector, or not injected in order to constitute negative controls.

c- Voltage clamp measurement

The oocytes are first placed in a regular ND96 medium bath and stung with two capillaries filled with a 3 M KCl solution, acting as electrodes, one imposing the voltage generated by an amplifier (15 mV steps from -155 mV to 40 mV), and the other measuring the global cell depolarization. A third capillary is placed in the ND96 to be used as a reference electrode.

The first measurement, the control measurement, is performed in the ND96 bath. The second measurement is performed in ND96 supplemented with 1mM zinc (the bath is progressively replaced during 1 minute of wash with the supplemented medium). And the third measurement is performed in ND96 supplemented with 1mM cadmium (the bath is progressively replaced during 1 minute of wash with the supplemented medium).

Every condition has been tested on 6 oocytes.

The data analyses have been made using the Clampfit software.

F. Mineral content measurement

The mineral contents measurements were performed by the US 1118 *USRAVE* laboratory at the INRA of Bordeaux.

1- Mineral content of tomato fruit pericarp measurement

The mineral content in tomato fruit pericarp was measured using two techniques, depending on the element quantities. The quantities of lyophilized fruit pericarp powders provided for the measurement were not less than 1 g.

The nature of the major elements and their respective quantity were determined using inductively coupled plasma - optical emission spectrometry (ICP-OES).

For traces elements, their respective quantity were determined using inductively coupled plasma - mass spectrometry (ICP-MS), more sensitive than the ICP-OES.

2- Mineral content of BY2 cells measurement

The trace elements contents in the BY2 cells were measured using three techniques, as the material quantity used is not more than 1g.

The nature of the major elements and their respective quantity were determined using ICP-MS

The traces elements contents were determined by coupling electrothermal vaporization to ICP-OES.

G. Sequence analysis

1- Isolation of new sequences

The homologues of FW2.2 in tomato were found using the Sol Genomics Network and the FLAGdb++ program available online.

The sequences were isolated by blasting the protein sequence of FW2.2 as a query and retrieved in a tomato database.

2- Protein alignment

The identification of the conserved domains and motifs in the protein sequences were performed using the ClustalW tool hosted at http://www.genome.jp/. The alignments were performed under the "Slow/Accurate" pairwise alignment and the default parameters were applied.

3- Phylogenetic analysis

The amino acid sequences used to generate the phylogenetic tree were aligned using the MUSCLE tool of the European Bioinformatics Institute (EBI). The alignment performed was then treated with the Gblocks tool (http://molevol.cmima.csic.es/castresana/Gblocks_server.html) in order to identify the more conserved domain of the proteins aligned.

Once the sequences cured, they were input in the MEGA5 software in order to generate a phylogenetic tree. The Maximum Likelihood statistic method was applied under the JTT (Jones-Taylor-Thornton) model with the Nearest Neighbor Interchange method. The tree was calculated with 1000 bootstraps.

Appendices

Appendix 1: Total mineral content measure in the M82 transgenic line

M82 transgenic fruits (M82+ small-fruit alleles)									
		10 DPA	20 DPA	30 DPA		40 DPA			
		Plant 1	Plant 1	Plant 1	Plant 2	Plant 1	Plant 2		
HUT residual humidity	%	6.13 +/- 0.12	8.13 +/- 0.16	11.8 +/- 0.24	14.8 +/- 0.30	14.6 +/- 0.29	15.4 +/- 0.31		
CBR raw ashes	%	7.54 +/- 0.15	8.30 +/- 0.17	7.90 +/- 0.16	7.54 +/- 0.15	9.35 +/- 0.19	7.93 +/- 0.16		
MOR organic matter	%	92.5 +/- 1.8	91.7 +/- 1.8	92.1 +/- 1.8	92.5 +/- 1.8	90.6 +/- 1.8	92.1 +/- 1.8		
PHO Phosphorus total	mg/100 g	568 +/- 28	526 +/- 26	552 +/- 28	461 +/- 23	604 +/- 30	524 +/- 26		
POT Potassium total	mg/100 g	2940 +/- 290	3670 +/- 370	3450 +/- 340	3240 +/- 320	3900 +/- 390	3750 +/- 380		
CAL Calcium total	mg/100 g	98.9 +/- 9.9	77.5 +/- 7.7	134 +/- 13	136 +/- 14	193 +/- 19	149 +/- 15		
MAG Magnesium total	mg/100 g	188 +/- 19	157 +/- 16	194 +/- 19	141 +/- 14	172 +/- 17	174 +/- 17		
SOD Sodium total	mg/100 g	106	62.0	102	71.8	110	94.5		
FER Iron total	mg/100 g	8.44 +/- 1.3	5.26 +/- 0.79	6.52 +/- 0.98	6.10 +/- 0.92	7.35 +/- 1.1	4.72 +/- 0.71		
MAN Manganese total	mg/100 g	* < 1	0.967 +/- 0.097	1.74 +/- 0.17	0.934 +/- 0.093	1.35 +/- 0.13	1.35 +/- 0.13		
ZIN Zinc total	mg/100 g	2.14 +/- 0.21	1.83 +/- 0.18	2.18 +/- 0.22	1.52 +/- 0.15	1.90 +/- 0.19	2.10 +/- 0.21		
BOR Boron total	mg/100 g	1.36	1.11	1.18	1.47	1.09	1.26		
CUI Copper total	mg/kg	0.583 +/- 0.12	0.593 +/- 0.12	0.802 +/- 0.16	0.266 +/- 0.053	0.590 +/- 0.12	0.738 +/- 0.15		
ALU Aluminium total	mg/kg	50.9 +/- 7.6	42.8 +/- 6.4	72.8 +/- 11	63.5 +/- 9.5	243 +/- 36	181 +/- 27		
MOL Molybdenum total	mg/kg	1.01 +/- 0.20	0.788 +/- 0.16	1.31 +/- 0.26	0.698 +/- 0.14	1.05 +/- 0.21	0.936 +/- 0.19		
CAD Cadmium total	mg/kg	0.117 +/- 0.023	0.0477 +/- 0.0095	0.0597 +/- 0.012	0.0574 +/- 0.011	0.0648 +/- 0.013	0.0545 +/- 0.011		
CHR Chromium total	mg/kg	4.83 +/- 0.97	1.12 +/- 0.22	1.69 +/- 0.34	2.43 +/- 0.49	1.22 +/- 0.24	2.04 +/- 0.41		
NIC Nickel total	mg/kg	55.7 +/- 11	3.89 +/- 0.78	1.18 +/- 0.24	0.894 +/- 0.18	1.14 +/- 0.23	1.17 +/- 0.23		
PLO Lead total	mg/kg	* < 0.4	* < 0.1	* < 0.2	* < 0.2	* < 0.3	* < 0.2		
COB Cobalt total	mg/kg	0.223 +/- 0.045	* < 0.05	* < 0.07	* < 0.07	* < 0.08	0.0778 +/- 0.016		
ARS Arsenic total	mg/kg	* < 0.1	* < 0.05	* < 0.07	* < 0.07	* < 0.08	* < 0.06		

Appendix 2: Total mineral content measure in the M82 control wild type plant

		M82 fruits (control)							
		10 DPA	20 DPA	30 DPA		40 DPA	
		Plant 1	Plant 1	Plant 1	Plant 2	Plant 1	Plant 2
HUT residual humidity	%	8.33 +/- 0.17	10.6 +/- 0.21	14.5 +/- 0.29	11.7 +/- 0.23	15.2 +/- 0.30	15.5 +/- 0.31
CBR raw ashes	%	8.64 +/- 0.17	9.07 +/- 0.18	8.30 +/- 0.17	8.52 +/- 0.17	10.9 +/- 0.22	10.6 +/- 0.21
MOR organic matter	%	91.4 +/- 1.8	90.9 +/- 1.8	91.7 +/- 1.8	91.5 +/- 1.8	89.1 +/- 1.8	89.4 +/- 1.8
PHO Phosphorus total	mg/100 g	544 +/- 27	534 +/- 27	607 +/- 30	534 +/- 27	702 +/- 35	591 +/- 30
POT Potassium total	mg/100 g	3510 +/- 350	3960 +/- 400	3630 +/- 360	3570 +/- 360	4250 +/- 420	4400 +/- 440
CAL Calcium total	mg/100 g	118 +/- 12	45.3 +/- 4.5	181 +/- 18	93.9 +/- 9.4	202 +/- 20	158 +/- 16
MAG Magnesium total	mg/100 g	212 +/- 21	176 +/- 18	143 +/- 14	207 +/- 21	165 +/- 17	190 +/- 19
SOD Sodium total	mg/100 g	114	113	98.6	90.7	185	173
FER Iron total	mg/100 g	8.33 +/- 1.2	5.48 +/- 0.82	6.09 +/- 0.91	6.67 +/- 1.0	6.03 +/- 0.90	5.60 +/- 0.84
MAN Manganese total	mg/100 g	1.51 +/- 0.15	0.777 +/- 0.078	1.63 +/- 0.16	1.04 +/- 0.10	* <	0.862 +/- 0.086
ZIN Zinc total	mg/100 g	2.52 +/- 0.25	1.65 +/- 0.17	1.98 +/- 0.20	2.58 +/- 0.26	1.66 +/- 0.17	2.02 +/- 0.20
BOR Boron total	mg/100 g	1.52	1.41	1.34	1.08	* <	1.30
CUI Copper total	mg/kg	0.889 +/- 0.18	0.370 +/- 0.074	0.630 +/- 0.13	0.796 +/- 0.16	* < 0.5	0.643 +/- 0.13
ALU Aluminium total	mg/kg	145 +/- 22	153 +/- 23	189 +/- 28	90.4 +/- 14	194 +/- 29	190 +/- 29
MOL Molybdenum total	mg/kg	1.36 +/- 0.27	1.19 +/- 0.24	0.974 +/- 0.19	1.42 +/- 0.28	1.12 +/- 0.22	1.37 +/- 0.27
CAD Cadmium total	mg/kg	0.132 +/- 0.026	0.0605 +/- 0.012	0.108 +/- 0.022	0.0489 +/- 0.0098	0.390 +/- 0.078	0.124 +/- 0.025
CHR Chromium total	mg/kg	2.91 +/- 0.58	0.817 +/- 0.16	1.43 +/- 0.29	0.840 +/- 0.17	2.25 +/- 0.45	1.16 +/- 0.23
NIC Nickel total	mg/kg	2.40 +/- 0.48	1.25 +/- 0.25	0.408 +/- 0.082	0.814 +/- 0.16	1.15 +/- 0.23	0.764 +/- 0.15
PLO Lead total	mg/kg	0.453 +/- 0.091	* < 0.2	* < 0.3	* < 0.2	* < 0.5	* < 0.2
COB Cobalt total	mg/kg	0.415 +/- 0.083	* < 0.06	* < 0.09	* < 0.06	* < 0.2	* < 0.08
ARS Arsenic total	mg/kg	* < 0.1	* < 0.06	* < 0.09	* < 0.06	* < 0.2	* < 0.08

Appendix 3: Total mineral content measure in the TA1143 and TA1144 nearly isogenic line

		TA1143		TA1144	
		15 DPA	30 DPA	15 DPA	30 DPA
HUT residual humidity	%	10,9	12,7	9,93	14,7
CBR raw ashes	%	10,3	10,7	9,57	10,3
MOR organic matter	%	89,7	89,3	90,4	89,7
PHO Phosphorus total	mg/100 g	5,82	5,98	5,51	5,68
POT Potassium total	mg/100 g	43,3	44,7	40,2	42,8
CAL Calcium total	mg/100 g	0,981	1,29	0,996	1,15
MAG Magnesium total	mg/100 g	1,74	1,47	1,63	1,37
SOD Sodium total	mg/100 g				
FER Iron total	mg/100 g	69,3	63,9	64,6	55,6
MAN Manganese total	mg/100 g	18,1	19	18,1	16,8
ZIN Zinc total	mg/100 g	41,4	35,4	34,4	32,6
BOR Boron total	mg/100 g				
CUI Copper total	mg/kg	8,82	7,56	7,01	7,7
ALU Aluminium total	mg/kg				
MOL Molybdenum total	mg/kg				
CAD Cadmium total	mg/kg	0,0312	0,0425	0,0252	0,0292
CHR Chromium total	mg/kg				
NIC Nickel total	mg/kg				
PLO Lead total	mg/kg	0,206	< 0.2	0,417	< 0.2
COB Cobalt total	mg/kg				
ARS Arsenic total	mg/kg				

Appendix 4: Total mineral content measure in the BY2 cell lines

		Control			35S::FW2.2				
		GFP4	GFP5	GFP9	YF37	YF39	YF53	HA8	HA44	HA51
HUT residual humidity	%	14,1	14,5	14,5	10,5	8,89	9,9	11	7,79	11
CBR raw ashes	%	6,55	5,8	6,13	5,84	6,6	5,67	6,3	6,49	7,55
MOR organic matter	%	93,4	94,2	93,9	94,2	93,4	94,3	93,7	93,5	92,4
PHO Phosphorus total	mg/100 g	5,75	7,68	5,8	10,9	8,59	10,9	9,33	12,5	14
POT Potassium total	mg/100 g	22,1	19,7	20,4	15,3	23,9	16,9	23,1	19,8	24,3
CAL Calcium total	mg/100 g	1,16	0,897	0,996	0,996	0,848	0,818	1,02	0,975	0,973
MAG Magnesium total	mg/100 g	2,2	1,65	1,53	1,85	1,29	1,26	1,41	1,15	1,6
SOD Sodium total	mg/100 g									
FER Iron total	mg/100 g	36,8	80,1	61,7	143	68,7	50,7	66,2	178	82,9
MAN Manganese total	mg/100 g	402	619	343	733	531	400	612	1020	895
ZIN Zinc total	mg/100 g	163	112	154	159	155	263	162	188	182
BOR Boron total	mg/100 g									
CUI Copper total	mg/kg	< 3	< 3	< 3	6,03	< 3	< 3	< 3	< 3	3,52
ALU Aluminium total	mg/kg									
MOL Molybdenum total	mg/kg									
CAD Cadmium total	mg/kg	< 0.04	< 0.04	< 0.04	< 0.04	< 0.04	< 0.04	< 0.04	< 0.04	0,0383
CHR Chromium total	mg/kg									
NIC Nickel total	mg/kg									
PLO Lead total	mg/kg	< 0.3	< 0.3	< 0.3	< 0.3	< 0.3	< 0.3	< 0.3	< 0.3	< 0.3
COB Cobalt total	mg/kg									
ARS Arsenic total	mg/kg									

References

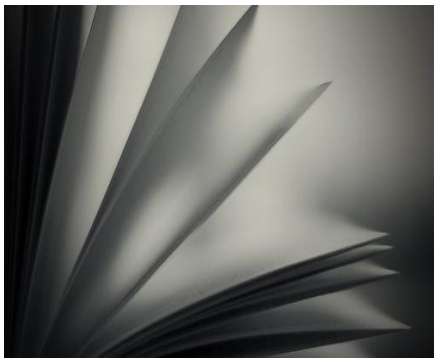

Abbà S, Vallino M, Daghino S, Di Vietro L, Borriello R, Perotto S. (2010). A PLAC8-containing protein from an endomycorrhizal fungus confers cadmium resistance to yeast cells by interacting with Mlh3p. Nucleic Acids Res. 39(17) pp 7548-7563.

Adachi S, Minamisawa K, Okushima Y, Inagaki S, Yoshiyama K, Kondou Y, Kaminuma E, Kawashima M, Toyoda T, Matsui M, Kurihara D, Matsunaga S, Umeda M. (2011). Programmed induction of endoreduplication by DNA double-strand breaks in Arabidopsis. Proc Natl Acad Sci U S A 108(24) pp 10004-10009.

Alpert KB, Grandillo S, Tanksley SD. (1995). fw2.2: a major QTL controlling fruit weight is common to both red- and green-fruited tomato species. Theor Appl Genet. 91 pp 994-1000.

Alpert KB, Tanksley SD. (1996). High-resolution mapping and isolation of a yeast artificial chromosome contig containing fw2.2: a major fruit weight quantitative trait locus in tomato. Proc Natl Acad Sci USA. 93 pp 15503-15507.

Azpiroz R, Wu Y, LoCascio JC, Feldmann KA. (1998). An Arabidopsis brassinosteroid-dependent mutant is blocked in cell elongation. Plant Cell 10(2) pp 219-230.

Beemster GTS, Fiorani F, Inze D. (2003). Cell cycle: the key to plant growth control? Trends Plant Sci. 8(4) pp 154-158.

Bergervoet JHW, Verhoeven HA, Gilissen LJW, Bino RJ. (1996). High amounts of nuclear DNA in tomato (*Lycopersicon esculentum Mill*.) pericarp. Plant Science 116 pp 141-145.

Bernard A, Domergue F, Pascal S, Jetter R, Renne C, Faure JD, Haslam RP, Napier JA, Lessire R, Joubès J. (2012). Reconstitution of plant alkane biosynthesis in yeast demonstrates that Arabidopsis ECERIFERUM1 and ECERIFERUM3 are core components of a very-long-chain alkane synthesis complex. Plant Cell 24(7) pp 3106-3118.

Bertin N, Lecomte A, Brunel B, Fishman S, Genard M. (2007). A model describing cell polyploidization in tissues of growing fruit as related to cessation of cell proliferation. Journal of Experimental Botany 58 pp 1903–1913.

Boudolf V, **Vlieghe K**, **Beemster GT**, **Magyar Z**, **Torres Acosta JA**, **Maes S**, **Van Der Schueren E**, **Inzé D**, **De Veylder L**. **(2004).** The plant-specific cyclin-dependent kinase CDKB1;1 and transcription factor E2Fa-Dpa control the balance of mitotically dividing and endoreduplicating cells in Arabidopsis. Plant Cell 16(10) pp 2683-2692.

Boudolf V, Lammens T, Boruc J, Van Leene J, Van Den Daele H, Maes S, Van Isterdael G, Russinova E, Kondorosi E, Witters E, De Jaeger G, Inzé D, De Veylder L. (2009). CDKB1;1 forms a functional complex with CYCA2;3 to suppress endocycle onset. Plant Physiology 150 pp 1482-1493.

Bourdon M, Frangne N, Mathieu-Rivet E, Nafati M, Cheniclet C, Renaudin JP, Chevalier C. (2010). Endoreduplication and growth of fleshy fruits. Progress in Botany 71 pp 101–132.

Bourdon M, Pirrello J, Cheniclet C, Coriton O, Bourge M, Brown S, Moise A, Peypelut M, Rouyere V, Renaudin JP, Chevalier C, Frangne N. (2012). Evidence for karyoplasmic

homeostasis during endoreduplication and a ploidydependent increase in gene transcription during tomato fruit growth. Development 139 pp 3817-3826.

Bradford MM. (1976). A rapid and sensitive method for the quantitation of microgram quantities of protein utilizing the principle of protein-dye binding. Anal Biochem. 72 pp 248-254.

Buer CS, Weathers PJ, Swartzlander GA Jr. (2000). Changes in Hechtian strands in cold-hardened cells measured by optical microsurgery. Plant Physiology 122(4) pp 1365-1377.

Burstenbinder K, Savchenko T, Muller J, Adamson AW, Stamm G, Kwong R, Zipp BJ, Dinesh DC. (2013). Arabidopsis Calmodulin-binding Protein IQ67-Domain 1 Localizes to Microtubules and Interacts with Kinesin Light Chain-related Protein-1. J Biol Chem. 288(3) pp 1871-1882.

Abel, SChakrabarti M,Zhang N, Sauvage C, Munos S, Blanca J, Canizares J, Diez MJ, Schneider R, Mazourek M, McClead J, Causse M, van der Knaap E. (2013). A Cytochrome P450 regulates a domestication trait in cultivated tomato. Proc Natl Acad Sci USA. 110 (42) pp 17125-17230.

Cannon SB, Mitra A, Baumgarten A, Young ND, May G. (2004). The roles of segmental and tandem gene duplication in the evolution of large gene families in *Arabidopsis thaliana. BMC Plant Biology 4(10).*

Carrari F, Baxter C, Usadel B, Urbanczyk-Wochniak E, Zanor MI, Nunes-Nesi A, Nikiforova V, Centero D, Ratzka A, Pauly M, Sweetlove LJ, Fernie AR. (2006). Integrated analysis of metabolite and transcript levels reveals the metabolic shifts that underlie tomato fruit development and highlight regulatory aspects of metabolic network behaviour. Plant Physiology 142 pp 1380-1396.

Cebolla A, Vinardell JM, Kiss E, Oláh B, Roudier F, Kondorosi A, Kondorosi E. (1999). The mitotic inhibitor ccs52 is required for endoreduplication and ploidy-dependent cell enlargement in plants. EMBO Journal 18(16) pp 4476-4484.

Cheniclet C, Rong WY, Causse M, Frangne N, Bolling L, Carde JP, Renaudin JP. (2005). Cell expansion and endoreduplication show a large genetic variability in pericarp and contribute strongly to tomato fruit growth. Plant Physiology 139 pp 1984-1994.

Chevalier C, Nafati M, Mathieu-Rivet E, Bourdon M, Frangne N, Cheniclet C, Renaudin JP, Gévaudant F, Hernould M. (2011). Elucidating the functional role of endoreduplication in tomato fruit development. Annals of Botany 107 pp 1159-1169.

Churchman ML, Brown ML, Kato N, Kirik V, Hulskamp M, Inze D, De Veylder L, Walker JD, Zheng Z, Oppenheimer DG, Gwin T, Churchman J, Larkin JC. (2006). SIAMESE, a plant-specific cell cycle regulator, controls endoreplication onset in *Arabidopsis thaliana*. The Plant Cell 18 pp 3145-3157.

Clough SJ, Bent AF. (1998). Floral dip: a simplified method for Agrobacterium-mediated transformation of Arabidopsis thaliana. Plant J. 16(6) pp 735-743.

Cong B, Liu J, Tanksley SD. (2002). Natural alleles at a tomato fruit size quantitative trait locus differ by heterochronic regulatory mutations. Proc Natl Acad Sci USA. 99 pp 13606-13611.

Cong B, Tanksley SD. (2006). FW2.2 and cell cycle control in developing tomato fruit: a possible example of gene co-option in the evolution of a novel organ. Plant Molecular Biology 62 pp 867-880.

Conn SJ, Gilliham M, Athman A, Schreiber AW, Baumann U, Moller I, Cheng NH, Stancombe MA, Hirschi KD, Webb AA, Burton R, Kaiser BN, Tyerman SD, Leigh RA. (2011). Cell-specific vacuolar calcium storage mediated by CAX1 regulates apoplastic calcium concentration, gas exchange, and plant productivity in Arabidopsis. The Plant Cell 23 pp 240-257.

Cowan AK, Moore-Gordon CS, Bertling I, Wolstenholme BN. (1997). Metabolic Control of Avocado Fruit Growth (Isoprenoid Growth Regulators and the Reaction Catalyzed by 3-Hydroxy-3-Methylglutaryl Coenzyme A Reductase). Plant Physiology 114(2) pp 511-518.

Dahan Y, Rosenfeld R, Zadiranov V, Irihimovitch V. (2010). A proposed conserved role for an avocado FW2.2-like gene as a negative regulator of fruit cell division. Planta 232(3) pp 663-676.

De Franceschi P, Stegmeir T, Cabrera A, van der Knaap E, Rosyara UR, Sebolt AM, Dondini L, Dirlewanger E, Quero-Garcia J, Campoy JA, Iezzoni AF. (2013). Cell number regulator genes in Prunus provide candidate genes for the control of fruit size in sweet and sour cherry. Mol Breed. 32 pp 311-326.

De Veylder L, Beeckman T, Beemster GT, Krols L, Terras F, Landrieu I, van der Schueren E, Maes S, Naudts M, Inzé D. (2001). Functional analysis of cyclin-dependent kinase inhibitors of Arabidopsis. Plant Cell 13(7) pp 1653-1668.

De Veylder L, Larkin JC, Schnittger A. (2011). Molecular control and function of endoreduplication in development and physiology. Trends in Plant Science 16 pp 624-634.

Dewitte W, Riou-Khamlichi C, Scofield S, Healy JM, Jacqmard A, Kilby NJ, Murray JA. (2003). Altered cell cycle distribution, hyperplasia, and inhibited differentiation in Arabidopsis caused by the D-type cyclin CYCD3. Plant Cell 15(1) pp 79-92.

Dewitte W, Scofield S, Alcasabas AA, Maughan SC, Menges M, Braun N, Collins C, Nieuwland J, Prinsen E, Sundaresan V, Murray JA. (2007). Arabidopsis CYCD3 D-type cyclins link cell proliferation and endocycles and are rate-limiting for cytokinin responses. Proc Natl Acad Sci U S A 104(36) pp 14537-14542.

Doebley J, Stec A, Hubbard L. (1997). The evolution of apical dominance in maize. Nature 386(6624) pp 485-488.

Dubin MJ, Bowler C, and Benvenuto G. (2008).A modified Gateway cloning strategy for overexpressing tagged proteins in plants. Plant Methods 4:3.

Edgar BA, Orr-Weaver TL. (2001). Endoreplication cell cycles: more for less. Cell 105(3) pp 297-306.

Eshed Y, Zamir D. (1994). Introgressions from Lycopersicon pennellii can improve the soluble-solids yield of tomato hybrids. Theor Appl Genet. 88(6-7) pp 891-897.

Eshed Y, Zamir D. (1995). An introgression line population of Lycopersicon pennellii in the cultivated tomato enables the identification and fine mapping of yield-associated QTL. Genetics 141(3) pp 1147-1162.

Espunya MC, Combettes B, Dot J, Chaubet-Gigot N, Martínez MC. (1999). Cell-cycle modulation of CK2 activity in tobacco BY-2 cells. The Plant Journal 19(6) pp 655-666.

Espunya MC, López-Giráldez T, Hernan I, Carballo M, Martínez MC. (2005). Differential expression of genes encoding protein kinase CK2 subunits in the plant cell cycle. Journal of Experimental Botany 56(422) pp 3183-3192.

Frary A, Nesbitt TC, Grandillo S, Knaap E, Cong B, Liu J, Meller J, Elber R, Alpert KB, Tanksley SD. (2000). fw2.2 : a quantitative trait locus key to evolution of tomato fruit size. Science 289 pp 85-88.

Freeling M. (2009). Bias in plant gene content following different sorts of duplication: tandem, whole-genome, segmental, or by transposition. Annu Rev Plant Biol 60 pp 433-453.

Giaginis C, Gatzidou E, Theocharis S. (2006). DNA repair systems as targets of cadmium toxicity. Toxicol Appl Pharmacol. 213(3) pp 282-290.

Gillaspy G, Ben-David H, Gruissem W. (1993). Fruits: A Developmental Perspective. The Plant Cell 5(10) pp 1439-1451.

Gisler SM, Kittanakom S, Fuster D, Wong V, Bertic M, Radanovic T, Hall RA, Murer H, Biber J, Markovich D, Moe OW, Stagljar I. (2008). Monitoring protein-protein interactions between the mammalian integral membrane transporters and PDZ-interacting partners using a modified split-ubiquitin membrane yeast two-hybrid system. Mol Cell Proteomics 7(7) pp 1362-1377.

Grandillo S, Ku HM, Tanksley SD. (1999). Identifying the loci responsible for natural variation in fruit size and shape in tomato. Theor Appl Genet. 99 pp 978-987.

Guo M, Rupe MA., Dieter JA, Zou J, Spielbauer D, Duncan KE, Howard RJ, Hou Z, Simmons CR. (2010). Cell Number Regulator1 affects plant and organ size in maize: implications for crop yield enhancement and heterosis. The Plant Cell 22 pp 1057-1073.

Gutierrez C, Ramirez-Parra E, Castellano MM, Del Pozo JC. (2002). G1 to S transition: more than a cell cycle engine switch. Current Opinion in Plant Biology 5 pp 480-486.

Hanna DE, Rethinaswamy A, Glover CV. (1995). Casein kinase II is required for cell cycle progression during G1 and G2/M in Saccharomyces cerevisiae. J Biol Chem. 270(43) pp 25905-25914.

Hase Y, Trung KH, Matsunaga T, Tanaka A. (2006). A mutation in the uvi4 gene promotes progression of endo-reduplication and confers increased tolerance towards ultraviolet B light. The Plant Journal 46(2) pp 317-326.

Homma MK, Wada I, Suzuki T, Yamaki J, Krebs EG, Homma Y. (2005). CK2 phosphorylation of eukaryotic translation initiation factor 5 potentiates cell cycle progression. Proc Natl Acad Sci USA. 102(43) pp 15688-15693.

Hu Y, Bao F, Li J. (2000). Promotive effect of brassinosteroids on cell division involves a distinct CycD3-induction pathway in Arabidopsis. The Plant Journal 24(5) pp 693-701.

Huang Z, Van Houten J, Gonzalez G, Xiao H, van der Knaap E. (2013). Genome-wide identification, phylogeny and expression analysis of SUN, OFP and YABBY gene family in tomato. Mol Genet Genomics. 288(3-4) pp 111-129.

Inzé D, De Veylder L. (2006). Cell cycle regulation in plant development. Annual Review in Genetics 40 pp 77-105.

Jimenez-Preitner M, Berney X, Uldry M, Vitali A, Cinti S, Ledford JG, Thorens B. (2011). Plac8 is an inducer of C/EBPβ required for brown fat differentiation, thermoregulation, and control of body weight. Cell Metab. 14(5) pp 658-670.

Jimenez-Preitner M, Berney X, Thorens B. (2012). Plac8 is required for white adipocyte differentiation *in vitro* and cell number control in vivo. PLoS One. 7(11) e48767.

Joubès J, Phan TH, Just D, Rothan C, Bergounioux C, Raymond P, Chevalier C.(1999). Molecular and biochemical characterization of the involvement of cyclin-dependent kinase CDKA during the early development of tomato fruit. Plant Physiology 121 pp 857-869.

Joubès J, Chevalier C. (2000). Endoreduplication in higher plants. Plant Molecular Biology 43 pp 737-747.

Joubès J, **Chevalier C**, **Dudits D**, **Heberle-Bors E**, **Inzé D**, **Umeda M**, **Renaudin JP. (2000).** CDK-related protein kinases in plants. Plant Molecular Biology 43 (5-6) pp 607-620.

Joubès J, Walsh D, Raymond P, Chevalier C. (2000). Molecular characterization of the expression of distinct classes of cyclins during the early development of tomato fruit.Planta 211(3) pp 430-439.

Kim TW, Michniewicz M, Bergmann DC, Wang ZY. (2012). Brassinosteroid regulates stomatal development by GSK3-mediated inhibition of a MAPK pathway. Nature 482(7385) pp 419-422.

Kondorosi E, Redondo-Nieto M, Kondorosi A. (2005). Ubiquitin mediated proteolysis. To be in the right place at the right moment during nodule development. Plant Physiology 137 pp 1197-1204.

Ku H-M, Doganlar S, Chen K-Y, Tanksley SD.(1999). The genetic basis of pear-shaped tomato fruit. Theor Appl Genet. 99 pp 844–850.

Ku HM, Tanksley SD. (1999). Identifying the loci responsible for natural variation in fruit size and shape in tomato. Theor Appl Genet. 99 pp 978-987.

Ku HM, Grandillo G, Tanksley SD. (2000). fs8.1, a major QTL, sets the pattern of tomato carpel shape well before anthesis. Theor Appl Genet. 101 pp 873-878.

Kuppusamy KT, Chen AY, Nemhauser JL. (2009). Steroids are required for epidermalcellfate establishment in Arabidopsis roots. Proc Natl Acad Sci U S A. 106(19) pp 8073-8076.

Kurusu T, Yamanaka T, Nakano M, Takiguchi A, Ogasawara Y, Hayashi T, Iida K, Hanamata S, Shinozaki K, Iida H, Kuchitsu K. (2012). Involvement of the putative Ca^{2+}-permeable mechanosensitive channels, NtMCA1 and NtMCA2, in Ca^{2+} uptake, Ca^{2+}- dependent cell proliferation and mechanical stress induced gene expression in tobacco (*Nicotiana tabacum*) BY-2 cells. J Plant Res. 125 pp 555-568.

Laemmli UK. (1970). Cleavage of structural proteins during the assembly of the head of bacteriophage T4. Nature 15;227(5259) pp 680-685.

Lammens T, Boudolf V, Kheibarshekan L, Zalmas LP, Gaamouche T, Maes S, Vanstraelen M, Kondorosi E, La Thangue NB, Govaerts W, Inzé D, De Veylder L. (2008). Atypical E2F activity restrains APC/CCCS52A2 function obligatory for endocycle onset. Proc Natl Acad Sci USA 105(38) 14721-14726.

Larson-Rabin Z, Li Z, Masson PH, Day CD. (2009). FZR2/CCS52A1 expression is a determinant of endoreduplication and cell expansion in Arabidopsis. Plant Physiology 149(2) pp 874-884.

Libault M., Zhang X. C., Govindarajulu M., Qiu J., Ong Y. T., Brechenmacher L., Berg R. H., Hurley-Sommer A., Taylor C. G., Stacey G. (2010). A member of the highly conserved FWL (tomato FW2.2-like) gene family is essential for soybean nodule organogenesis. The Plant Journal 62 pp 852–864.

Liu J, Van Eck J, Cong B, Tanksley SD. (2002). A new class of regulatory genes underlying the cause of pear-shaped tomato fruit. Proc Natl Acad Sci USA. 99 pp 13302-13306.

Liu J, Cong B, Tanksley SD. (2003). Generation and analysis of an artificial gene dosage series in tomato to study the mechanisms by which the cloned quantitative trait locus fw2.2 controls fruit size. Plant Physiology 132 pp 292–299.

Marrocco K, Bergdoll M, Achard P, Criqui MC, Genschik P. (2010). Selective proteolysis sets the tempo of the cell cycle. Current Opinion in Plant Biology 13 pp 631-639.

Mathieu-Rivet E, Gévaudant F, Sicard A, Salar S, Do PT, Mouras A, Fernie AR, Gibon Y, Rothan C, Chevalier C, Hernould M. (2010). Functional analysis of the anaphase promoting complex activator CCS52A highlights the crucial role of endo-reduplication for fruit growth in tomato. The Plant Journal 62(5) pp 727-741.

Mathieu-Rivet E, Gévaudant F, Cheniclet C, Hernould M, Chevalier C.(2010). The Anaphase Promoting Complex activator CCS52A, a key factor for fruit growth and endoreduplication in Tomato. Plant Signaling and Behavior 5(8) pp 985-987.

Melaragno JE, Mehrotra B, Coleman AW. (1993). Relationship between endopolyploidy and cell size in epidermal tissue of *Arabidopsis*. The Plant Cell 5 pp 1661-1668.

Miyazawa Y, Nakajima N, Abe T, Sakai A, Fujioka S, Kawano S, Kuroiwa T, Yoshida S. (2003). Activation of cell proliferation by brassinolide application in tobacco BY-2 cells:

effects of brassinolide on cell multiplication, cell-cycle-related gene expression, and organellar DNA contents. Journal of Experimental Botany 54(393) pp 2669-2678.

Mongrand S, Stanislas T, Bayer EM, Lherminier J, Simon-Plas F. (2010). Membrane rafts in plant cells. Trends in Plant Science 15(12) pp 656-663.

Moreno-Romero J, Espunya MC, Platara M, Ariño J, Martínez MC. (2008). A role for protein kinase CK2 in plant development: evidence obtained using a dominant-negative mutant. The Plant Journal 55(1) pp 118-130.

Muños S, Ranc N, Botton E, Bérard A, Rolland S, Duffé P, Carretero Y, Le Paslier MC, Delalande C, Bouzayen M, Brunel D, Causse M. (2011). Increase in Tomato Locule Number Is Controlled by Two Single-Nucleotide Polymorphisms Located Near WUSCHEL. Plant Physiology 156 pp 2244-2254.

Nafati M, Frangne N, Hernould M, Chevalier C, Gévaudant F. (2010). Functional characterization of the tomato cyclin-dependent kinase inhibitor SlKRP1 domains involved in protein-protein interactions. New Phytologist 188(1) pp 136-149.

Nafati M, Cheniclet C, Hernould M, Do PT, Fernie AR, Chevalier C, Gévaudant F. (2011). The specific overexpression of a cyclin-dependent kinase inhibitor in tomato fruit mesocarp cells uncouples endoreduplication and cell growth. The Plant Journal 65(4) pp 543-556.

Nakagawa Y, Katagiri T, Shinozaki K, Qi Z, Tatsumi H, Furuichi T, Kishigami A, Sokabe M, Kojima I, Sato S, Kato T, Tabata S, Iida K, Terashima A, Nakano M, Ikeda M, Yamanaka T, Iida H. (2007). Arabidopsis plasma membrane protein crucial for Ca^{2+} influx and touch sensing in roots. Proc Natl Acad Sci USA. 104(9) pp 3639-3644.

Nakano M, Iida K, Nyunoya H, Iida H. (2011). Determination of Structural Regions Important for Ca^{2+} Uptake Activity in Arabidopsis MCA1 and MCA2 Expressed in Yeast. Plant Cell Physiol. 52(11) pp 1915-1930.

Nemhauser JL, Mockler TC, Chory J. (2004). Interdependency of Brassinosteroid and Auxin signaling in Arabidopsis. PLOS Biology 2(9) e258.

Nesbitt TC, Tanksley SD. (2001). fw2.2 directly affects the size of developing tomato fruit, with secondary effects on fruit number and photosynthate distribution. Plant Physiology 127 pp 575-583.

Nesbitt TC, Tanksley SD. (2002). Comparative sequencing in the genus *Lycopersicon*: implications for the evolution of fruit size in the domestication of cultivated tomatoes. Genetics 162 pp 365-379.

Olmstead JW, Iezzoni AF, Whiting MD. (2007). Genotypic differences in sweet cherry fruit size are primarily a function of cell number. J Am Soc Hort Sci. 132 pp 697-703.

Paterson AH, Damon S, Hewitt JD, Zamir D, Rabinowitch HD, Lincoln SE, Lander ES, Tanksley SD. (1991). Mendelian factors underlying quantitative traits in tomato: comparison across species, generations, and environments. Genetics 127(1) pp 181-197.

Sicard A, Petit J, Mouras A, Chevalier C, Hernould M. (2008). Meristem activity during flower and ovule development in tomato is controlled by the mini zinc finger gene INHIBITOR OF MERISTEM ACTIVITY. The Plant Journal 55(3) pp 415-427.

Song WY, Martinoia E, Lee J, Kim D, Kim DY, Vogt E, Shim D, Choi KS, Hwang I, Lee Y. (2004). A novel family of Cys-Rich membrane proteins mediates cadmium resistance in *Arabidopsis*. Plant Physiology 135 pp 1027-1039.

Song WY, Choi KS, Kim DY, Geisler M, Park J, Vincenzetti V, Schellenberg M, Kim SH, Lim YP, Noh EW, Lee Y, Martinoia E. (2010). Arabidopsis PCR2 is a zinc exporter involved in both zinc extrusion and long-distance zinc transport. The Plant Cell 22 pp 2237-2252.

Song WY, Choi KS, Alexis de A, Martinoia E, Lee Y. (2011). Brassica juncea plant cadmium resistance 1 protein (BjPCR1) facilitates the radial transport of calcium in the root. Proc Natl Acad Sci U S A. 108(49) pp 19808-198013.

Stagljar I, Korostensky C, Johnsson N, te Heesen S. (1998). A genetic system based on split-ubiquitin for the analysis of interactions between membrane proteins in vivo. Proc Natl Acad Sci USA. 95 pp 5187-5192.

Tanksley SD, Ganal MW, Prince JP, De Vicente MC, Bonierbale MW, Broun P, et al. (1992). High density molecular linkage maps of the tomato and potato genomes. Genetics 132 pp 1141-1160.

Torres-Acosta JA, Fowke LC, Wang H. (2011). Analyses of phylogeny, evolution, conserved sequences and genome-wide expression of the ICK/KRP family of plant CDK inhibitors. Annals of Botany 107 pp 1141-1157.

Vahisalu T, Kollist H, Wang YF, Nishimura N, Chan WY, Valerio G, Lamminmäki A, Brosché M, Moldau H, Desikan R, Schroeder JI, Kangasjärvi J. (2008). SLAC1 is required for plant guard cell S-type anion channel function in stomatal signaling. Nature 452(7186) pp 487-491.

van der Knaap E, Lippman ZB, Tanksley SD. (2002). Extremely elongated tomato fruit controlled by four quantitative trait loci with epistatic interactions. Theor Appl Genet. 104(2-3) pp 241-247.

Verkest A, Manes CL, Vercruysse S, Maes S, Van Der Schueren E, Beeckman T, Genschik P, Kuiper M, Inzé D, De Veylder L. (2005a). The cyclin-dependent kinase inhibitor KRP2 controls the onset of the endoreduplication cycle during Arabidopsis leaf development through inhibition of mitotic CDKA;1 kinase complexes. Plant Cell 17(6) pp 1723-1736.

Vilhar B, Kladnik A, Blejec A, Chourey PS, Dermastia M. (2002). Cytometrical evidence that the loss of seed weight in the miniature1 seed mutant of maize is associated with reduced mitotic activity in the developing endosperm. Plant Physiology 129 pp 23-30.

Villiers F, Jourdain A, Bastien O, Leonhardt N, Fujioka S, Tichtincky G, Parcy F, Bourguignon J, Hugouvieux V. (2012). Evidence for functional interaction between brassinosteroids and cadmium response in Arabidopsis thaliana. Journal of Experimental Botany 63(3) pp 1185-1200.

Wang RL, Stec A, Hey J, Lukens L, Doebley J. (1999). The limits of selection during maize domestication. Nature 398(6724) pp 236-239.

Weinl C, Marquardt S, Kuijt SJ, Nowack MK, Jakoby MJ, Hülskamp M, Schnittger A. (2005). Novel functions of plant cyclin-dependent kinase inhibitors, ICK1/KRP1, can act non-cell-autonomously and inhibit entry into mitosis. Plant Cell 17(6) pp 1704-1722.

Winicur ZM, Zhang GF, Staehelin LA. (1998). Auxin Deprivation Induces Synchronous Golgi Differentiation in Suspension-Cultured Tobacco BY-2 Cells. Plant Physiology 117(2) pp 501-513.

Wu S, Xiao H, Cabrera A, Meulia T, van der Knaap E. (2011). SUN regulates vegetative and reproductive organ shape by changing cell division patterns. Plant Physiology 157(3) pp 1175-1186.

Xiao H, Jiang N, Schaffner E, Stockinger EJ, and van der Knaap E. (2008). A Retrotransposon-Mediated Gene Duplication Underlies Morphological Variation of Tomato Fruit. Science 319 pp 1527-1530.

Xu J, Xiong W, Cao B, Yan T, Luo T, Fan T, Luo M. (2013). Molecular characterization and functional analysis of "fruit-weight 2.2-like" gene family in rice. Planta 238(4) pp 643-655.

Study of the FW2.2 role during tomato fruit development

The *FW2.2* gene corresponds to the major Quantitative Trait Locus (QTL) governing fruit size in tomato. *FW2.2* belongs to a multigene family and encodes a transmembrane protein of 163 amino acids whose actual function remains unknown. Although described as a negative regulator of cell divisions and consequently as a regulator of fruit size, any definitive biochemical, physiological and developmental function assigned to FW2.2 is still lacking although the gene was cloned more than twelve years ago. Especially the fundamental question of what kind of link is there between the FW2.2 protein function and cell cycle regulation is all even more relevant. The analysis of the recently released genome of tomato identified 17 new sequences related to FW2.2 (*SlFW2.2-like* genes) and the protein sequence alignments showed the conservation of the PLAC8 motif common to this multigene family. Our phylogenetic studies did not give any clues relative to the FW2.2 function even though it presents sequence characteristics described for heavy metal transporters. Electrophysiology experiments did not allow the confirmation of the ion transporter function but a total ion content measurement on tomato fruit pericarps differing by their levels of *FW2.2* expression showed a difference in the fruit pericarp cadmium content. We also investigated the role of the FW2.2 protein on the plant development using plant and cell lines that overexpress this gene and it appeared that this protein may be involved in the brassinosteroid signal pathway. The regulatory mechanisms mediated by the action of FW2.2 on mitotic activity during fruit development have also been analyzed by looking for potential partners interacting with the FW2.2 protein using the technique of split-ubiquitin.

Étude du rôle de FW2.2 pendant le développement du fruit de tomate

Le gène *FW2.2* correspond au locus de caractère quantitatif (QTL) majeur impliqué dans le contrôle de la taille finale du fruit de tomate. *FW2.2* appartient à une famille multigénique et code une protéine transmembranaire de 163 acides aminés dont la fonction demeure de nos jours inconnue. Pourtant décrite comme un régulateur négatif des mitoses, par conséquent comme un régulateur de la taille du fruit et cloné plus de 12 ans auparavant, aucune fonction biochimique, physiologique ni même développementale n'a été déterminée concernant cette protéine. Ce qui est d'autant plus étonnant car aucun lien n'a été révélé entre sa fonction protéique et sa capacité à influencer le cycle cellulaire. L'analyse d'une nouvelle version du génome de la tomate nous a permis d'identifier 17 nouvelles séquences homologues à FW2.2 (que nous avons nommé FW2.2-like) et l'alignement de ces séquences nous a permis d'observer une importante conservation du motif PLAC8 commun à cette famille multigénique. L'étude phylogénétique que nous avons réalisée ne nous a donné aucune indication quant à la fonction potentielle de transporteur de métaux lourds de la protéine FW2.2 malgré le fait que sa séquence protéique présente les mêmes caractéristiques que celles décrites chez des transporteurs de métaux lourds. Des expériences d'électrophysiologie ne nous ont pas permis de confirmer son rôle de transporteur, mais des dosages de contenu minéral réalisés sur des péricarpes de fruits de tomate présentant des niveaux d'expression différents pour *FW2.2* nous ont permis d'observer une différence de stockage du cadmium dans le péricarpe de ces fruits. Nous avons également étudié le rôle de la protéine FW2.2 dans le développement des plantes en utilisant des lignées de plantes et des lignées cellulaires surexprimant le gène *FW2.2.* Ceci nous a mené à l'hypothèse que la protéine FW2.2 pouvait être impliquée dans la voie de signalisation des brassinostéroïdes. Pour terminer, nous avons tenté de comprendre quels mécanismes de régulation étaient déclenchés par FW2.2 en recherchant ses partenaires potentiels par le biais de l'application de la technique du Split-Ubiquitin.